Prepared for
New England Interstate Water Pollution Control Commission
(NEIWPCC)
Lowell, MA

Flushing Analysis in the Acushnet River Estuary

ASA Report 01–123 **Final Report**

January 2003

Hyun-Sook Kim
J. Craig Swanson
Jiganesh Patel

Applied Science Associates, Inc.
70 Dean Knauss Drive
Narragansett, RI 02882

Executive Summary

A flushing study was performed for the Acushnet River estuary (New Bedford Inner Harbor), supported by the New England Interstate Water Pollution Control Commission (NEIWPCC) and U. S. EPA-New England. This work consisted of two parts: field program and numerical computations. The field study was conducted to support the numerical computations. The ultimate goal of this study is to determine the flushing characteristics of the estuary and residence time of the wastewater discharged from the Fairhaven Wastewater Treatment Plant (WWTP) in the lower estuary. This study will eventually serve as a preliminary step in determining the nitrogen TMDL (Total Maximum Daily Load) that the estuary can assimilate.

A dye study was conducted as part of the field program in the lower estuary, at the Fairhaven WWTP discharge outfall. This study was designed with three parts. The first was a survey to measure background level of fluorescence at eleven stations, and the second was the dye release study by pumping at the Fairhaven WWTP at a rate of 21 mg/s for a 5-day period from 9:00 18 October to 9:00 23 October. The last was three surveys to monitor dye distribution once before and twice after the termination of dye injection. The survey observations exhibited that dye rose to the surface as soon as it was discharged through the outfall, and it immediately spread out forming a localized plume mostly residing near the outfall. There was no significant vertical distribution of dye observed during the observation. Four hours after the cessation of dye injection, the spatial coverage of dye distribution became much smaller than the survey six hours earlier. Twenty-two hours later, the dye concentration became at the same level as background fluorescence concentration, indicating that the residence time of dye was less than 22 hours.

The dye simulation was conducted to estimate residence time of dye in the lower estuary, using BFMASS (Boundary Fitted Pollutant Transport) model, a component of Water Quality Analysis and Mapping Package (WQMAP). The simulation resulted in 21 hours (0.88 days) of residence time, which implied a good agreement with the observation.

Also performed was a long-term dye release simulation in the Acushnet River estuary, having a unit source strength at the Fairhaven WWTP outfall. The results suggested that the estuary system took six months to reach steady state, and estimated residence time for the lower estuary was on the order of 15 days. A comparison of estimated residence time between the 5-day and long-term dye simulations implied that the reason for the shorter residence time from the 5-day simulation was due to the dye lost not only by dispersion in the inner harbor but also to transport to the outer harbor. Therefore, the actual dye study was unable to determine an accurate estimate of residence time since the amount of dye pumped into the system was not sufficient for the system to reach steady state.

For the flushing time estimate, three different approaches were employed: Freshwater exchange method (Mills et al., 1984), modified tidal prism method (Ketchum, 1951) and BFMASS (Boundary Fitted Pollutant Transport Model) numerical simulation. The first approach uses salinity information in a series of segments, and the modified tidal prism

method utilizes sub-tidal and inter-tidal volume of the area of interest. In addition, the study also employed local/system residence time to compare results.

The estimate of flushing time was based on the hydrologic conditions for 1 November. Estimated flushing times from the freshwater ratio and modified tidal prism methods were 15.6 days and 18.8 days, respectively. The BFMASS simulation used a fixed river flow on 1 November but time-varying hydrodynamics that were ambient currents and played an important role for the pollutant advection. The simulation results yielded 10.6 days of flushing time. As the freshwater budget increased to 2.5 times of the river flow on 1 November (24 October), estimated flushing times decreased to 6.4 days, 17.8 days and 7.1 days for the freshwater exchange and modified tidal prism methods, and numerical simulation, respectively.

Table of Contents

List of Figures

List of Tables

1. Introduction

A study of flushing time was performed for the Acushnet River estuary (New Bedford Inner Harbor), supported by the New England Interstate Water Pollution Control Commission (NEIWPCC) and U. S. EPA-New England. This work consisted of two parts: field program and numerical simulations. The goal of this study is to provide the flushing characteristics of the estuary as a preliminary step in determining the nitrogen TMDL (Total Maximum Daily Loading) that the estuary can assimilate.

The Acushnet River estuary is a unique area that is confined by Hurricane Barriers with an opening 46 m wide between New Bedford and Fairhaven (Figure 1-1). The barrier restricts exchange of waters between the Inner and Outer Harbors and possibly reduces flushing of the estuary. Furthermore, freshwater input from the Acushnet River is relatively low in the vicinity of an annual average of 0.54 m^3/s (Abdelrhmann and Dettmann, 1995) or 0.75 m^3/s (ASA, 1990). These conditions result in elevated levels of nutrients, as observed by Howes (1999). The nitrogen loading from the watershed, the Fairhaven Wastewater Treatment Plant (WWTP) and the New Bedford combined sewage outflows (Costa, 2000) all contribute to the water quality problem.

To improve water quality in the system, the important question to be answered is to what level must the nitrogen sources be reduced. Since water quality improves as excess nutrient loading decreases and flushing time decreases, the first order approach to find the assimulative capacity is to determine how quickly the estuary flushes.

The objective of this work is to analyze flushing characteristics of the Acushnet River estuary. There are three different approaches employed for the study, using either data or numerical models. They are freshwater exchange method, a modified tidal prism method, and BFMASS (Boundary Fitted Pollutant Transport Model) numerical simulation. The former uses salinity information in a series of segments in the estuary system, which is determined *a priori*, and the latter uses sub-tidal and inter-tidal volumes of a study area. The difference of the modified tidal prism method and the conventional tidal prism method is to take into account the morphology of the estuary system, by employing variations of cumulative sub-tidal and inter-tidal volumes as function of upstream distance and by determining tidal excursion from the volume functions. The BFMASS model is to simulate the fate and transport of pollutants with a single or multiple sources. Employment of the model for this work further extends the capability to predict residence time of the waste matter or flushing time for an area of interest, either part or the whole estuary. In addition to the three approaches, we also adopt a method of local/system residence time for the flushing time comparison.

Another objective of this work is to estimate residence time of the wastewater discharged from the Fairhaven WWTP. This will be separately accomplished by a dye release study and numerical simulations.

This report is organized in six sections. Following the introduction, Section 2 presents a summary of the field study, analysis of salinity and dye observations, and description of

hydrodynamic conditions during the field investigation. Section 3 presents a brief description of WQMAP, followed by the BFHYDRO and BFMASS model applications to the Acushnet River estuary. Section 4 documents flushing time results from the three separate methods and sensitivity analysis for each method. Also included in the section is the flushing time results computed using a local/system residence time methods. Finally section 5 presents discussion and conclusions, followed by the list of references in section 6. There are three appendices describing the field observations: Salinity data in Appendix A, dye study area in Appendix B and currents in Appendix C.

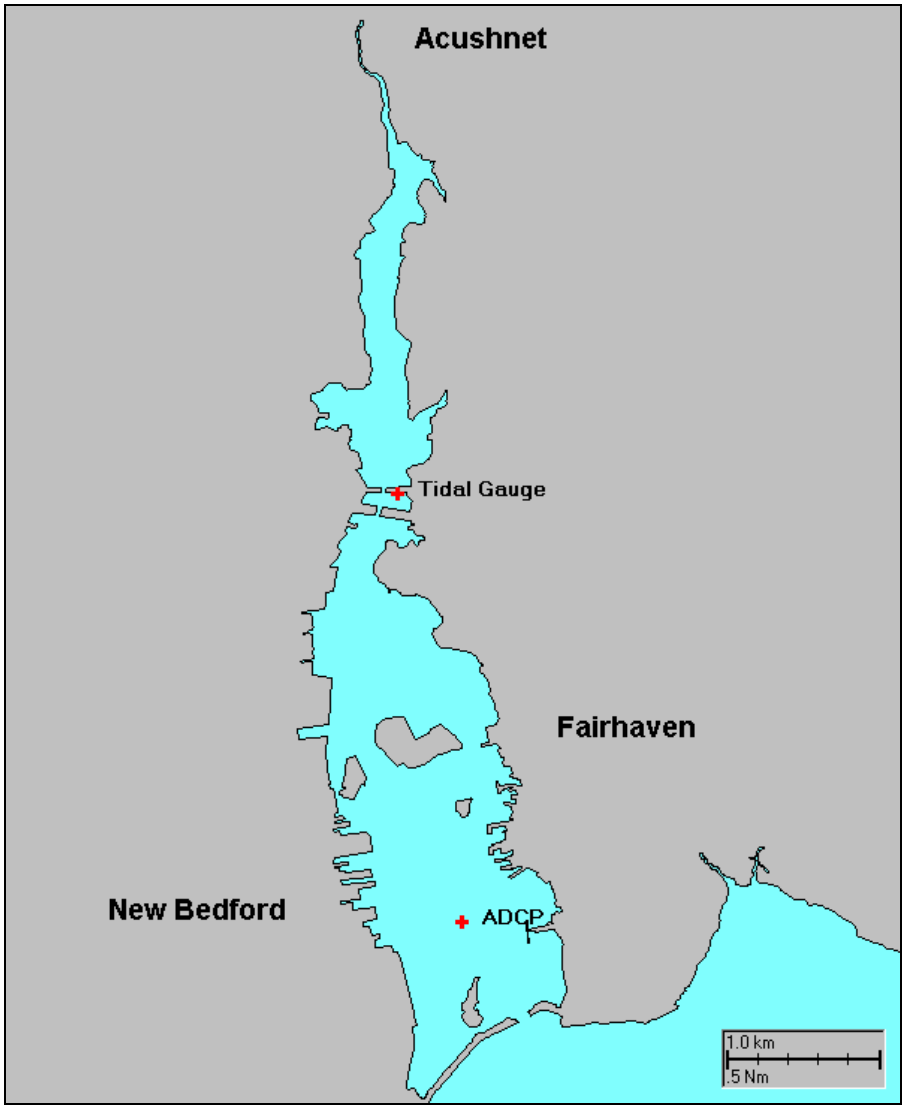

Figure 1-1. Mooring locations for BBADCP (BroadBand Acoustic Doppler Current Profilers) and tide gauge.

2. Field Study

The field study was designed as an integrated program of intensive collection of various data. The measurements included salinity, dye concentrations, freshwater run-off, and time series of surface elevations and currents. The goal of the study was to utilize these

data to determine flushing times in the estuary using various approaches, and to provide data for the model calibration.

Figure 2-1 shows a summary of the field program schedules. This figure differentiates time series and discrete samplings, represented by solid arrows and cross symbols, respectively. The observations not collected during this field program but available from different sources are also shown in the figure as broken arrows.

The strategy to collecting salinity data is to measure synoptically over the estuary at high and low tides for a minimum of three tidal cycles during the execution of the dye survey. The measurement at low slack provides the best indication of flushing as it provides the largest longitudinal salinity gradient. The high slack measurement offers some indications on the variability of the salinity gradient and is a useful check on the predicted range of flushing times for the estuary. The difficulty is to measure synoptically in an area composed of 20 sub-zones in an estuary 6.1 km long. To minimize the problem of non-synopticity, two boats were operated simultaneously but in different sections of the estuary. Vertical casts were taken at approximately 55 stations using SEACAT or YSI instruments on each boat to obtain the vertical structure of salinity. Mode details are presented in Appendix A.

The dye study was conducted for the Fairhaven Waste Water Treatment Plant (WWTP) discharge, and was performed during average tidal conditions (tidal range ~ 1m) based on tidal predictions for the second half of October 2001. For the study, Rhodamine WT dye was chosen because of its low toxicity, high detectability and is a conservative tracer. A 20% solution of Rhodamine WT dye was added into the WWTP discharge water to reach a target concentration of at least 1330 ppb in the effluent (see QAPP). Rhodamine WT dye was continuously injected into the Fairhaven WWTP effluent, starting on 18 October, 5 days prior to the start of the actual plume monitoring. Dye concentrations were monitored daily at selected 11 stations (Table B-1 in Appendix B) to confirm that a steady state had been reached prior to commencing the intensive synoptic surveys. A sample of the effluent was taken from the discharge, tagged with dye at the start of the injection and monitored throughout the study to determine dye depletion. More details of methodology and sampling strategy for the dye study may be referred to in the QAPP.

Stage and flow of the Acushnet River were monitored just downstream of Saw Mill Dam during the dye study, whereas only the stage was measured for the salinity surveys. Using the stage to flow correlation, estimates of river flow were made during the period of the salinity survey. A comparison of stream flow was made between the estimate and USGS observation in an area close to the study region, in order to determine the appropriate estimate.

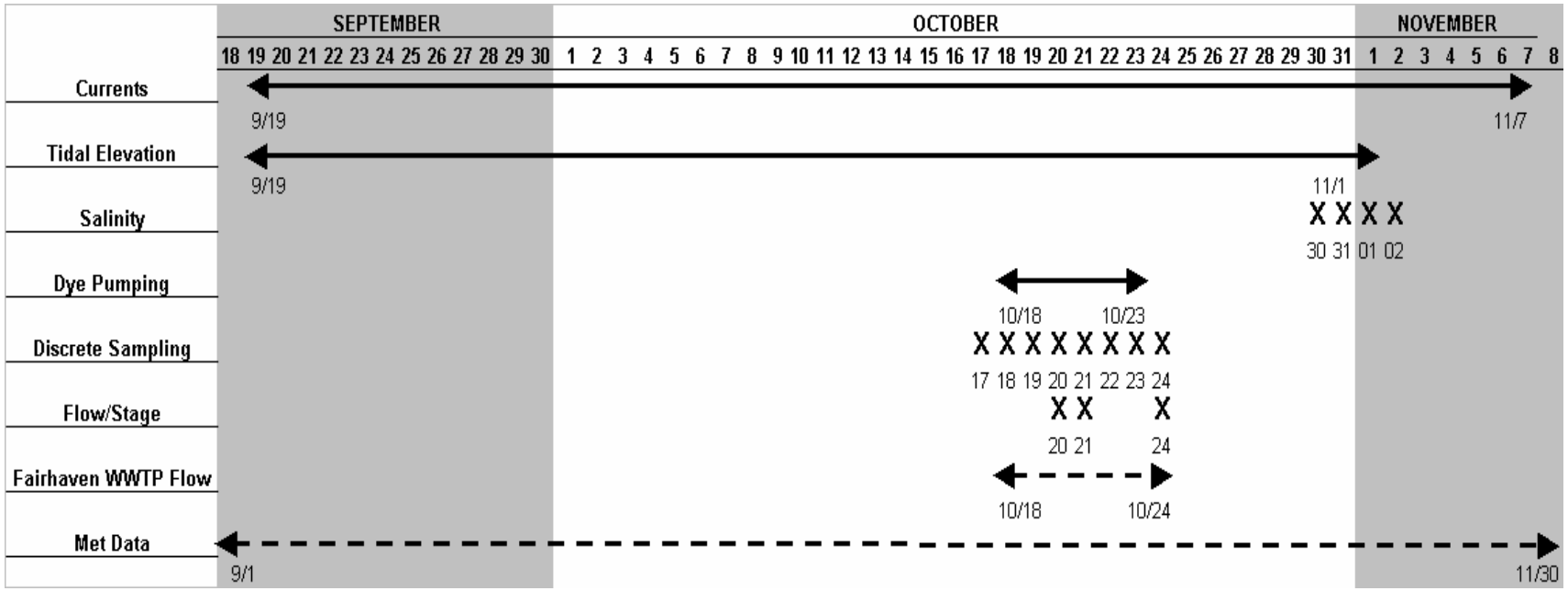

Figure 2-1. Data collection schedule for time series and discrete surveys, and other data available from different sources.

A tidal gauge was deployed at 0.3 m (1 ft) off the bottom in 2.4 m (8 ft) of water at high water (HW) at (41° 39.350′N, 70° 54.952′W), south of the Coggeshall Street Bridge (Figure 1-1), for the period from 19 September to 1 November 2001. The measurements were taken for the period that included the salinity and dye surveys. The 42-day deployment was sufficient to perform a tidal constituent analysis.

A BroadBand Acoustic Doppler Current Profilers (BBADCP) with a set of 610 kHz convex transducers was moored in 10.4 m water (HW) at a site (41° 37.808′N, 70° 54.643′W), west of the federal navigation channel (Figure 1-1). The deployment period was from 19 September to 7 November 2001. The BBADCP was designed to collect currents every 5 min (200 ensemble pings at 1.5 sec per ping; see Table C-1 in Appendix C) and over the whole water column at 0.5 m vertical sampling intervals. These data sets were to be used to calibrate the hydrodynamic model. However, beam 3 failed one-and-half days after deployment. This was evident in echo intensity (Figures C-1a to C-1g) and correlation profile data (Figure C-2a and C-2g) with zero amplitude and relatively low correlation, respectively. Furthermore, the *percent good* data for beams 2 and 4 indicated that a majority of data from the beams did not pass quality-screening criteria (Figures C-3a to C-3g). Judging from the quality of the standard profile data, the BBADCP measurements were not useful.

2.1. Salinity Study

The sampling area for salinity measurements were divided into three zones; A, B and C (Figure 2-2). Each zone was further divided into 8 (A1 to A8), 7 (B1 to B7) and 6 (C1 to C6) segments, respectively. Salinity measurements were taken at two or three locations in each segment in zone A and zones B and C, respectively, comprising a total of 55 sampling locations (Figure 2-3). The original schedule for salinity sampling was set-up so that measurements would take place at two consecutive tidal stages per day. However, due to instrument malfunctioning on 30 October and a broken shifter cable on one of the boats on 31 October measurements collected twice on high tide and four times on low tide over a 4-day period (Table 2-1).

Table 2-1. Salinity sampling schedule and salinity measurements missing stations. Due to low water level, salinity at stations with + mark were not taken.

Date and Time	Tidal Stage	Missing Stations
10/30/2001 from 11:58 AM	Low	$A1B^{+}$
10/31/2001 from 11:41 AM	Low	$A1B^{+}$
11/1/2001 from 06:47 AM	High	
11/1/2001from 12:09 PM	Low	$A1A^{+}$, $A1B^{+}$
11/2/2001 from 07:07 AM	High	
11/2/2001 from 01:14 PM	Low	$A1A^{+}$, $A1B^{+}$, B5A, B5B, B5C

Observed salinity range for the estuary varied from about 12 ppt to 32 ppt. The lower salinity existed in the upper estuary and the higher salinity occurred in the lower estuary, showing a negative gradient with downstream. Variation of the gradient depended on the

freshwater inflow from the Acushnet River. For most of the time, the largest gradient existed in zone A.

During the salinity survey, there were two rain events whose precipitation was less than 0.2 inches, on 23-24 October and 25 October 2001. Figure 2-4 shows the salinity distribution in the upper 20-cm layer. It is revealed that the surface water on 30 October (Figure 2-4a)

Figure 2-2. The Acushnet River estuary segments defined for flushing time estimate.

was relatively fresh, compared to the other days. The field data indicated that freshwater also existed in the lower estuary (Figure 2-4). However, one day later the salinity became similar to the following two days, having freshwater in the upper estuary adjacent to the Acushnet River. The reason for the low salinity on 30 October was a time-lagged impact by freshwater input from precipitation via surface stream flow.

Different salinity gradients at different tidal stages are also evident in Figure 2-4. Comparing Figures 2-5c and 2-5e with Figures 2-5d and 2-5f, the salinity gradually increases toward the lower estuary during high tide but it increases relatively rapidly over the same latitudinal span during low tide.

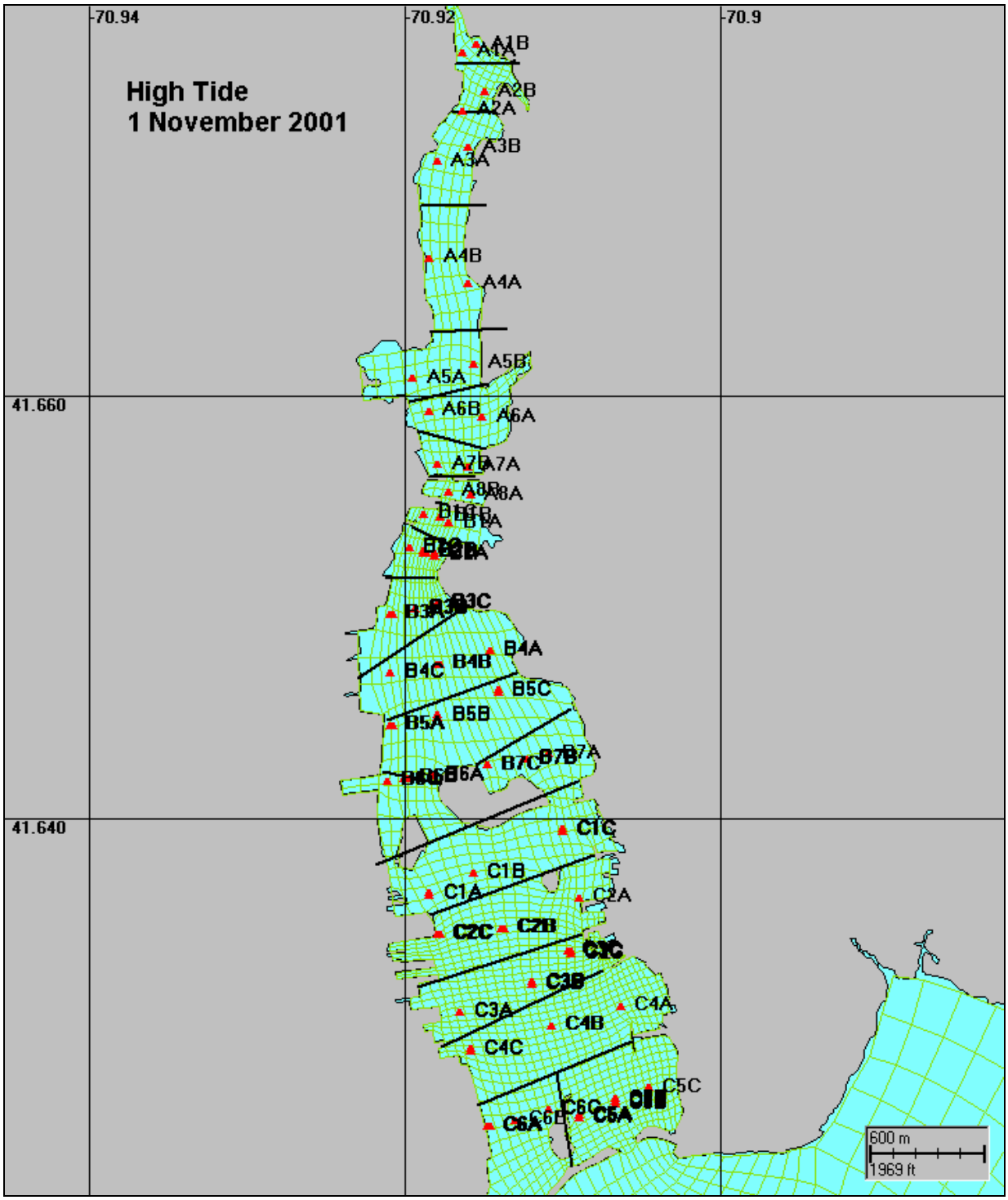

Figure 2-3. Salinity sampling stations during high tide (06:27 am) on 1 November 2001.

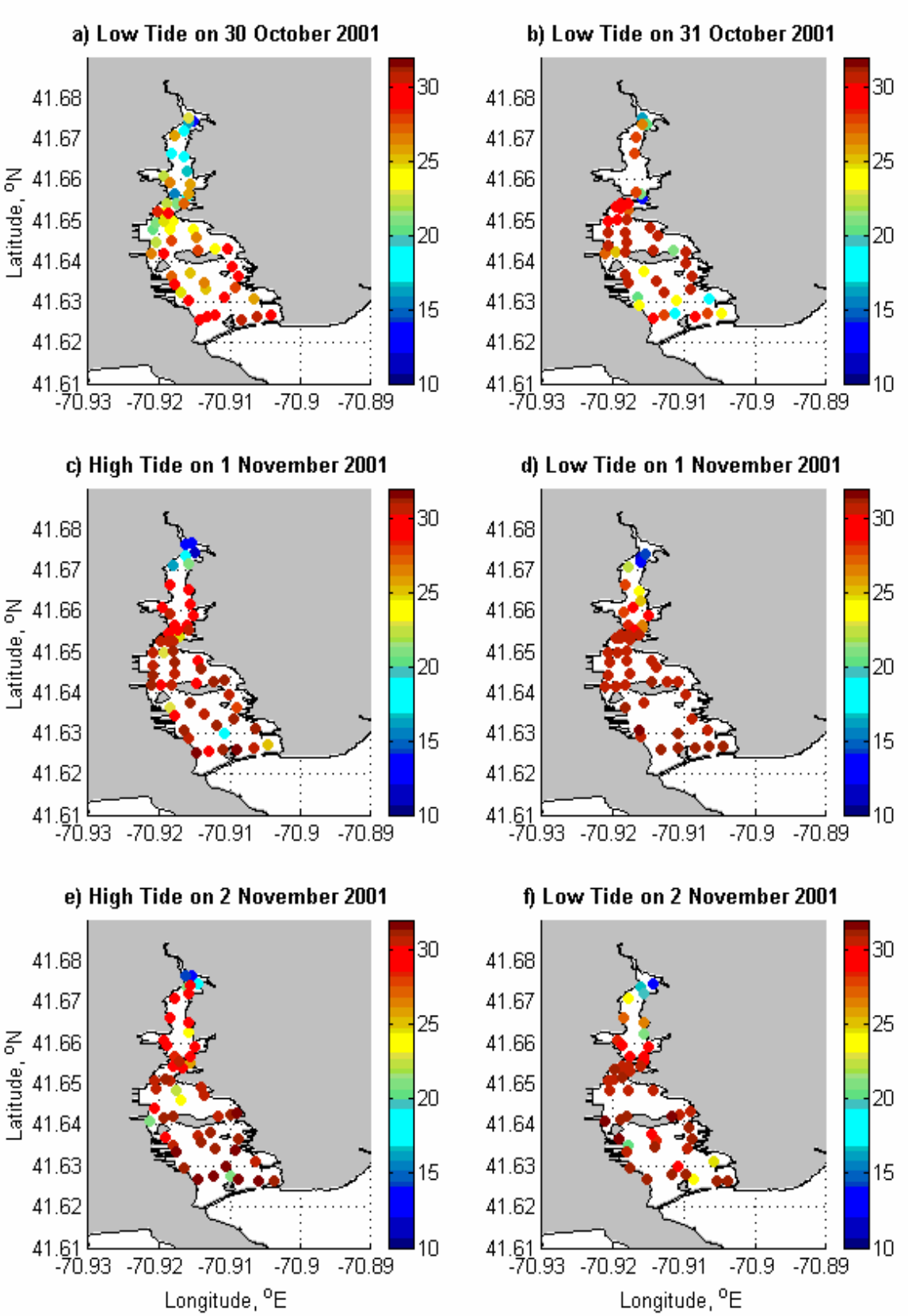

Figure 2-4. Salinity field in the upper 20 cm surface-layer.

Salinity change with depth was very small. Figure 2-5 shows salinity profiles, for example, at shallow and deep locations in segment C4. Regardless of the water depth, the salinity variation with depth was insignificant. Mean salinity in the shallow area (C4A and C4C) was 31.2 ppt, excluding the top-layer sample at C4C, with a variation less than ±0.2 ppt. Similar variation was observed at the deep channel, C4B, where presumably salinity might be higher because the water was confined within the channel and the only exchange occurring was with the water from the Outer Harbor.

However, there were substantial variations existing in the near surface layer. Figure 2-6 presents an example of salinity fields at two different depths. The salinity in the lower layer (40 cm below the surface) ranged from 22 to 31 ppt, and its distribution was rather homogeneous. In contrast, the upper layer (19 cm below the surface) exhibited freshwater (12-31 ppt), about 4.5 ppt on average lower than salinity in the lower layer. This indicates the surface layer thickness varies across the estuary.

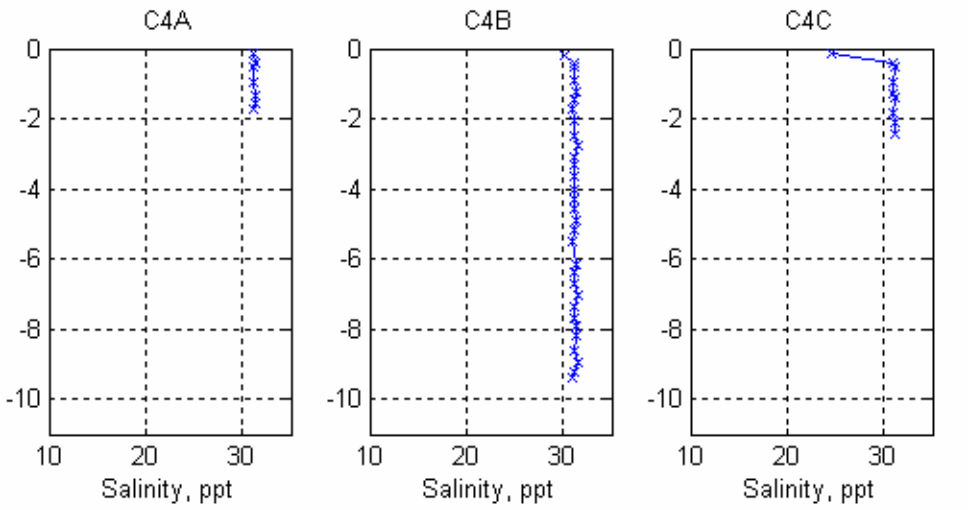

Figure 2-5. Salinity profiles measured in segment C4 on 2 November 2001. Station C4B is located in the navigation channel, and stations C4a and C4C are west and east of C4B in shallow areas, respectively.

2.2. Dye Study

Dye was pumped into the waste water at the Fairhaven WWTP from 9:00AM 18 October to 9:00AM 23 October. A total of 45.4 kg (100 lb) of dye (as a 20% Rhodamine WT solution) was released at a 1.8 MGD (million gallon per day) rate of the waste water, for a 5-day period. This is equivalent to 1330 ppb dye solution release per day or 21 mg/s release rate.

Figures 2-8 to 2-10 show the dye distributions during and after the termination of injection. These synoptic measurements were obtained over the course of 24 hours,

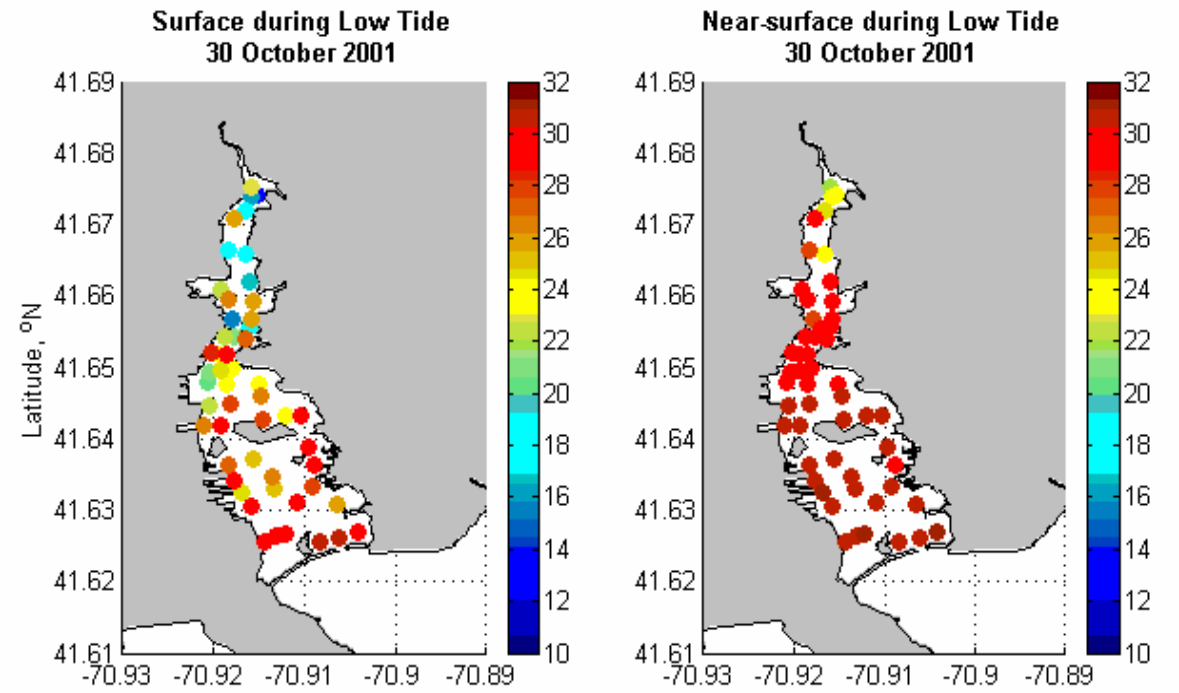

Figure 2-6. Salinity fields in the 20 cm depth (left) and in the 40 cm depth below the surface (right) on 30 October 2001. Spatial mean salinity is 25.0 ppt and 29.5 ppt for the upper and lower layers, respectively.

beginning 2.5 hours before and 23 hours after the termination. The monitoring surveys showed that the released dye was observed nowhere but at the surface, and the magnitude of the concentration was drastically decreased as one moves away from the discharge outfall. For the first survey (Figure 2-7) conducted in the morning of 23 October, the maximum concentration was 46 ppb and was observed at the outfall. However, the concentrations in areas away from the outfall were substantially lower. For instance, the distance to the e-folding concentration (17 ppb) was about 300 m in the morning of 23 October and decreased by a factor of 3 over the next 4 hours (Figure 2-8). A similar rapid decrease appeared in the following 20 hours (Figure 2-9). Since the dye was still observed during the second survey and completely disappeared by the third survey, the residence time of dye at the discharge area therefore was estimated to be between 5 and 22 hours.

For the second survey (Figure 2-8), the concentration level at the outfall was still the same level as measured during the pumping (Figure 2-7). This may be the fact that residual dye from the pipe was still flowing into the Harbor even after the termination. The treatment plant is about 2.8 km landward from the discharge outfall and has the outfall pipe of 91 cm (36 inches) diameter. With 1.8 MGD average daily flow, the effluent flows at a speed of 0.12 m/s and takes about 6.5 hours to reach the end of the outfall pipe. Therefore, it is possible to find elevated dye 6.5 hours after the cessation of the pumping.

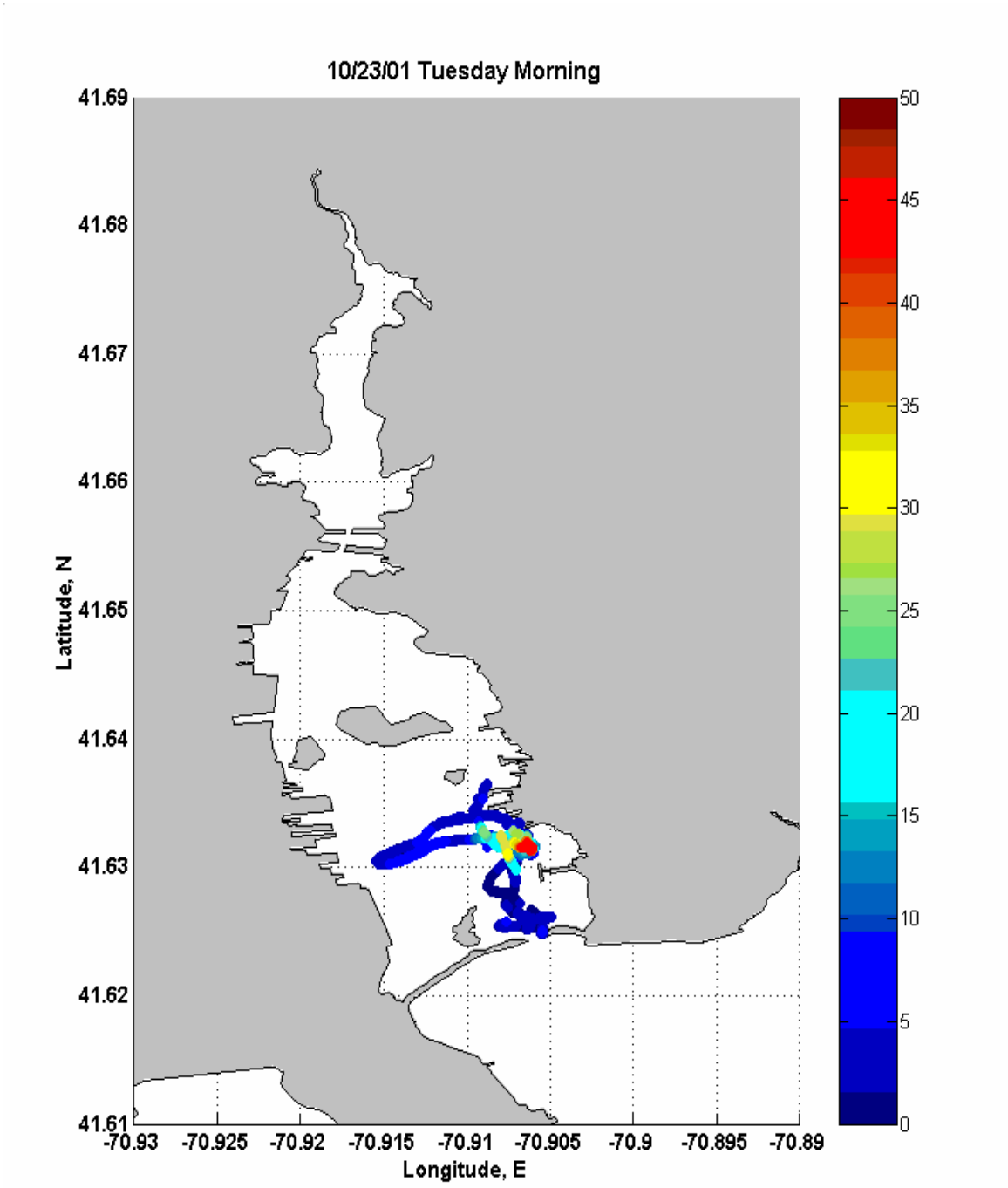

Figure 2-7. Dye distribution at the surface layer observed from 6:44 AM to 9:22 AM on 23 October. Units are ppb.

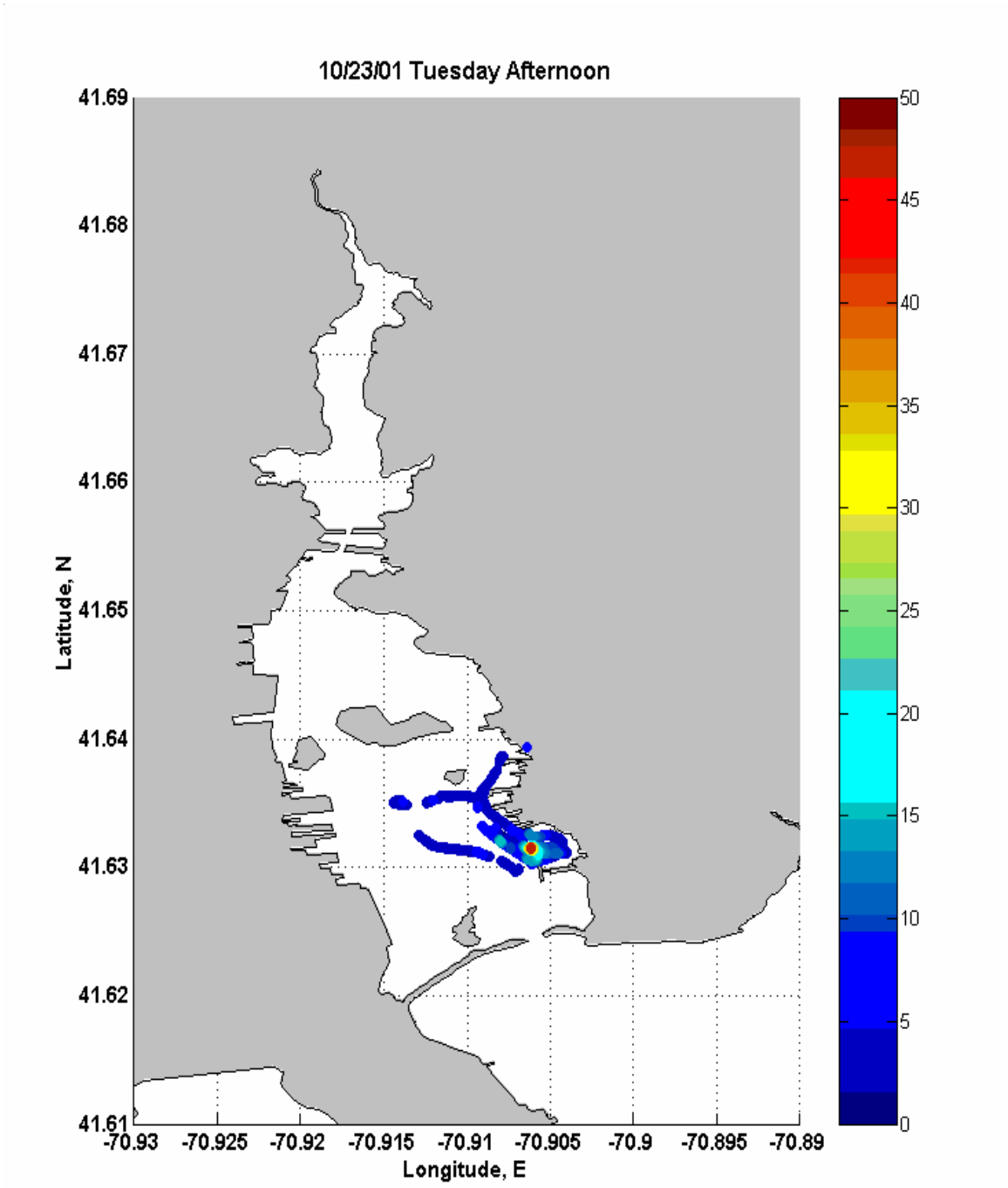

Figure 2-8. Dye distribution in the surface layer observed from 1:00 PM to 2:13 PM on 23 October. Units are ppb.

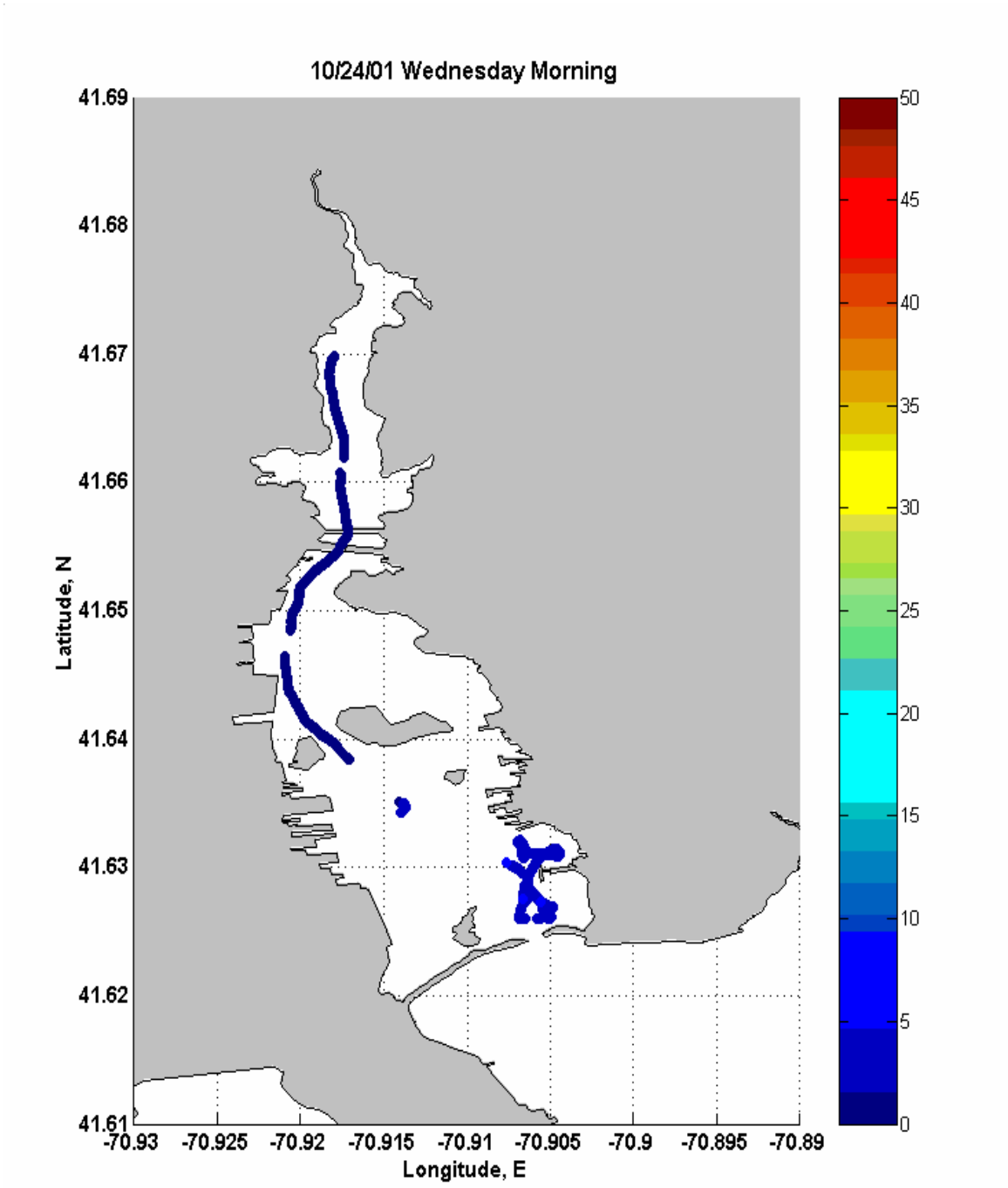

Figure 2-9. Dye distribution in the surface layer observed between 7:00 AM and 10:00 AM on 24 October. Units are ppb.

2.3. River Flow

According to three discrete samplings collected downstream of the Saw Mill Dam (19-20 and 24 October 2001), freshwater entering from the Acushnet River varied between 0.29 m^3/s (10.15 ft^3/s) and 1.14 m^3/s (40.42 ft^3/s), with an average of 0.5 m^3/s (Figure 2-10). Concurrently observed stage data indicated the water elevations varied from 0.43 to 0.51 m. For the sampling period, flow and stage are highly correlated showing a squared correlation coefficient of 0.998.

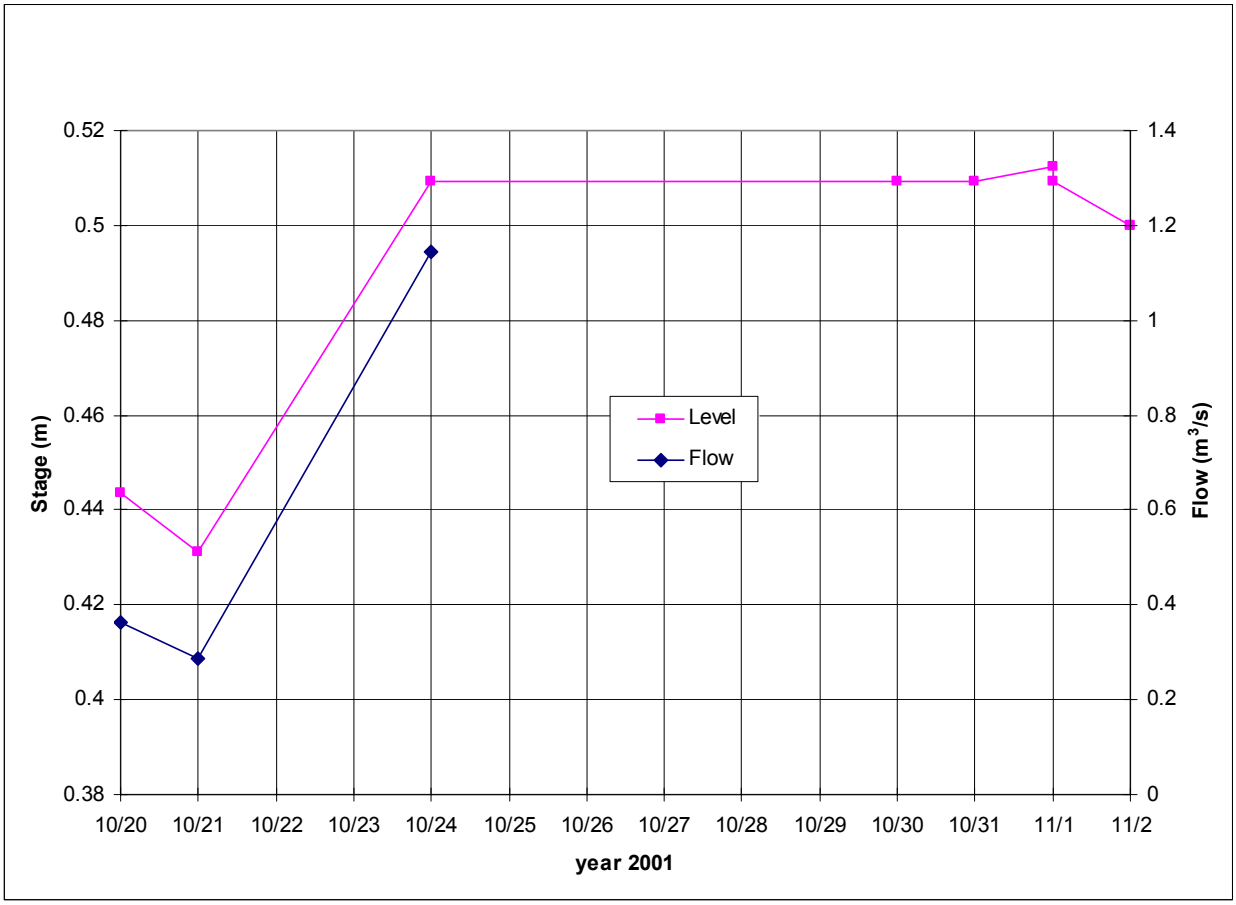

Figure 2-10. Discrete flow and level measurements of the Acushnet River downstream the Saw Mill Dam. Additional level data collected during the salinity survey (30 October – 2 November) are plotted.

Variations in freshwater input may play an important role in the flushing time estimate for an estuary, typically reducing residence time of a contaminant with higher flow rate. To estimate freshwater entering from the Acushnet River, three methods were employed. Method 1 used a regression equation obtained from the discrete three samples of flow (Q) and stage (η) measurements ($Q = -4.6 + 11.3\ \eta$). Method 2 scaled the USGS Paskamanset River flow data (gaging station 01105933) by a factor of 1.87 that was determined from three discrete flow observations and the daily averaged Paskamanset River flow data. Method 3 applied a regression equation (Abdelrhman, 2002).

Figure 2-11 shows Acushnet River flow estimates from the three methods, compared with observed data. Estimates from method 1 and 2 appear similar to the observations, except hat method 2 indicate a larger variation for the period where no observations were taken (22 - 23 October). After 23 October, the two curves diverge. While the estimate from the stage regression (method 1) show a steady flow of 1.1 m^3/s on average, the flow scaled from the Paskamanset River data (method 2) rapidly decreases to 0.46 m^3/s on 1 November. The flow estimate from method 3 is 3 to 12 times smaller than the data, and shows no high flow episode on 23 October. In general, method 3 under-estimates the Acushnet River flow. Therefore, the estimate from method 2 was used in scenarios of the flushing analysis study.

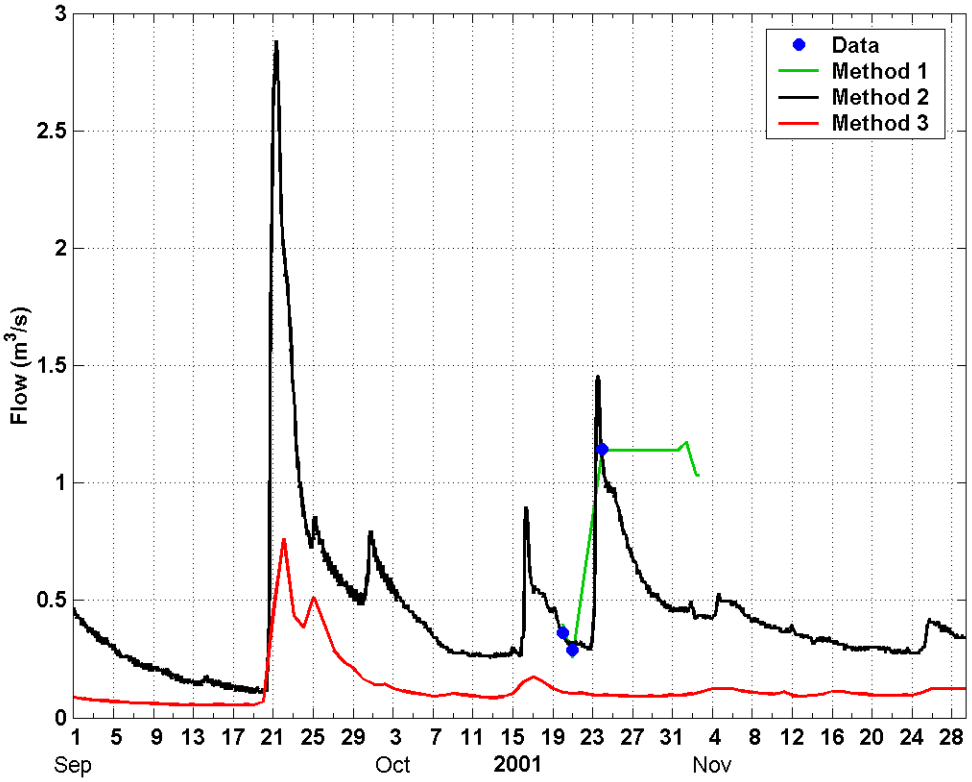

Figure 2-11. Observed and estimated Acushnet River flows from three methods (see text for details).

To validate the scale used to estimate flow in Acushnet River with Paskamanset River flow, a comparison of sub-basin area and surficial characteristics was made. Results implied that the Acushnet River sub-basin (at Saw Mill Dam) is about 72% of the Paskamanset basin (Personal communication with Costa, 2002). This appears inconsistent with the flow differences. However, there are substantial differences in well recharge and impervious areas between the basins. Different ground-flow recharge and discharge rates due to dissimilarity in characteristics of surficial deposits in each basin (USGS, 1995) can also contribute to the difference in flow. This may explain the streamflow differences.

2.4. Hydrodynamic Conditions

The tidal height data from the Coggeshall Street Bridge is shown in Figure 2-12. The tides in the upper estuary primarily varied at semi-diurnal and fortnight cycles. It was observed from the tidal height measurements at the Coggeshall Street Bridge that the tidal height measurements at the Coggeshall Street Bridge indicated that the water elevations were dominated by semi-diurnal tides, with a large variation at a fortnight cycle (Figure 2-12). The tidal range for a spring tide (18 October) was 1.6 m, while the range for neap tides (24 September and 24 October was 0.7 m with a mean range of 1.14 m (Figure 2-12).

A harmonic analysis was performed for the diurnal (Q_1, O_1 and K_1), semi-diurnal (N_2, M_2, L_2 and S_2) and overtide (M_4, M_6 and M_8) constituents. The results (Figure 2-13) showed that the M_2 semi-diurnal tide dominates the elevation with amplitude of 52.3 cm and phase of 230°, followed by the other semi-diurnal constituents (S_2 and N_2) and the M_4 overtide, and the diurnal components (O_1 and K_1). A similar result was observed in power spectrum analysis of the tides (Figure 2-14). The largest peak existed at the semi-diurnal tides, and the secondary peaks were at the overtide M_4 and diurnal components. The governing semi-diurnal tides account for 83% of the total tidal energy.

Currents in the Inner Harbor were not available from the failed BBADCP or from any other source during the field study. Historical observations from a study of the circulation and dispersion in New Bedford Harbor during summer (Geyer and Grant, 1986), showed that the typical peak speed of tidal currents north of Hurricane Barrier was 15 cm/s, flowing mainly in the north-south direction, whereas the peak tidal currents in the Outer Harbor were on the order of 10 cm/s and were oriented northwest-southeast. The current response to wind forcing was significant at the Outer Harbor, but not in the Inner Harbor.

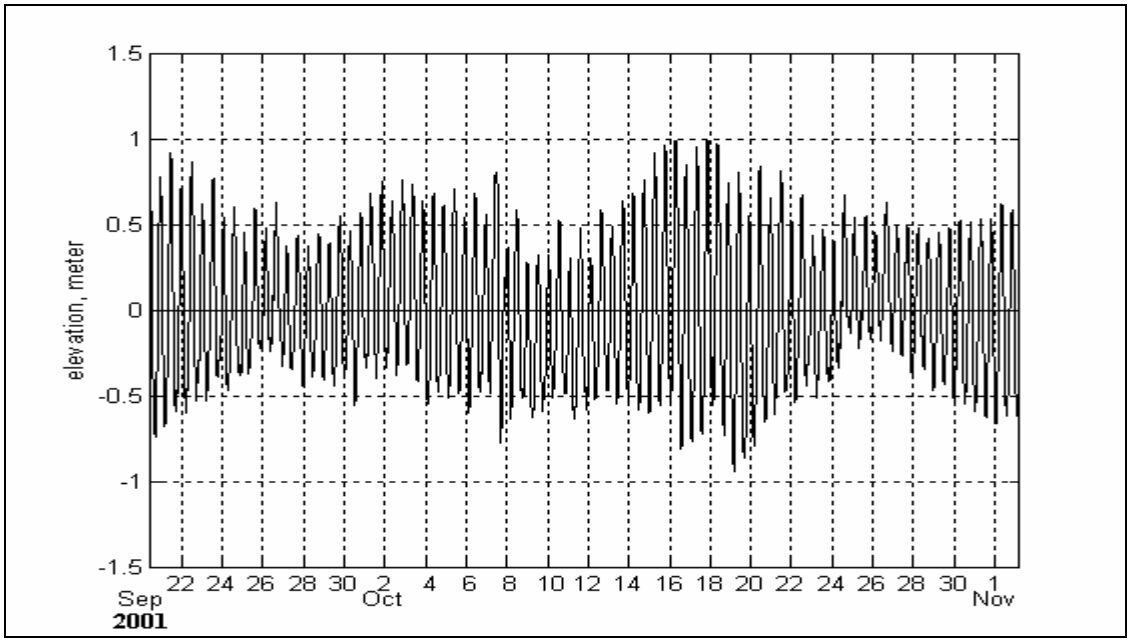

Figure 2-12. Observed tidal heights at the Coggeshall Street Bridge.

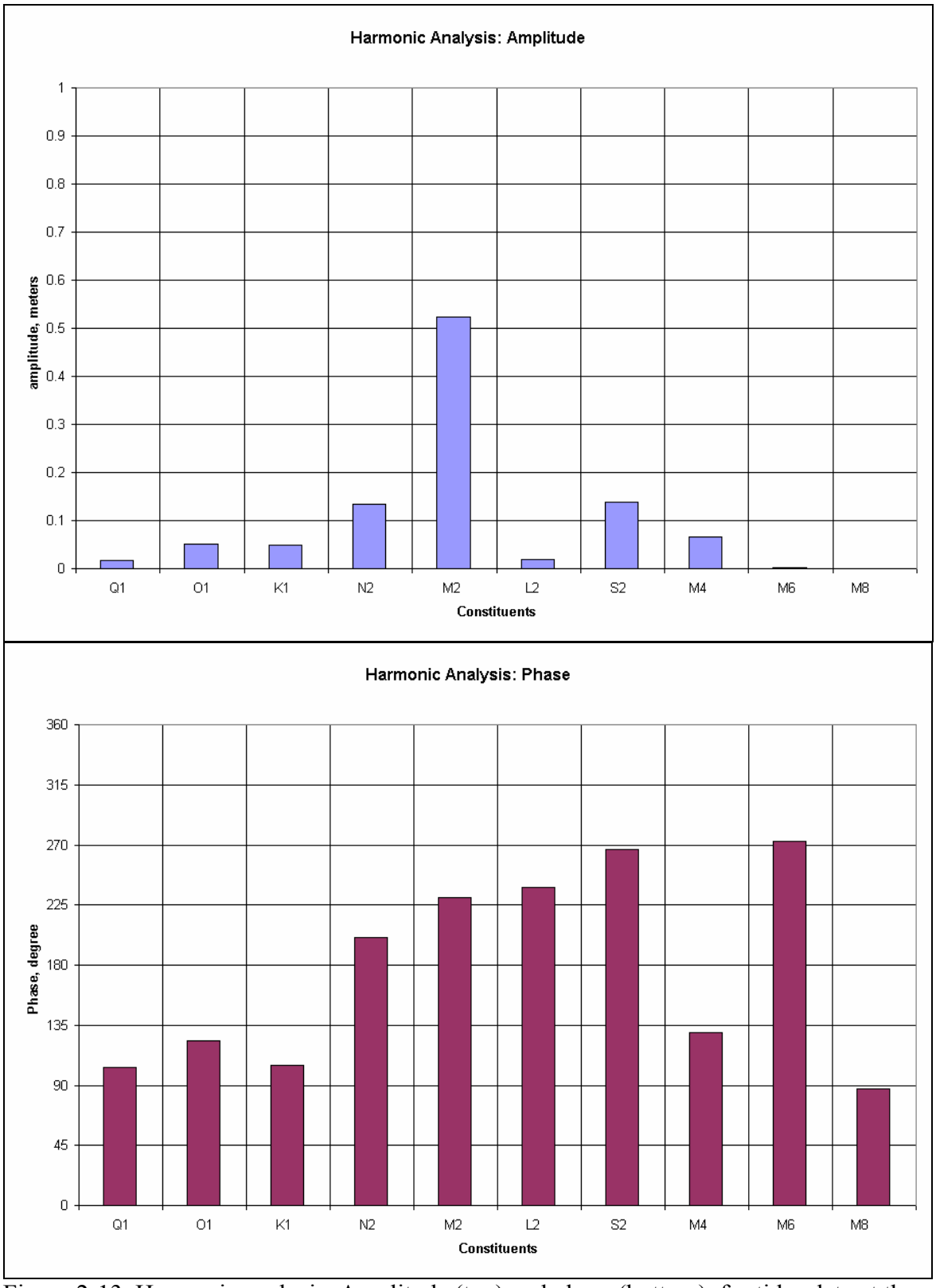

Figure 2-13. Harmonic analysis: Amplitude (top) and phase (bottom), for tides data at the Coggeshall Street Bridge.

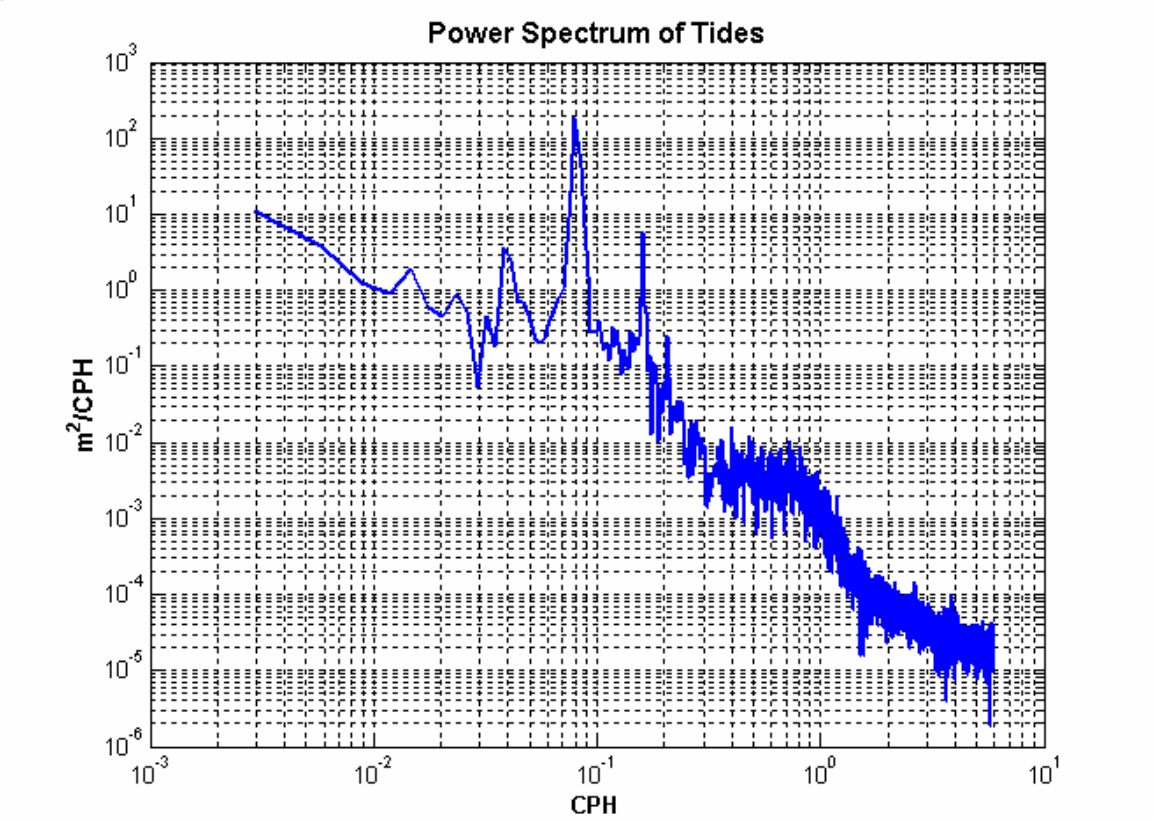

Figure 2-14. Power spectrum density analysis of tides at the Coggeshall Street Bridge.

3. Flushing Time Analysis Using WQMAP

3.1. WQMAP Description

WQMAP (Water Quality Mapping and Analysis Package) is a PC-based system that integrates geographic information (coastlines, land use, watersheds, etc.) and models (analytical and numerical, hydrodynamic, pollutant transport, etc.) to provide the user with a tool to analyze (with a graphical user interface) many alternatives to determine the optimum solution to a particular problem. It has been applied, with different models, as appropriate, to Total Maximum Daily Load (TMDL) analysis of Greenwich Bay, RI; to wastewater treatment facility effluent impacts to Cohasset Harbor, MA; to fecal coliform impacts from combined sewer overflows to the Providence River and upper Narragansett Bay, RI; to flushing estimates for alternative development configurations for Enighed Pond located on St. John, USVI; to circulation and flushing estimates for Nantucket Harbor, MA; and to dredging and disposal operations in Boston, MA, Providence, RI and New Bedford Harbor, MA; among other applications.

The geographic information component of WQMAP holds user-specified layers of data appropriate for the task. Such layers might include shorelines, land use, pollutant point source locations, sampling locations, shell fishing closure areas, habitat maps, etc. Each data layer can be easily input, either directly into WQMAP with a mouse and screen

forms or through import from existing geographic information systems such as ArcInfo. Data can be exported as well. Each layer can be displayed separately or in any combination. Graphics can be generated and sent directly to a printer (color or black and white) or stored for later use in a computer driven slide show.

The modeling component of WQMAP is uniquely versatile with its ability to link one or more of a suite of models of varying complexity into the system. These range from simple analytic calculations of flushing time in a single basin to full three dimensional, time dependent, boundary fitted numerical models of hydrodynamics and water quality. For the Acushnet River estuary flushing study we used a boundary fitted, two- and three-dimensional hydrodynamic model to simulate currents and surface elevation. A pollutant transport calculation used the hydrodynamic model output and estimated the flushing time based on a dye release simulation in the estuary.

3.1.1. Hydrodynamic Model (BFHYDRO)

BFHYDRO, a component of WQMAP, solves the three dimensional, conservation of water mass, momentum, salt and energy equations on a spherical, non-orthogonal, boundary conforming grid system and is applicable for estuarine and coastal areas (Muin, 1993; Muin and Spaulding, 1996, 1997a,b).

The velocities are represented in their contra-variant form. A sigma stretching system is used to map the free surface and bottom to resolve bathymetric variations. The model employs a split mode solution methodology (Madala and Piaseck, 1977). In the exterior (vertically averaged) mode the Helmholtz equation, given in terms of the sea surface elevation, is solved by a semi-implicit algorithm to ease the time step restrictions normally imposed by gravity wave propagation. In the interior (vertical structure) mode the flow is predicted by an explicit finite difference method, except that the vertical diffusion term is treated implicitly. The time step generally remains the same for both exterior and interior modes. Computations are performed on a space staggered grid system in the horizontal and a non-staggered system in the vertical. Time is discretized using a three level scheme. Muin and Spaulding (1996, 1997a) provide a detailed description of the governing equations, numerical solution methodology, and in depth testing against analytic solutions for two and three dimensional flow problems. additional applications are given in Swanson and Mendelsohn (1993, 1996) and Mendelsohn et al. (1995).

3.1.2. Pollutant Transport Model (BFMASS)

There are three separate models within the WQMAP pollutant transport model system. The first is a single constituent transport model, which includes first order reaction terms. This model is suitable for a single constituent contaminant that is conservative, settles, decays, or grows. This model can be used to predict the temporally and spatially varying concentrations associated with treatment of sewage effluent or other constituents (e.g. fecal coliform, residual chlorine, dye). The second is a multi-constituent transport and fate model with a reaction matrix that can be specified by the user. This model can be

used to custom design a multi-component water quality model system (e.g. dissolved oxygen and biochemical oxygen demand). The third is a multi-constituent eutrophication model (e.g. nitrogen, phosphorous, dissolved oxygen), which incorporates EPA WASP5 kinetic rate equations (Ambrose et al., 1994). The user can set the parameters of the rate equations via the user interface or select default values. The suite of models allows the system to be used for a wide range of pollutant transport and fate studies, extending from simple single parameter systems to complex multi-constituent problems with interacting components.

In each model the three-dimensional advective diffusion equation is solved on a boundary conforming grid for each constituent of interest. The model employs the same grid system and obtains the face-centered, contra-variant velocity vector components from the hydrodynamic model. This procedure eliminates the need for aggregation or spatial interpolation of the flows from the hydrodynamic model and assures mass conservation. The transport model is solved using a simple explicit finite difference technique on the boundary conforming grid. The vertical diffusion, however, is represented implicitly to ease the time step restriction caused by the normally small vertical length scale that characterizes many coastal applications. The horizontal diffusion term is solved by a centered-in-space, explicit technique. The solution to the advective diffusion equation has been validated by comparison to one and two-dimensional analytic solutions for a constant plane and line source loads in a uniform flow field and for a constant step function at the upstream boundary. The model has also been tested for salinity intrusion in a channel (Muin, 1993).

3.2. Model Applications to the Acushnet River Estuary

3.2.1. BFHYDRO Application and Calibration

The modeling domain was designed to include New Bedford Inner and Outer Harbor as well as a portion of Buzzards Bay. The model grid was generated using BFGRID to represent the domain, which is a component of WQMAP, and is ideal for an area of complex shoreline like New Bedford Harbor. A total of 3,310 curvilinear, non-orthogonal elements composed the domain (Figure 3-1). Almost half (1,637 cells) of the total cells represented the Inner Harbor covering surface area (3.85×10^6 m^2) of 2.5% of the total domain, in order to capture complex bathymetric and shoreline variations and flow patterns. The rest of cells were used to represent the Outer Harbor, adjacent bay and cove, and a portion of Buzzards Bay. The reason including the area outside the Inner Harbor was to not only facilitate open boundary specifications but also to include the influence of the Bay-wide dynamics in the Inner Harbor. The smallest cell in the domain was 17 m × 18 m and the largest was 820 m × 639 m, located in Clark's Cove.

Source of the shoreline used for modeling was the Massachusetts State GIS data. Figure 3-2 shows the model bathymetry with a depth specified for each cell. Depths were assigned based on the Buzzards Bay project, the BBP web-site http://www.buzzardsbay.org/gisdownload.htm and NOAA National Ocean Service (NOS) data were used together. The former was employed to meet the finely resolved

grids in the Inner Harbor, while the latter was used to specify depths in the area outside the Inner Harbor.

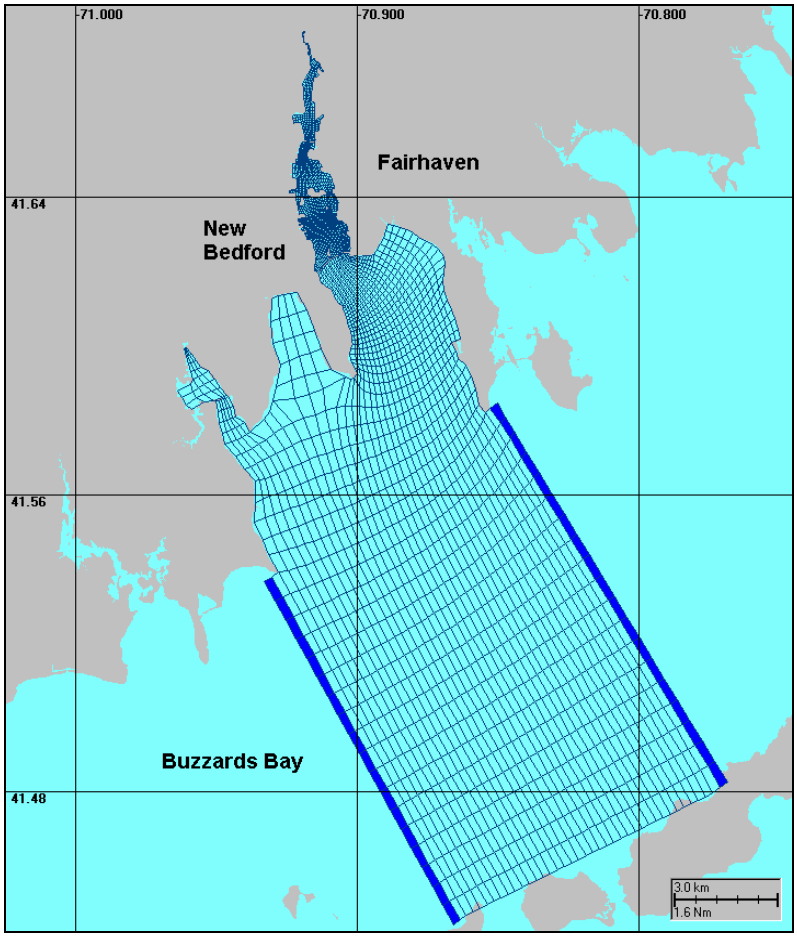

Figure 3-1. Model domain and grids. Cells in dark blue are open boundaries.

There are two major forcings important in driving the circulation in the study area. They are surface elevations and winds. The surface level variations cause the influx and efflux of a significant volume of water on each tidal cycle to the interior. For the Acushnet River estuary model application, two open boundaries (east and west) were specified in Buzzards Bay (Figure 3-1). The first reason to have the boundaries located as far away from the area of interest as possible is to minimize the boundary impact on the interior dynamics. The second reason is to simulate tides, since tides in the Buzzards Bay flow in and out parallel to the Bay axis and their phase and amplitude vary linearly with the axial direction. Since the phase difference over a distance between the head and mouth of the Bay is 0.5 lunar hours, and the amplitude difference is 15 cm (Signell, 1987), we applied 15 min phase lag and 3 cm amplitude difference between the west and east boundaries, which were computed by projecting the maximum phase and amplitude differences onto 9 km distance between the open boundaries.

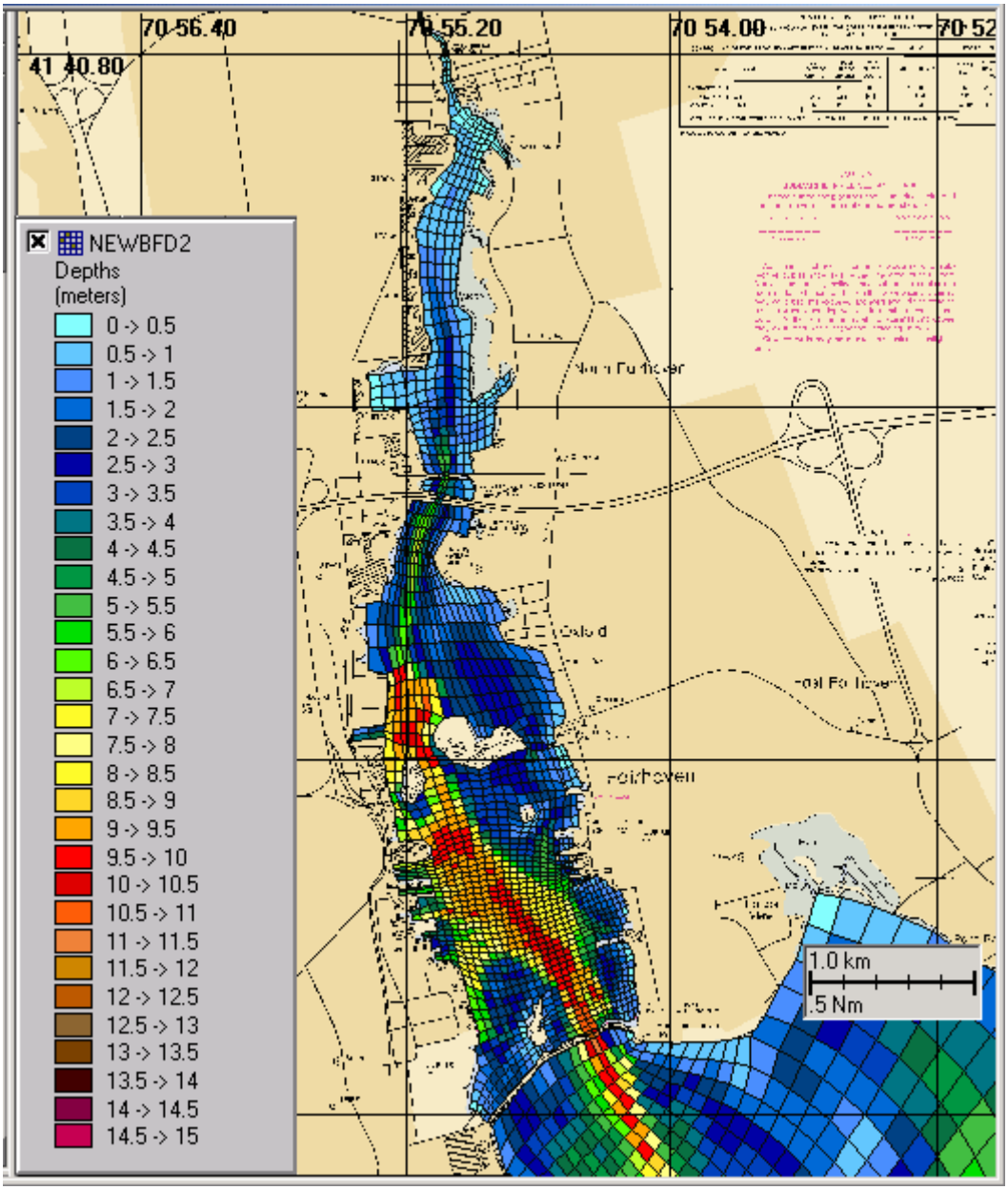

Figure 3-2. Bathymetry (m) in the New Bedford Inner Harbor (the Buzzards Bay Project).

Wind forcing induces a shear stress on the water surface causing it to move in the general direction of the wind, and transfer energy to the water column. Also the wind energy causes mixing in the upper layers that tends to reduce vertical gradients of density. For the Acushnet River estuary application, hourly wind observations at New Bedford Municipal Airport were applied at the sea surface. Figure 3-3 shows the winds during October 2002. The monthly mean speed was 3.6 m/s, blowing from the southwest. The wind stress friction and bottom friction used were quadratic and their coefficients were 0.0014 and 0.001, respectively.

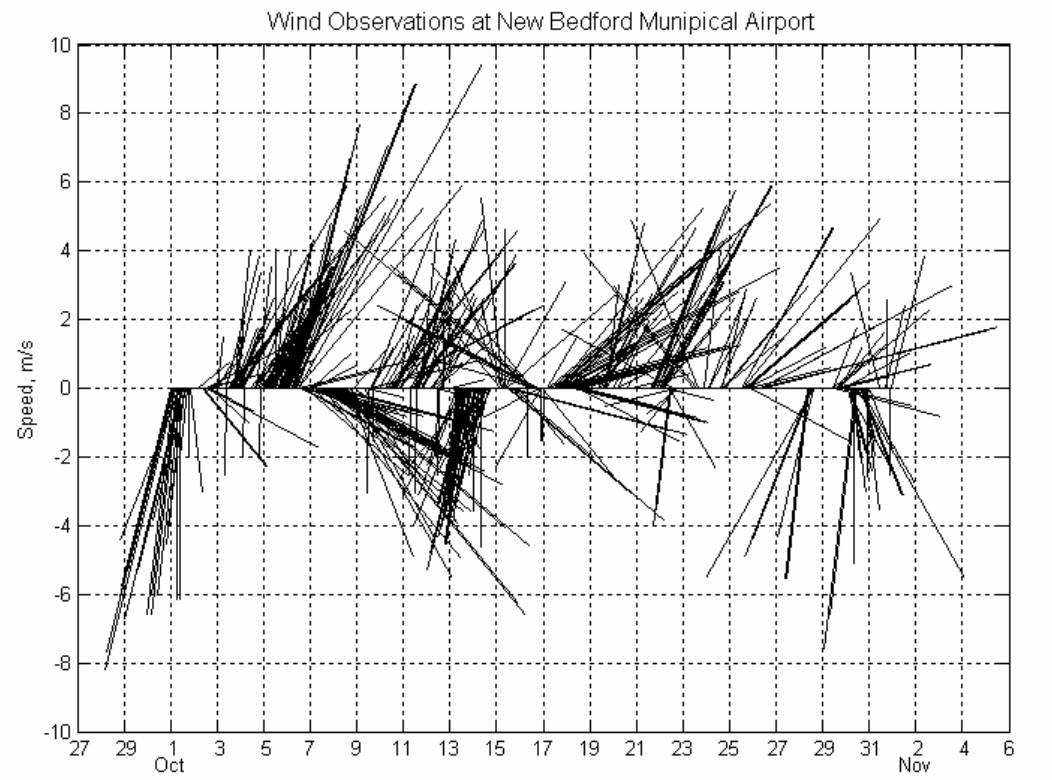

Figure 3-3. Wind data collected at the New Bedford Municipal Airport.

For calibration of hydrodynamic model, a simulation period was chosen from 1 October to 2 November, the same period as the tide observations available in the Inner Harbor. The 3-layer, 3-dimensional model was used for the simulation. The model was forced by tides at the open boundary and by wind forcing uniformly at the surface. The tidal forcing data were generated from a composite of 16 tidal constituents (Table 3-1) by an iteration process to minimize the difference between the Tides and Currents prediction and the model simulation at Dumpling Rocks. Figure 3-4 shows the time series. Predicted mean range is 0.6 m, with a tidal range of 1.8 m during spring tides and 0.5 m during neap tides.

Calibration of tidal elevations was performed using time series data obtained from the tide gauge located south of the Coggeshall Street Bridge. Figure 3-5a shows observed (light line) and predicted (dark line) tides at the Coggeshall Street Bridge. The predicted tidal heights are the results of simulations without wind forcing. Differences between the data and predictions are quite small. These discrepancies are probably due to forcing other than tides. This is evident in Figure 3-5b that presents a comparison of time series of model prediction to the tidal composite time series. Mean difference between the harmonically extracted observation and simulation is –0.002 m, the standard error is 0.1 m and the square of correlation coefficient (r^2) is 0.97.

Therefore, the difference found in the periods 7-11 October, 16-19 October and 23-27 October (Figure 3-5a), which almost disappears in Figure 3-5b, might be caused by non-

Table 3-1. Tidal constituents amplitudes and phases used for a composite of tides.

Constituent	Amplitude, m	Phase, °
MM	0.003	352.81
MSF	0.004	105.42
Q1	0.014	111.45
O1	0.052	128.88
K1	0.059	91.90
J1	0.004	81.32
NO1	0.004	78.81
MU2	0.022	245.10
ETa2	0.002	305.49
N2	0.121	193.78
M2	0.554	216.29
L2	0.012	190.12
S2	0.160	222.58
M4	0.060	111.36
M8	0.001	233.77

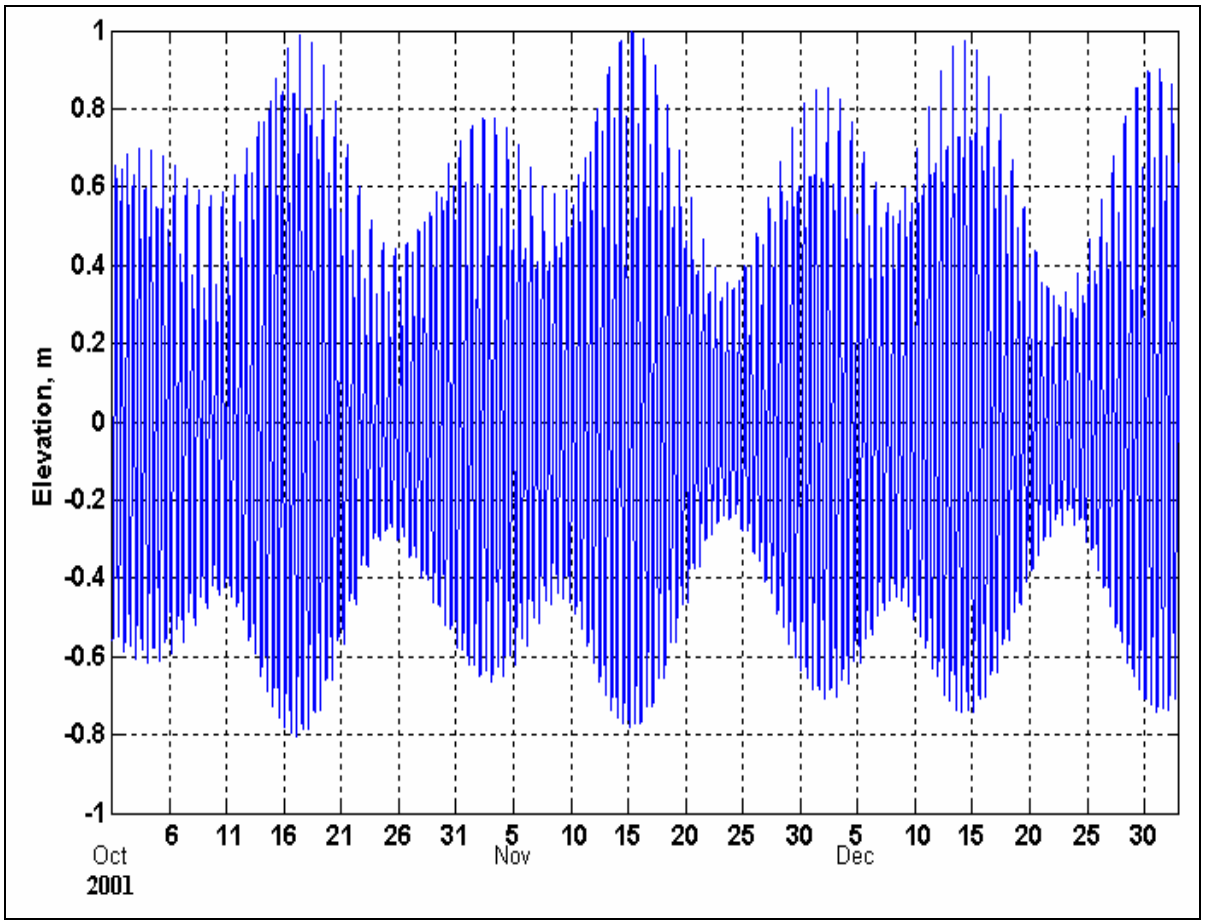

Figure 3-4. Time series of composite tidal height used as forcing at the open boundary.

tidal forcing. For instance, there were two storms during the last half of October, which explain the latter two periods. It is unknown what may have caused the difference during the first period.

Because the BBADCP instrument moored to measure currents in the Inner Harbor failed, a quantitative calibration of the model predicted velocity was not possible. Instead the calibration was performed using the statistics from historical data collected in the Inner and Outer Harbor. Simulated currents north of Hurricane Barrier (41°37.6'N, 70°54.4'W) and south of the Barrier, at Butlers Flats (41°36.3'N, 70°53.6'W) are shown in Figure 3-6 and 3-7, respectively. Also shown are the currents predicted with wind forcing (black thin line). The currents in the Inner Harbor (Figure 3-6) are primarily the N-S direction, with a variation of peak speed between 8 and 18 cm/s and typical peak speed of 15 cm/s, whereas the typical peak speed of the currents in the Outer Harbor (Figure 3-7) is on the order of 10 cm/s, flowing northwest-southeast. These values are very close to the observations collected for the period of 17 July – 14 august 1986 (Geyer and Grant, 1986). Typical peak speeds observed during 1986 were 15 cm/s and 10 cm/s north of Hurricane Barrier and Butlers Flats, respectively.

(a)

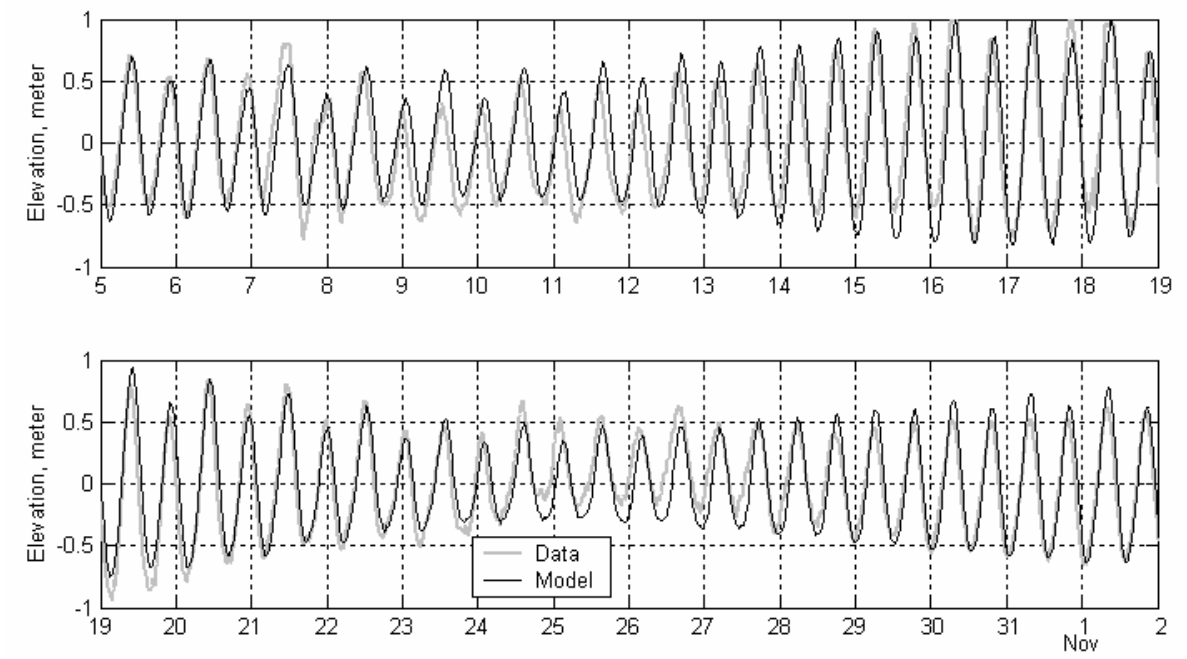

(b)

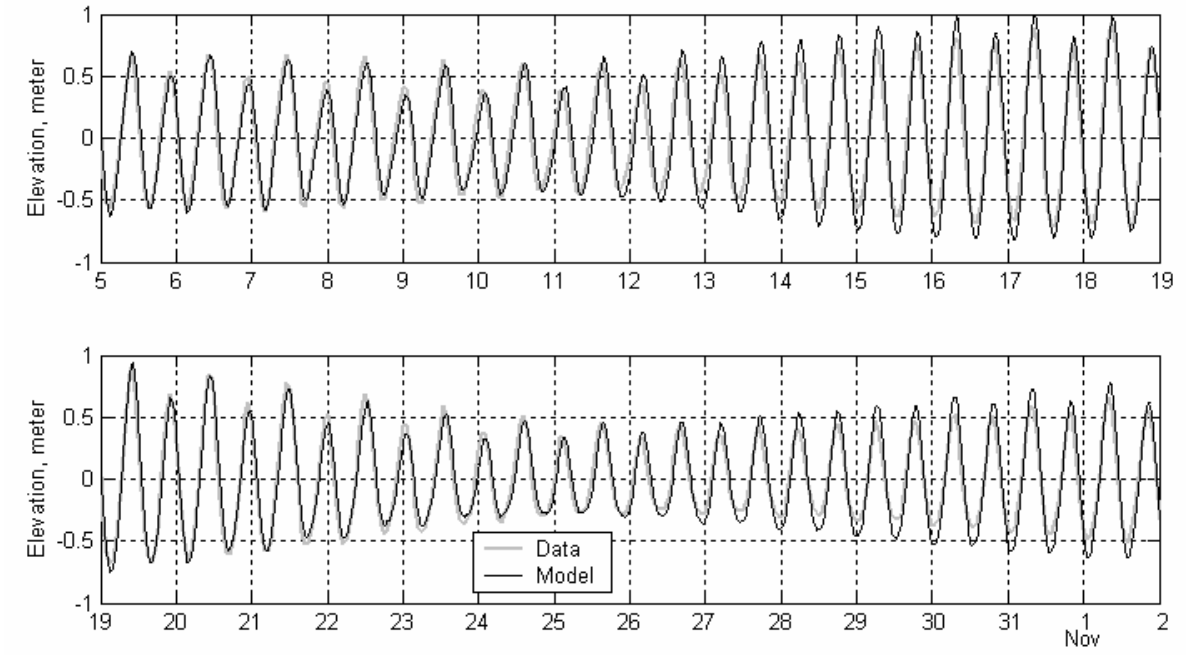

Figure 3-5. A comparison of tidal heights at the Coggeshall Street Bridge between the BFHYDRO prediction and the observations (a), and between the prediction and harmonically composite data (b).

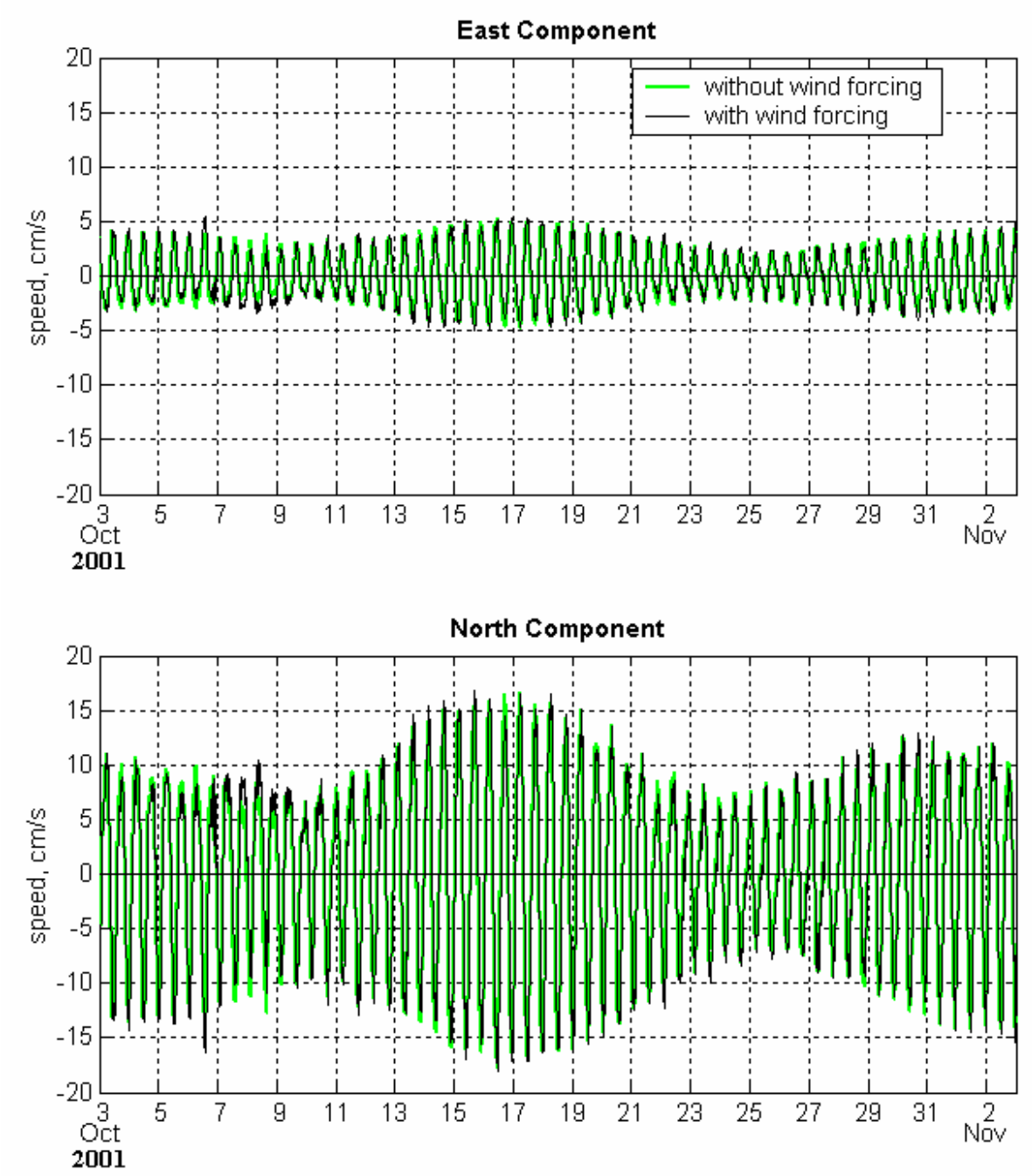

Figure 3-6. Simulated Currents north of Hurricane Barrier, (41°37.6'N, 70°54.4'W) without (green line) and with wind forcing (black thin line).

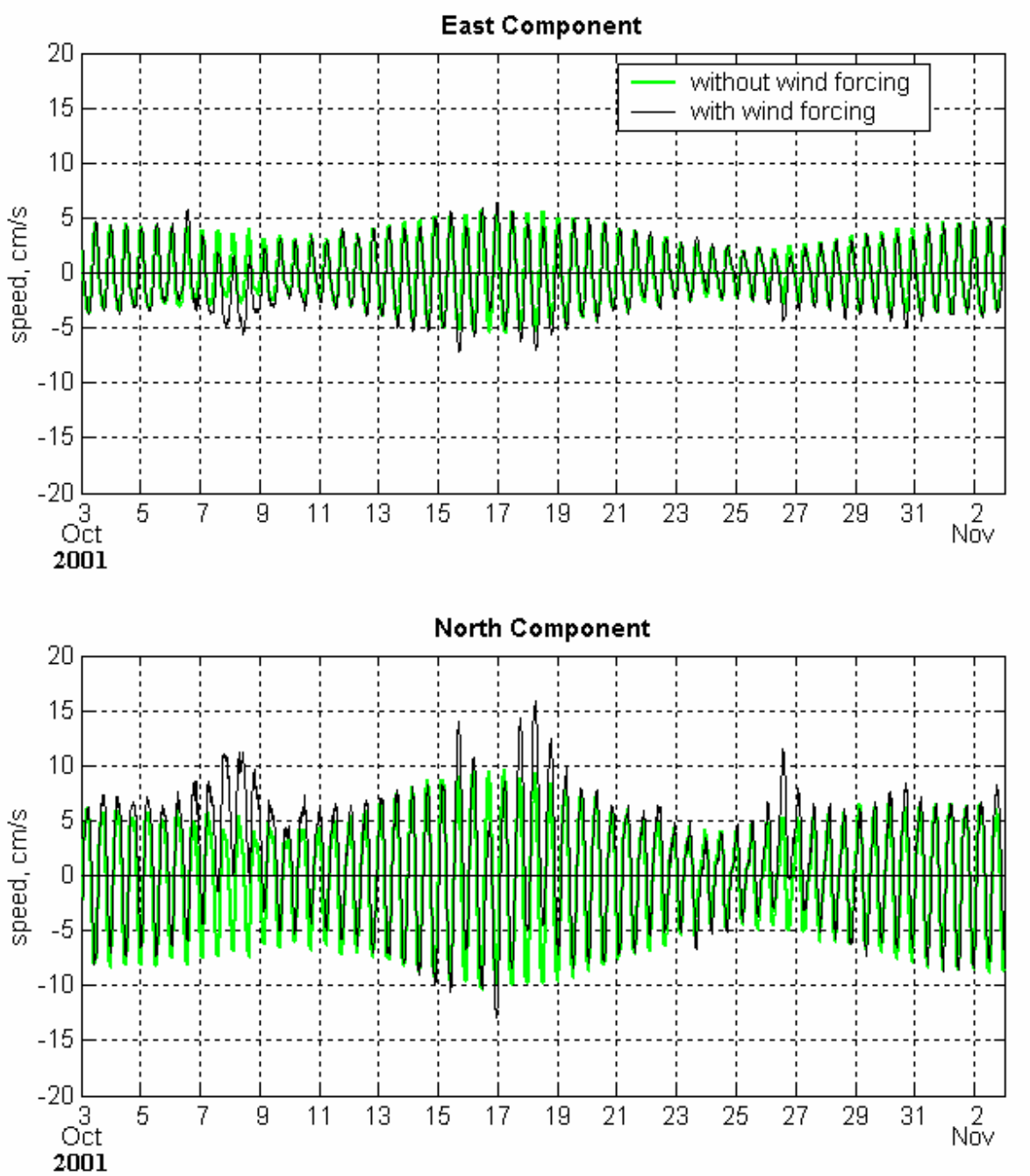

Figure 3-7. Simulated Currents at Bulters Flats, (41°36.3'N, 70°53.6'W) without (green line) and with wind forcing (black thin line).

3.2.2. BFMASS Application and Calibration

A common application of the BFMASS model is the simulation of the fate and transport of a pollutant discharged from either a point or non-point source. Employment of the model for the work further extends to predict residence time of the waste matter or flushing time for either a portion or the entire estuary.

Regardless of types of simulations, input parameters required for the BFMASS modeling are source strength, dispersion coefficient, settling velocity and decay rate, if appropriate. Settling velocity acts as a mechanism to transport the constituent from the water column to the bottom, whereas decay rate acts as a sink term to remove the constituent from the system. The source strength is the amount of material entering the system on a special rate. Types of the source strength specification for the BFMASS mode are an instantaneous release to the water column, a constant release over time, or a variable release over time. Multiple locations can be also simulated at the same time. An instantaneous source is the amount of material released to the water column over a second. The constant source, or continuous release, is defined as the mean loading to the water column over time. A variable source is the time varying load to the water column.

In this section, we set up the BFMASS model to simulate the dye release study conducted in the lower Acushnet River estuary. The goal of the application is to determine residence time of dye that represents the wastewater discharged from the Fairhaven WWTP. A 3-layer 3-D model was employed for the work. The scenario specifications replicated the dye study. Since dye used for the study was in dissolved form and a conservative tracer, no settling velocity and decay rate were applied. The source strength was a continuous release at a rate of 21 mg/s for a 5-day period from 9:00AM 18 October until 9:00 AM 23 October.

Actual dye injection occurred at the Fairhaven WWTP, and the dye was discharged at the outfall located in the lower estuary, 2.8 km (1.7 mile) southwest of the treatment facility. For modeling purposes the dye was released at the outfall represented by a cell of 35 m × 36 m ×0.8 m (depth) dimension. A linear decrease in the source strength was considered in order to simulate the travel time of dye along the pipe after the termination at the plant.

Observations during the dye surveys suggested that the dye quickly rose to the surface after the release from the diffuser at the sea bottom. Therefore the measurements were taken at the water surface. It was also found that the dye reached the surface immediately spread out forming a highly localized plume near the outfall. The dye distribution in the far field, however, was not well organized as in the near field. This is evident in Figures 2-8 and 2-9 showing substantial spatial variations.

Prior to the residence time simulation or flushing time simulation, calibration of the BFMASS model was conducted to select model coefficients to best match experimental data. The calibration should be based on two principles (McCutcheon et al., 1990): the simplest model formulation should be used to solve the problem at hand, and the model coefficients and parameters should be uniform in space and time unless there is strong evidence in the experimental data that they should change.

The primary focus of the calibration process is to adjust appropriate model parameters to optimize the comparison to an observation data set. For the dye simulation study, parameters of concern are horizontal and vertical dispersion coefficients. The calibration procedure McCutcheon et al. (1990) is adapted for the Acushnet River estuary application in order to reproduce observed dye field by adjusting the parameter values.

The goodness measure of the calibration was determined by the relative mean error, defined as follows:

$$rme = \frac{\left|\bar{x} - \bar{c}\right|}{\bar{x}},$$

where $\bar{x}$ is the mean of the observed dye concentration values and $\bar{c}$ is the mean of the model-predicted or calculated values.

In the calibration simulations, dye was released at the surface layer at the outfall cell. A combination of seven vertical dispersion coefficients and four horizontal diffusion coefficients were applied. The values for vertical dispersion coefficient are from 1×10^{-1} to 1×10^{-7} m^2/s with 1-order of magnitude intervals, and the horizontal dispersion coefficient values are 0.02, 0.2, 2, and 2.5 m^2/s. Since there were no stations to monitor the dye concentration continuously, we conveniently choose six sites located along a 75-m perimeter from the outfall (Figure 3-8). We used dye concentration observed at these locations for a comparison of the concentrations between observations and simulations.

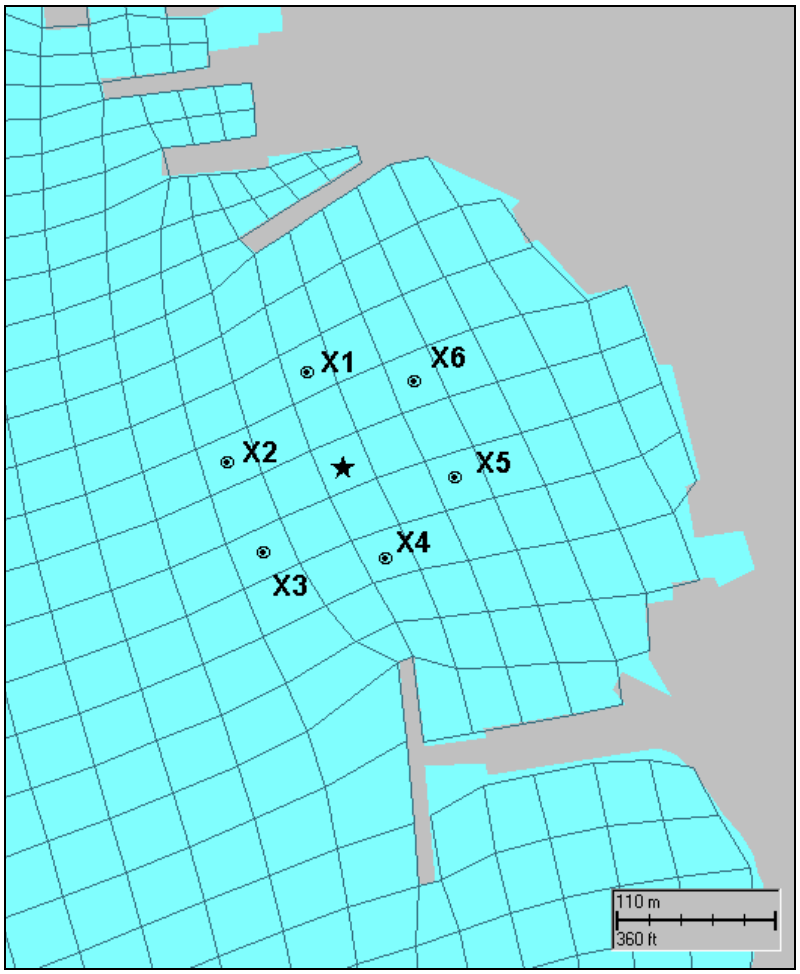

Figure 3-8 The Fairhaven WWTP discharge outfall (star) and six sites about 70 m from the outfall for the dye concentration monitoring.

Figure 3-9 shows the dye concentration comparisons between observations and simulations, for example. The predicted values were found at X1, X3, X4 and X5 at the times when the survey took place in an area within a 20-m radius from each site, which is a half of the average length of a cell representing the site.

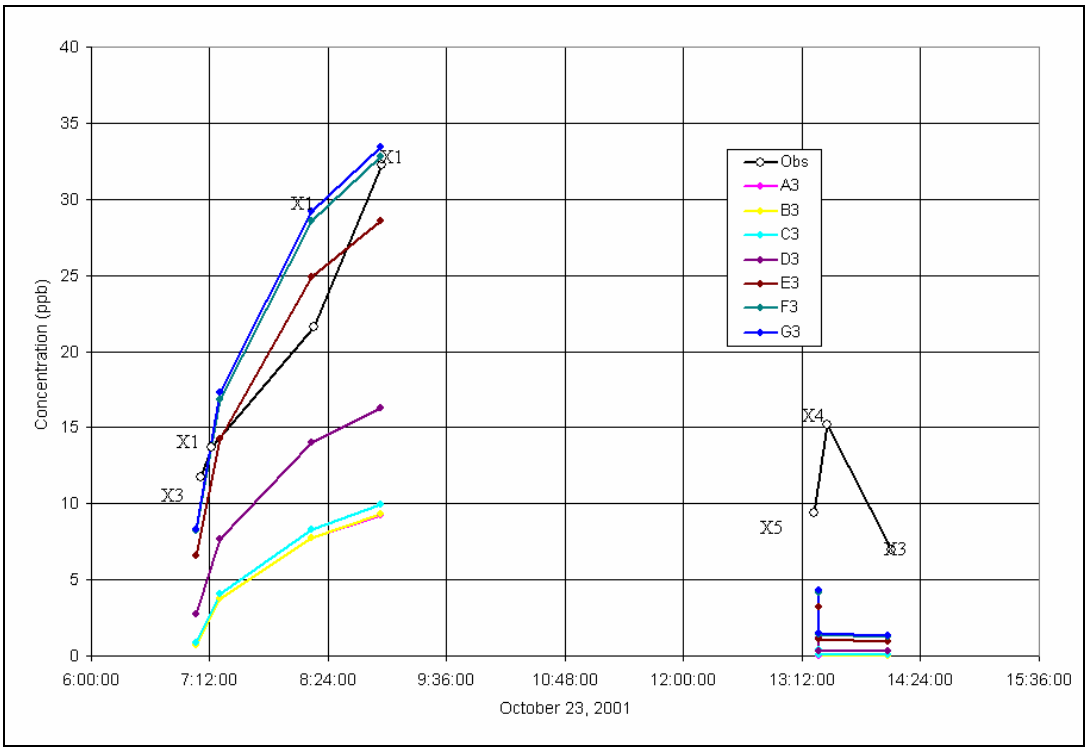

Figure 3-9 Observation vs. simulation of dye concentrations at locations along the 75-m perimeter from the discharge location. The predicted values are from simulations using 0.02 m^2/s horizontal dispersion coefficient but different vertical dispersion coefficients (color-coded): A3= 1×10^{-1}, B3=1×10^{-2}, C3= 1×10^{-3}, D3=1×10^{-4}, E3=1×10^{-5}, F3=1×10^{-6}, G3=1×10^{-7} m^2/s.

Figure 3-9 shows that although there exists relatively large difference between the simulations and observations for a period after the termination of dye pumping, overall variation of the simulated concentrations is similar to the observation, especially for the simulations using two lowest vertical dispersion coefficients (F3 and G3). The relative mean errors were computed for all the calibration simulations (Table 3-2), including the simulations shown in Figure 3-9. Table 3-2 suggests that the simulation G3 is the best, showing the lowest error of 0.14 ppb. Also shown in the table is that the larger value of vertical dispersion coefficient produces the larger error, while the smaller horizontal dispersion coefficient yields the smaller error.

Although the simulation G3 shows the lowest error, relatively large difference in dye concentration between observations and simulations still exists (see Figure 3-9). This is firstly due to sub-grid scale variations in the observation. The variation is more apparent in a time series plot (Figure 3-10), showing that the concentration can be as large as twice

Table 3-2. Relative mean errors for calibration simulations from seven vertical dispersion coefficients (column) and four horizontal dispersion coefficients (row). Units are ppb.

	1×10^{-1} m^2/s	1×10^{-2} m^2/s	1×10^{-3} m^2/s	1×10^{-4} m^2/s	1×10^{-5} m^2/s	1×10^{-6} m^2/s	1×10^{-7} m^2/s
2.5 m^2/s	0.934	0.933	0.920	0.867	0.753	0.664	0.647
2 m^2/s	0.926	0.925	0.912	0.853	0.726	0.629	0.611
0.2 m^2/s	0.865	0.864	0.849	0.720	0.479	0.361	0.339
0.02 m^2/s	0.804	0.802	0.786	0.617	0.283	0.159	0.140

over a distance equivalent to a one-cell size. The second reason is that the time of prediction does not always coincide with the observation time, neither do the survey track with the sites along the perimeter. These are shown with the open circle (simulation) and red dots (observation) in Figure 3-10.

Given the fact that the disagreement can always exist due to either the sub-grid scale variations or mismatch of time or locale, a combination of 1×10^{-7} m^2/s of vertical and 0.02 m^2/s of horizontal dispersion coefficients simulates the dye field as close as the observations, by showing the smallest rme value.

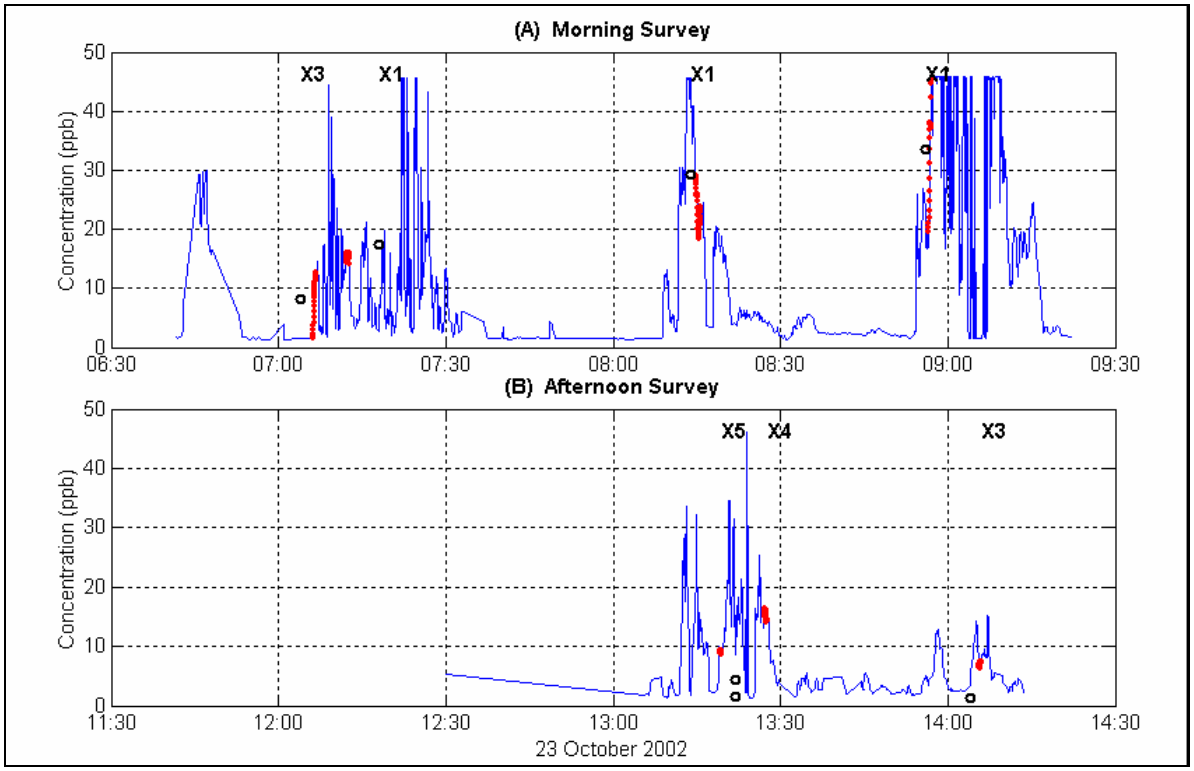

Figure 3-10. Time records of observed dye concentrations for the morning survey and afternoon survey (see Figures 2-8 to 2-10). Superimposed are the simulated concentrations at sites along the 75-m perimeter (open circle) and the observed concentrations (red dots) found within a 17-m radius centered each site.

4. Flushing analysis

The New Bedford Inner Harbor is a unique estuary where the water exchanges with the Outer Harbor only through the Hurricane Barrier opening (85 m wide [279 ft] and 13 m [43 ft] deep). Typical tidal currents in the opening are on the order of 30 cm/s (0.58 kt) for either flood or ebb, which is about three times larger than the speed inside. The peak total water volume transporting through the opening is approximately 330 m^3/s (11,654 ft^3/s). This flux is about 720 times larger than the average of the Acushnet River flow at the head of the estuary.

In the section, we present flushing time analysis for the Acushnet River estuary. Three independent approaches are employed to assess flushing time for the Acushnet River estuary. First is a freshwater exchange ratio method (Mills et al., 1985). This method requires segmentation of the estuary into a number of sections with salinity and mean-tidal volume specified for each section. Second is a modified tidal prism approach (Ketchum, 1951). This method assumes a steady state distribution of fresh and saline water in the estuary and uses sub-tidal and inter-tidal volume estimates as function of upstream distance from the estuary mouth. The last method employed is numerical simulations using the BFMASS model, a component of ASA's WQMAP model system. The simulation uses dispersion parameters determined from calibration using dye concentration data.

There are three terms commonly used to represent hydraulic turnover time (Costa et al., 1999), and they are turnover time, residence time and flushing time. The "flushing time" is defined as the length of time that is necessary to replace the freshwater contained within an estuary. Turnover time is the length of time that it takes for tidal flushing to remove 64% ($1-e^{-1}$) of marine water. Residence time is defined as the average time of a particle residing within the system. Turnover time and residence time, according to Costa et al (1999), yield very similar value, and they are approximately equivalent at equilibrium conditions.

The flushing time commonly used throughout the work is more generic term representing hydraulic turnover time and not the "flushing time" defined in Costa et al (1999). This section documents results of the flushing analysis using three separate methods together with sensitivity analysis, followed by comparisons of flushing time estimated using local/system residence time method (ACI, 1995) and from previous dye study conducted in the estuary in 1986 (ASA, 1987).

4.1. Freshwater Ratio

The freshwater fraction method involves five steps (Mills et al., 1985). They are:

1) Divide the estuary into segments and determine the mean volume and salinity of each segment. For the Acushnet River estuary application, twenty-two segments (n=22) were specified (Figure 2-3).

2) Calculate the fraction of fresh water (f_i) in each segment using the formula:

$$f_i = (S_o - S_i) / S_o, \quad (1)$$

where S_i and S_o are the mean salinity of the i^{th} segment and salinity at the open boundary, respectively.

For the Acushnet River estuary application, S_o was chosen to be the maximum salinity observation during the salinity survey, S_o=31.91 ppt, and S_i was determined with mean measurements collected in each segment. Figure 4-1 shows the S_i for 1 and 2 November. The values representing the A1A and A1B segments were the mean salinities computed by combining the measurements from the two sampling locations, because the water at the northern station was not deep enough during low tide to collect the measurement. The B6 and B7 segments were combined due to their lateral alignment.

The salinity in the upper estuary varies substantially over a 1.5 km distance (Figure 4-1), which means the finer segment is necessary to provide a better result. Hence we utilized the 7 sampling stations (A1A-B, A2A, A2B, A3A, A3B, A4A and A4B) in the area rather than the predefined four segments (A1 – A4).

3) Compute the fresh water volume in each segment, W_i, using the following formula:

$$W_i = V_i \times f_i, \quad (2)$$

where V_i is the mean tide volume of the segment.

4) Determine the exchange time for each segment, T_i, as follows:

$$T_i = W_i / R_i, \quad (3)$$

where R_i is the mean freshwater input for the i^{th} segment, measured over a tidal cycle, and it includes river flow, precipitation, ground-water discharge and combined sewage outfall (CSO) discharge.

Besides the Acushnet River flow, the estuary system has an additional point source of freshwater, which is the effluent of wastewater from the Fairhaven WWTP. The average of flow is 1.77 MGD (0.077 m^3/s) and 1.80 MGD (0.079 m^3/s) for 1 and 2 November, respectively. Since the discharge outfall is located at segment C4, the freshwater input will be added to that segment.

The freshwater volumes and sources are listed in Table 4-1. The river flow values were estimated from discrete measurements collected during the field survey (Section 2) by prorating the daily mean estimates of USGS Paskamanset River streamflow by multiplying by 1.87. The WWTP discharge averages 17% of the river discharge.

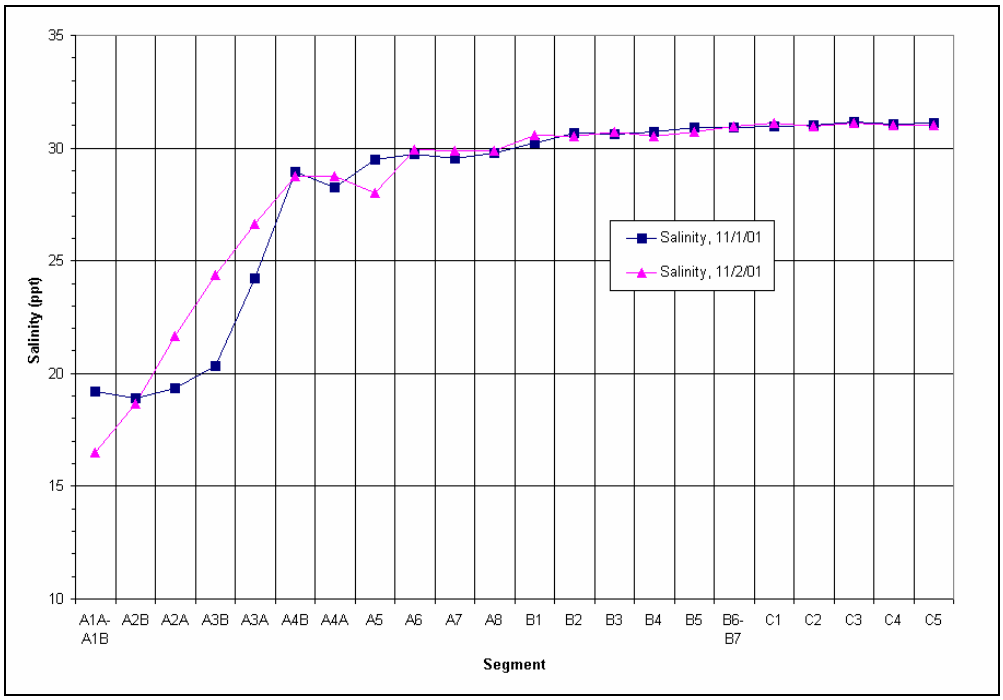

Figure 4-1. Mean salinity (ppt) over a tidal cycle for each segment on 1 and 2 November 2001.

Table 4-1. Freshwater sources and volume over a tidal cycle entering the Acushnet River estuary during the salinity survey.

Date	Freshwater Volume (m^3)	
	River	Fairhaven WWTP Outfall
1 Nov 01	20,567	3,448
2 Nov 01	21,015	3,527

5) Compute the flushing time for the entire estuary, T_f, by summing the exchange times for the individual segments:

$$T_f = \sum_{i=1}^{n} T_{i,} \qquad (4)$$

where n is the number of segments.

4.1.1. Results and Sensitivity analysis

Using the 1 November hydrologic condition, estimated flushing time for the Acushnet River estuary from the freshwater ratio method is 15.6 days. This means that if the estuary condition were persistently the same as the 1 November condition over a turnover period, it would take 15.6 days to flush the freshwater completely out of the estuary.

Table 4-2 shows the turnover time for the entire estuary as well as the individual segment, including freshwater fraction f_i and the freshwater volume W_i. It is noticed that the segment exchange time T_i generally increases with distance downstream direction.

This is because the T_i is determined primarily by the W_i, which is in turn caused by the mean volume V_i.

If hydrologic condition of the estuary changes to the 2 November condition, the flushing time decreases to 15.5 days (by less than 1%) due to the 2% higher volume from the freshwater sources than those of the previous day.

On 1 and 2 November, there was no precipitation in the study area. Historical records (Howes and Geohringer, 1996) indicated that the average rainfall for a month of November is on the order of 9 cm, equivalent to the 6,160 m^3 freshwater over a tidal cycle. If we consider the climatological rainfall, the flushing time estimate decreases to 15.4 days for the 1 November condition and 15.2 days for the 2 November condition.

Table 4-2. Flushing time for the Acushnet River estuary on 1 November 2001.

Segment #	Stations	S_i (ppt)	V_i (m^3)	f_i	W_i (m^3)	T_i (day)
0	A1A-A1B	19.22	46,378.36	0.398	18,441.73	0.46
1	A2A	18.92	100,697.38	0.407	41,000.72	1.03
2	A2B	19.37	69,614.02	0.393	27,350.71	0.69
3	A3A	20.32	45,276.07	0.363	16,442.10	0.41
4	A3B	24.22	134,542.89	0.241	32,431.45	0.82
5	A4A	28.95	114,001.68	0.093	10,559.39	0.25
6	A4B	28.25	104,676.98	0.115	11,998.28	0.33
7	A5	29.48	288,953.15	0.076	22,014.48	0.55
8	A6	29.73	257,138.50	0.068	17,550.87	0.44
9	A7	29.56	148,581.43	0.074	10,957.21	0.28
10	A8	29.80	80,025.58	0.066	5,292.40	0.13
11	B1	30.25	175,032.86	0.052	9,109.03	0.23
12	B2	30.67	242,768.59	0.039	9,447.84	0.23
13	B3	30.63	393,513.70	0.040	15,745.39	0.40
14	B4	30.73	764,572.49	0.037	28,322.00	0.71
15	B5	30.90	1,462,179.81	0.032	46,086.78	1.16
16	B6-B7	30.93	1,424,169.03	0.031	43,960.87	1.11
17	C1	30.96	1,698,271.33	0.030	50,711.70	1.28
18	C2	31.01	2,082,860.78	0.028	58,655.03	1.48
19	C3	31.16	2,048,000.92	0.024	48,365.35	1.22
20	C4	31.06	2,740,737.58	0.027	72,975.99	1.57
21	C5	31.13	1,579,623.08	0.025	38,708.47	0.83
			Total Flushing Time = 15.6 day			

Besides river flow and wastewater effluent, parameters governing the flushing time estimate are open boundary salinity, combined sewage outfall (CSO), precipitation, and ground water. Since the CSO discharge, for instance, contributes the freshwater similar to precipitation as non-point source, the freshwater parameter for the sensitivity test is therefore applied as point and non-point source. Non-point sources include the CSO

discharge, precipitation and ground water, while point sources are river flow, the WWTP effluent discharge and ground water.

The ground water freshwater budget can be point or non-point source. The ground water discharge at the upper estuary can be considered as a point source, whereas the discharge from the watershed in the lower estuary can be served as non-point source, the same as the CSO. Both the CSO and ground-water discharge are more evident during rainfall (Costa, 2000; USGS, 995), because they are recharged by a portion of the precipitation and flow into the estuary through drainages, and seepages or streams.

The CSOs in the Acushnet River estuary are primarily located in the lower part of the Acushnet River watershed. According to Costa (2000), the annual CSO flows into the Inner Harbor for dry weather is negligible but the total discharge for wet weather is 353 MG. This equals 0.04 m^3/s (1,895 m^3/tidal cycle), and is only 0.01% of the embayment volume and approximately one half the WWTP discharge. Since the CSO serves as a non-point source similar to precipitation, the CSO is treated as precipitation for the sensitivity test. The combined freshwater volume from both the CSO and the climatological rainfall is 8,055 m^3/tidal cycle and it is still small compared to the river freshwater budget or the estuary volume.

Figure 4-2 presents the results of model sensitivity to point and non-point sources and open boundary salinity S_o. Values in the x- and y-axis are normalized to the parameters used to estimate the flushing time for 1 November. The result is that the most sensitive parameter is S_o and the least is non-point source. When the S_o changes by a factor between 0.98 (31.27 ppt) and 1.04 (33.19 ppt), range in flushing time varies between 0.5 and 1.9 times of the base time 15.6 days (8.0 to 29.9 days). However, increase in non-point source budget (precipitation) by a factor of 1.5 (from 6,160 m^3 to 9,240 m^3) results in only 1% decrease from the base-line flushing time l5.4 days (15.25 days).

During the river flow survey, 21 October was dry and 24 October was wet. The flow measurements were 0.29 m^3/s (12,945 m^3/tidal cycle) on 21 October and 1.14 m^3/s (50,890 m^3/s) on 24 October, which are 0.64 and 2.5 times of the flow on 1 November, respectively. If we apply the dry and wet river flows to the salinity distribution on 1 November, flushing time increases to 24.5 days and decreases to 6.4 days, respectively. This assumption violates the steady state criteria for this method, because it requires time for salinity in the system to reach steady state.

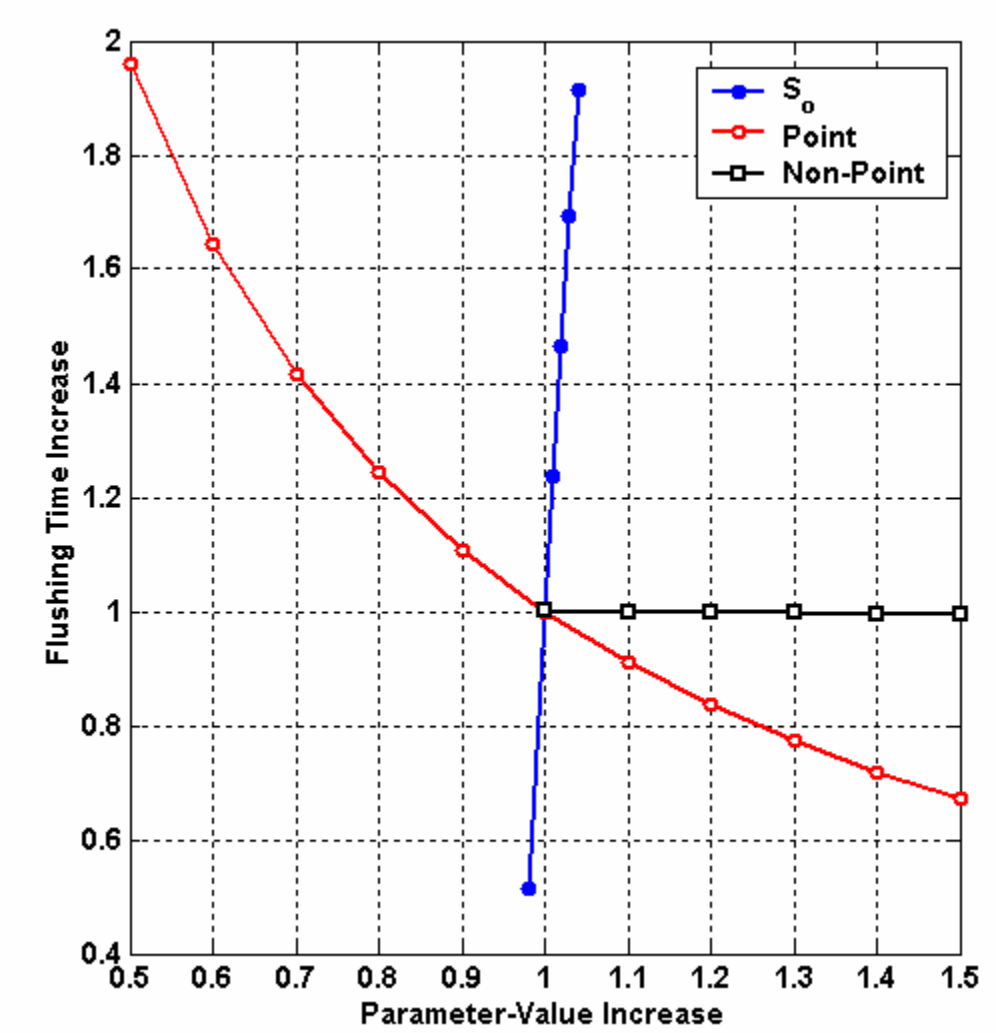

Figure 4-2. Sensitivity of flushing time to S_o, point source and non-point source. Values in the x- and y-axis are normalized.

In summary, the freshwater ratio method for the estimate of flushing time is the most sensitive to the open boundary salinity and the least sensitive to a non-point source like precipitation, CSO and ground-water discharges. Thus, the accuracy requires for non-point source flows is much less than for open boundary salinity. In reality, a system is rarely in true steady state since the hydrologic condition constantly changes in time as well as environment. Therefore, estimated flushing time should be updated continuously by counting the variation as well as resultant salinity distribution, to find accurate flushing time for the study area. This requires continuous salinity survey in order to provide current distribution and boundary salinity value. This method is not cost efficient.

4.2. Modified Tidal Prism

The underlying assumption of the modified tidal prism method is firstly a steady state distribution of fresh and saline water within the estuary (Ketchum, 1951). This method

also requires a set of segments, each of which is defined by tidal excursion over a cycle. The second assumption of the method is that complete mixing occurs within each volume segment. An ideal condition to obtain the beset result is the estuary that low river flow or a large number of segments and rapid downstream increase of cross-sectional area.

Parameters required for the flushing time estimate using the tidal prism method are river flow at the head of estuary, and cumulative sub-tidal and inter-tidal volumes as function of upstream distance. Both the cumulative volumes were computed by calculating the volume for the individual segment used for the freshwater exchange method. For the inter-tidal volume, a linear interpolation was applied between the Hurricane Barrier and the upper Acushnet River estuary where a tidal range is found from NOAA data in the Tides and Currents software. Figure 4-3 shows the upstream cumulative sub-tidal and inter-tidal volumes. The use of the cumulative volumes is to determine the excursion distance, which in turn define a segment where complete mixing takes place.

The modified tidal prism method requires four steps, and they are presented in the following. More details of this method can be referred to Ketchum (1951):

1) Segment the estuary. For this method an estuary must be segmented so that each segment length reflects the excursion distance a particle can travel during one tidal cycle. The innermost section must then have a tidal prism volume completely supplied by river flow. Thus:

$$P_o = R \tag{5}$$

where

P_o = tidal prism (inter-tidal volume) of segment ″o″
R = river discharge over one tidal cycle

The low tide volume in this section (V_o) is that water volume occupying the space under the inter-tidal volume P_o (which has just been defined as being equal to R). The seaward limit of the next seaward segment is placed such that its low tide volume (V_1) is defined by:

$$V_1 = P_o + V_o \tag{6}$$

P_1 is then that inter-tidal volume which, at high tide, resides above V_1. Successive segments are defined in an identical manner to this segment so that:

$$V_i = P_{i-1} + V_{i-1} \tag{7}$$

Thus, each segment contains, at high tide, the volume of water contained in the next seaward section at low tide.

2) Calculate the exchange ratio (r_i) by:

$$r_i = \frac{P_i}{P_i + V_i} \tag{8}$$

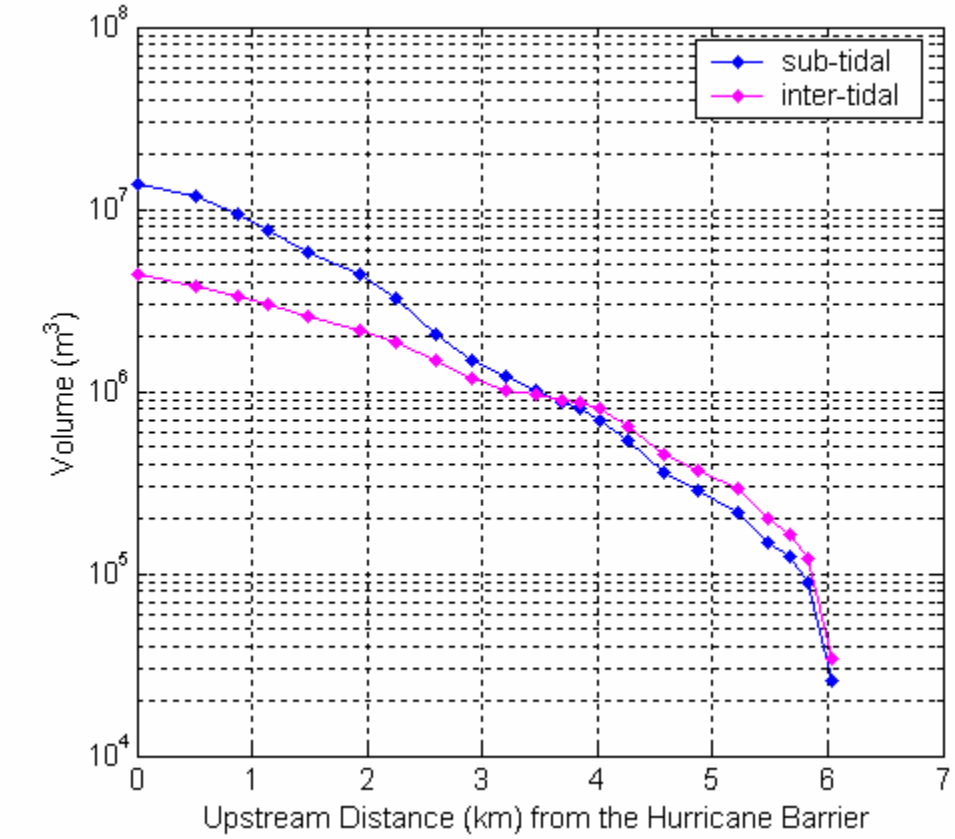

Figure 4-3. Cumulative sub-tidal and inter-tidal volumes as function of upstream distance.

Thus the exchange ratio for a segment is a measure of a portion of water associated with that segment which is exchanged with adjacent segments during each tidal cycle.

3) Calculate segment flushing time by:

$$T_i = \frac{1}{r_i} \tag{9}$$

where

T_i = flushing time for segment measured in tidal cycles.

4) Calculate total estuarine flushing time by summing the individual segment flushing times:

$$T_f = \sum_{i=1}^{n} T_i \tag{10}$$

where

T_f= total estuary flushing time
n = number of segments

The very first landward segment is denoted as i=0, and the tidal excursion distance is designated as X_i.

4.2.1. Results and Sensitivity Analysis

Estimated flushing time for the entire estuary from the modified tidal prism method is 18.77 days for 1 November and 18.75 days for 2 November. Results for 1 November are presented in Table 4-3, including turnover time for the individual segments.

Unless the fortnight variation of tidal height is considered (which will be presented later), the sub-tidal and inter-tidal volumes of the estuary are constant at a given location. Hence the only parameter governing flushing time is river flow. The sensitivity analysis for different river flow was performed and the results are presented in Figure 4-4. The x-axis is the flow variation in non-dimension and the y-axis is the flushing time estimate in dimension. Also shown in the figure are estimates of flushing time for the river flow on 1 November (black square) and 2 November (green square) for reference.

Table 4-3. Segment parameters and flushing time estimate of the Acushnet River estuary using the tidal prism method.

Segment #	X_i (m)	V_i (m^3)	P_i (m^3)	r_i	T_i (day)
0	6,139	15,311	20,567	0.573	0.90
1	5,950	35,878	48,194	0.573	0.90
2	5,583	84,072	112,933	0.573	0.90
3	4,672	197,005	243,359	0.553	0.94
4	3,899	440,365	416,148	0.486	1.07
5	2,835	856,513	405,016	0.321	1.61
6	2,356	1,261,529	491,017	0.280	1.85
7	1,868	1,752,546	500,196	0.222	2.33
8	1,281	2,252,742	610,322	0.213	2.43
9	823	2,863,063	533,319	0.157	3.30
10	122	3,396,383	872,933	0.204	2.53
	Total Flushing Time = 18.77 days				

The result suggests that as river flow increases, flushing time increases. Over a range of river flow variation by a factor of 3, flushing time increases by 1.15 times. However, the flushing time increase is not linear. The discontinuity is caused by the variation of the segment number. For a large river flow, the tidal excursion becomes long and therefore it generates a smaller number of segments compared to a small river flow.

The tidal prism used for the base cases was for the mean tide. If tide is a spring or neap tide, the estimated flushing time is altered because of the variation in the inter-tidal volume. For a spring tide, for example, the tidal prism of the estuary increases the mean tidal prism by 53%. This results in flushing time of 7.5 days. Conversely, for a neap tide, the estimated flushing time increases to 22.6 days due to decrease in the tidal prism by 36%.

If we consider the river flow for a wet weather, 24 October (50,890 m^3/tidal cycle), and assume the tide is mean, the flushing time decreases to 17.8 days from 18.8 days of the base condition (1 November).

Since the river flow and tide continuously change over the initially estimated turnover time in reality, the flushing time should be correspondingly revised to find an accurate estimate.

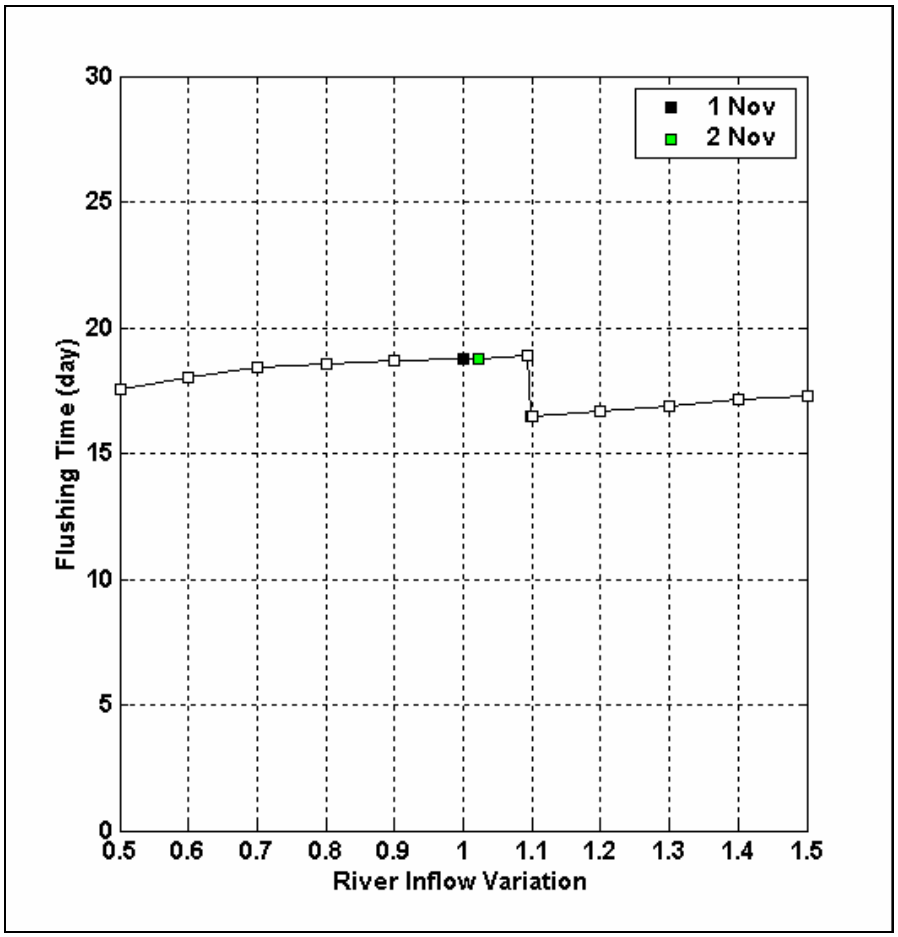

Figure 4-4. A relationship between river run-off and flushing time. Black and green square marks represent flushing time estimated using the river flow on 1 and 2 November, respectively.

4.3. BFMASS Simulation

This section documents results of two numerical simulations performed using three-dimensional BFMASS. One is the residence time simulation of wastewater in the lower Acushnet River estuary, and the other is the flushing time simulation for the entire estuary.

The ambient currents applied for these simulations are from the BFHDYRO results with wind forcing at the surface for October 2001. Important parameters governing the mass transport in the BFMASS model simulation are horizontal and vertical dispersion coefficients. These values were determined from the model calibration using the dye data, and the values are 0.02 m^2/s and 1×10^{-7} m^2/s for horizontal and vertical diffusion coefficients, respectively.

In the section, results of the residence time simulation with a short-term and long-term dye release at the Fairhaven WWTP outfall are presented, followed by the flushing time simulation for the entire estuary.

4.3.1. Residence Time Simulation

A Short-term Dye Release Study

Scenario for the residence time simulation replicates the dye release study conducted in the lower estuary, centered the Fairhaven WWTP outfall. In the actual dye study, the actual release was located at the treatment plant. For modeling purposes, however, the release occurred at the outfall in the lower estuary instead, which is 2.8 km (1.7 mile) northwest of the discharge site, and is represented by a cell of $35\times36\times0.8$ m^3 dimension.

The source type is a continuous release, and the strength is 21 mg/s. The release period is the same as the dye study, which starts 0900 October 18 and ends 0900 October 23. Since the actual termination of injection occurred at the facility, the dye travel time along the pipe over the distance is also added to the injection period with the strength linearly decreasing in time for 6.5 hours.

Figure 4-5 shows time series of simulated dye concentrations at three selected sites (X1, X3 and X5) out of six sites located along a 75-m perimeter from the outfall. Also shown in the figure are the average of the dye concentration computed from the six locations (thick line).

Simulated initial concentrations along the perimeter are not same. They vary from 4.9 at X6 (not shown in Figure 4-6) to 34.8 μg/l at X1 with an average of 12.5 μg/l. Definition of residence time is the length of time required for the initial concentration to reach its e-folding concentration, or the slope of logarithm of concentration on time-axis. Figure 4-6 shows the mean concentration in log-scale as function of time. If we consider the mean concentration, estimated e-folding time is approximately 0.88 days (21 hours).

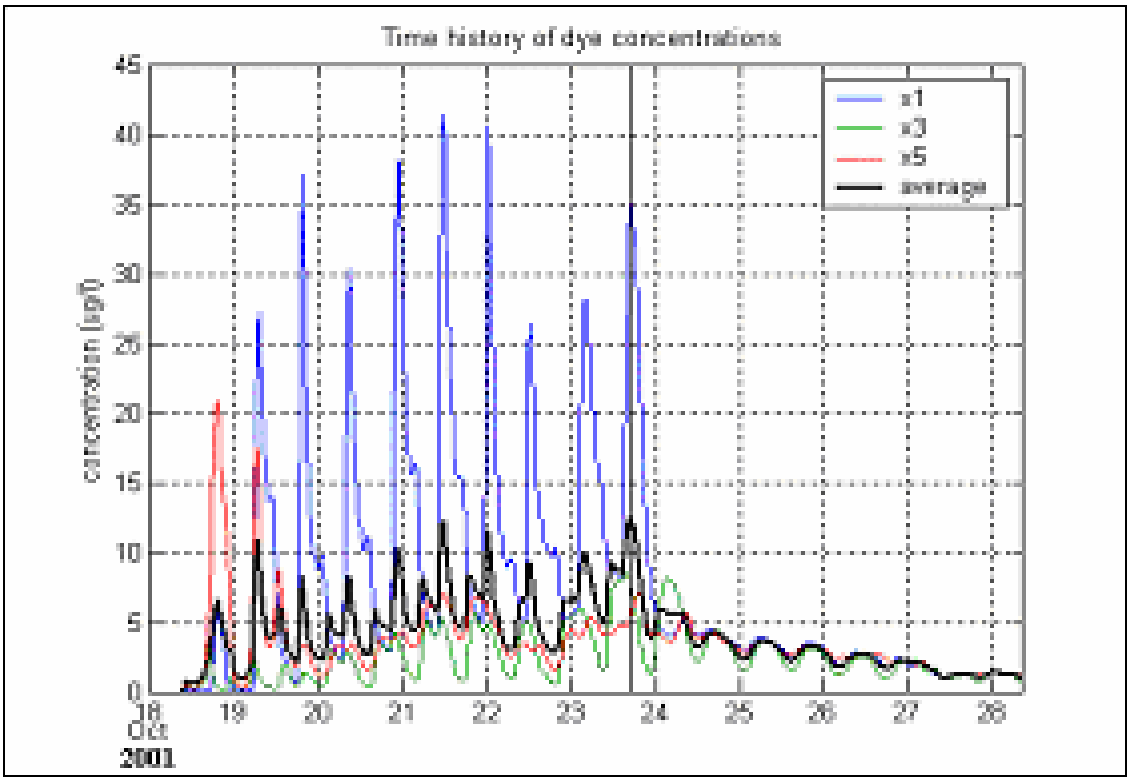

Figure 4-5. Time series of dye concentrations at sites X1, X3 and X5 (Figure 3-8), and the mean concentration determined from six locations (X1 to X6). A vertical line represents the time of the termination of dye release.

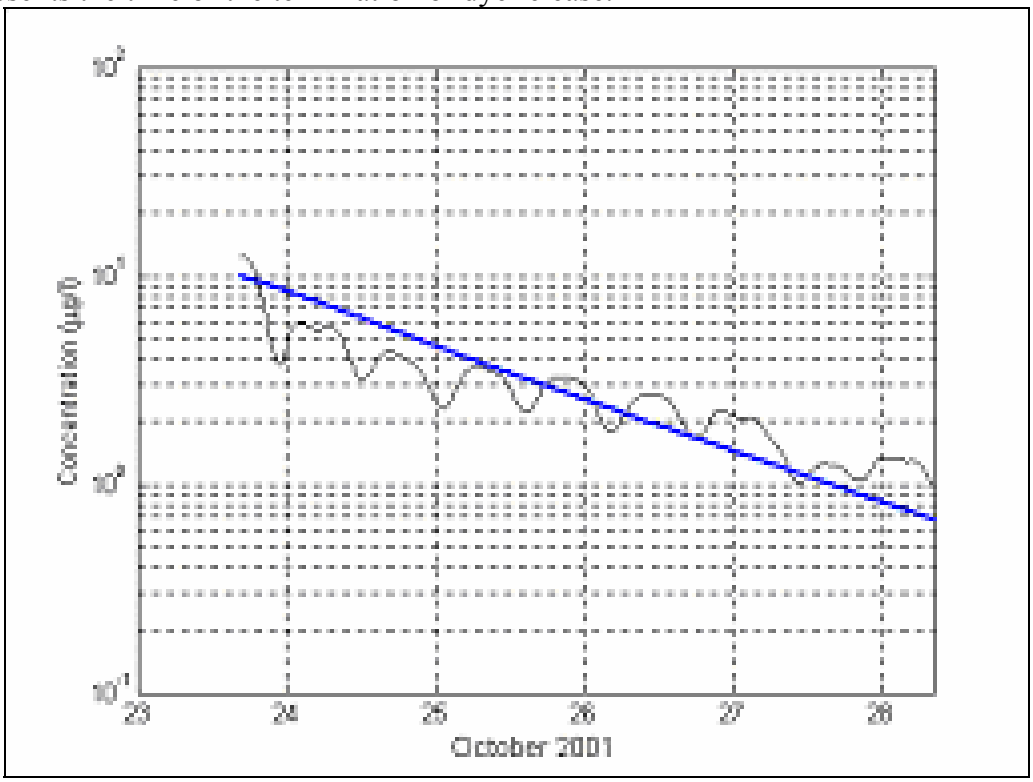

Figure 4-6. Logarithm of mean concentration vs. time after the termination of dye injection, superimposed on the slope (=1.14/day).

Figures 4-7a to 4-7c show simulations of dye distribution at 6-hour intervals after the cessation of dye injection (9:00 23 October).

In general, the shape of dye plume in the near field is a Gaussian, but in the far field it is in an elliptic shape whose principal axis is parallel with the estuary axis. The concentration at the outfall at 9:00 23 October was 9.8 μg/l (purple in Figure 4-7a), and its e-folding concentration of 3.6 μg/l was located in areas between 250 and 400 m from the outfall (bright yellow). Although the areal extent to the e-folding concentration was the same over 12 hours, the concentration gradient inside the area becomes smaller with time. The variation in the vertical also changed with time. For the 12-hour post-cessation period (Figure 4-7c), relative magnitude of the middle layer concentration increased from 27% to 60% of the surface-layer, implying that the concentration in the middle layer increases while that in the surface layer decreases. Similar process takes place in the bottom layer, showing an increase from 12% to 34%. This means that the dye gradually disperses to the lower layer with time.

A Long-term Dye Release Study

Figure 4.8 shows time series of simulated dye concentrations at three stations each in the upper, middle and lower estuary. The time series data were obtained from a simulation that was designed to find steady state conditions and residence time of a conservative pollutant. For the simulation, a unit source strength was continuously released at the Fairhaven WWTP outfall and eventually terminated eight months after the initial release. The simulation results presented in Figure 4.8 show that the concentrations gradually increase, reaching 99% of the final value at the beginning of April, suggesting that the Acushnet River estuary system takes about six months to reach steady state. Residence time determined by the -folding value of concentration at the time of termination is on the order of 15 days. This estimate is about 17 times larger than the residence time found from the 5-day dye simulation.

The reason for the shorter residence time for the 5-day dye simulation compared to the long-term dye simulation, is that the decrease of dye in the lower estuary is due not only to dispersion in the inner harbor but also to transport to the outer harbor. Figure 4.9 shows the volumetric mass transport to the outer harbor in terms of a ratio of instantaneous total mass in the inner harbor to the mass in the outer harbor. During the dye release period (18 –23 October), the mass in the inner and outer harbors increase in time to 9.4 kg (20.7lb) and 2.6 kg (5.7lb) of dye, respectively. However, after the termination of dye release the mass in the outer harbor continues to increase while the mass in the inner harbor decreases. The figure indicates the increase rate during the dye injection period is slower in the outer harbor than the inner harbor, and the amount of mass in the outer harbor ranges on average between 20 and 50% of the mass in the inner harbor.

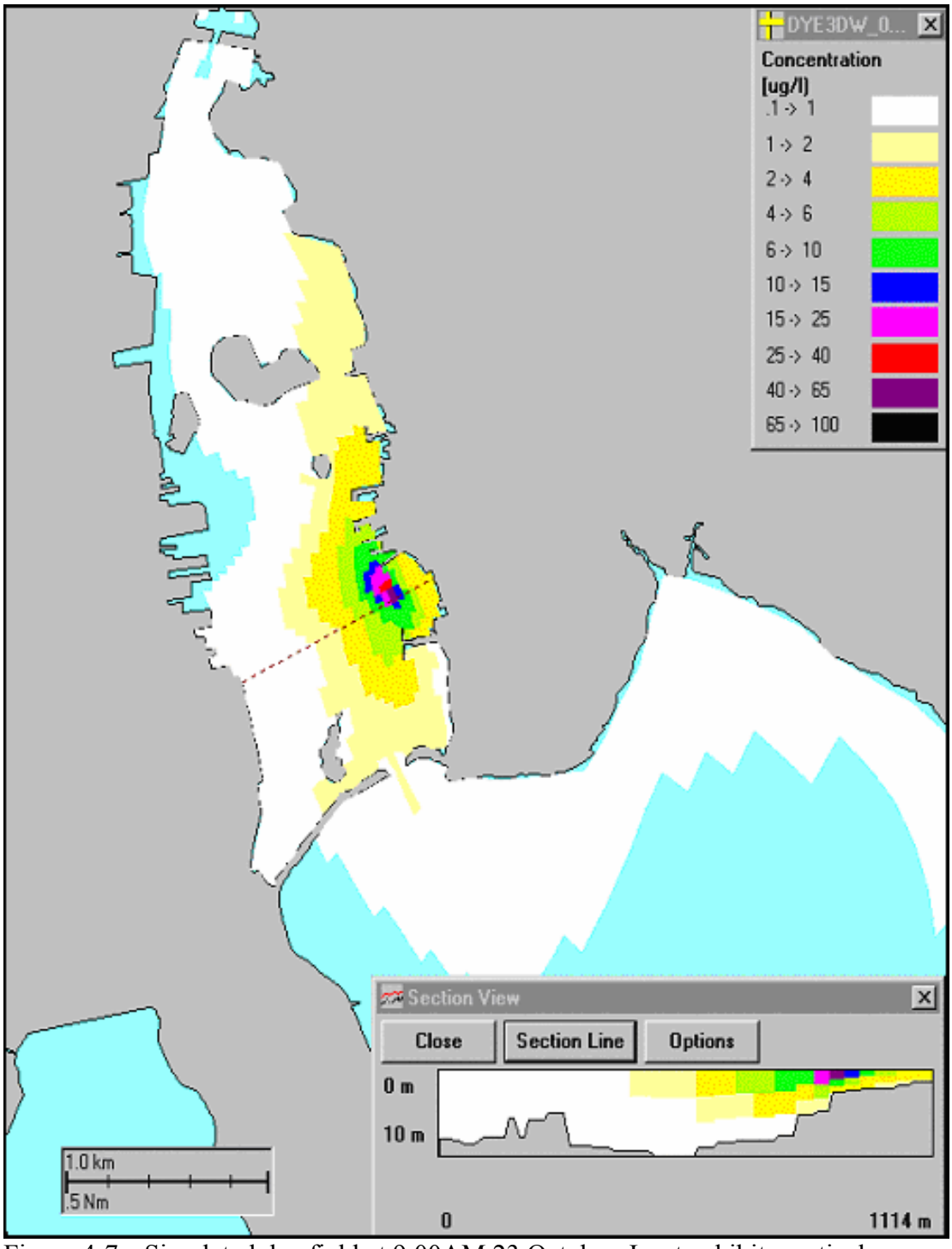

Figure 4-7a. Simulated dye field at 9:00AM 23 October. Inset exhibits vertical distribution across the outfall along a dashed line.

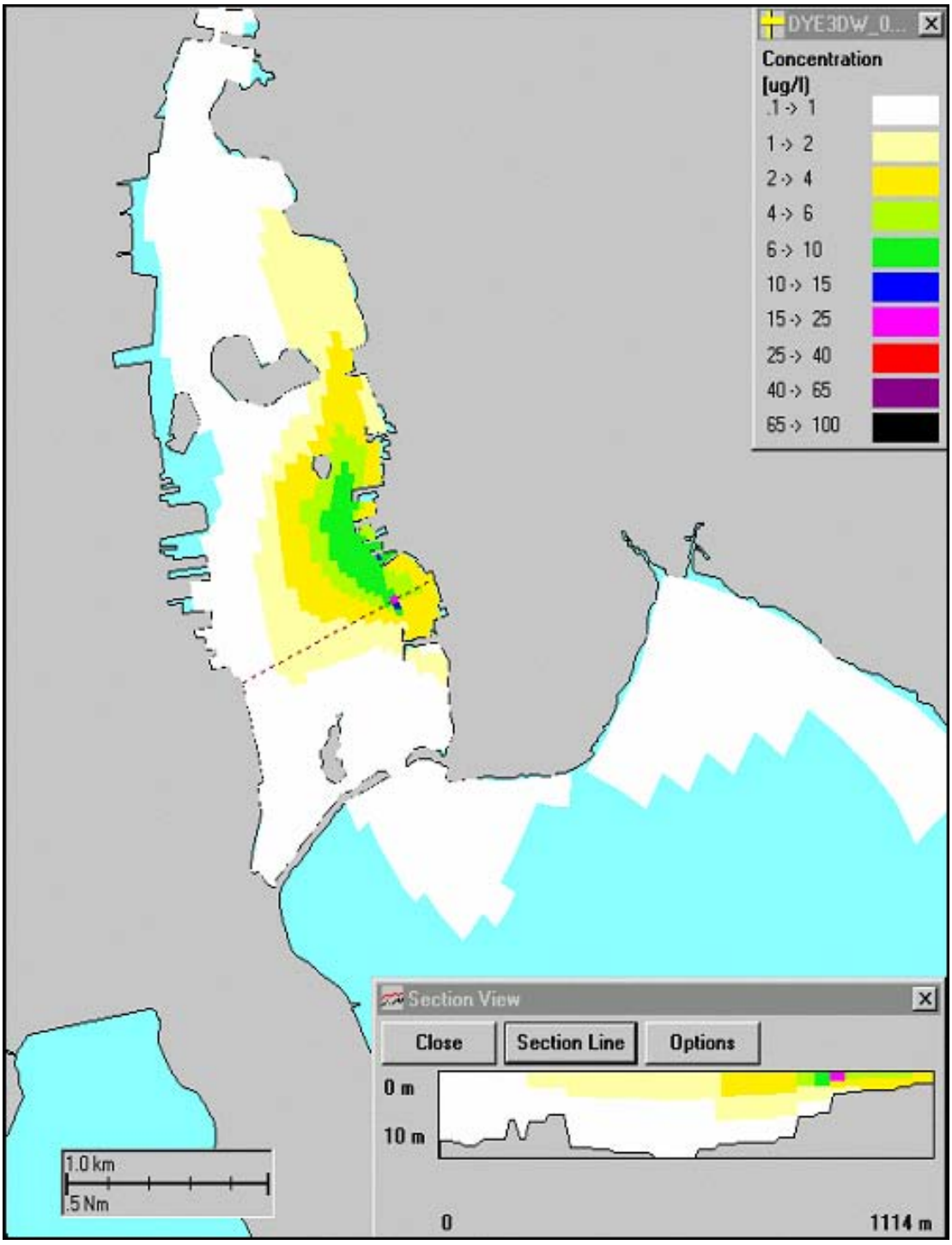

Figure 4-7b. Simulated dye field on 3:00PM 23 October. Inset exhibits vertical distribution across the outfall along a dashed line.

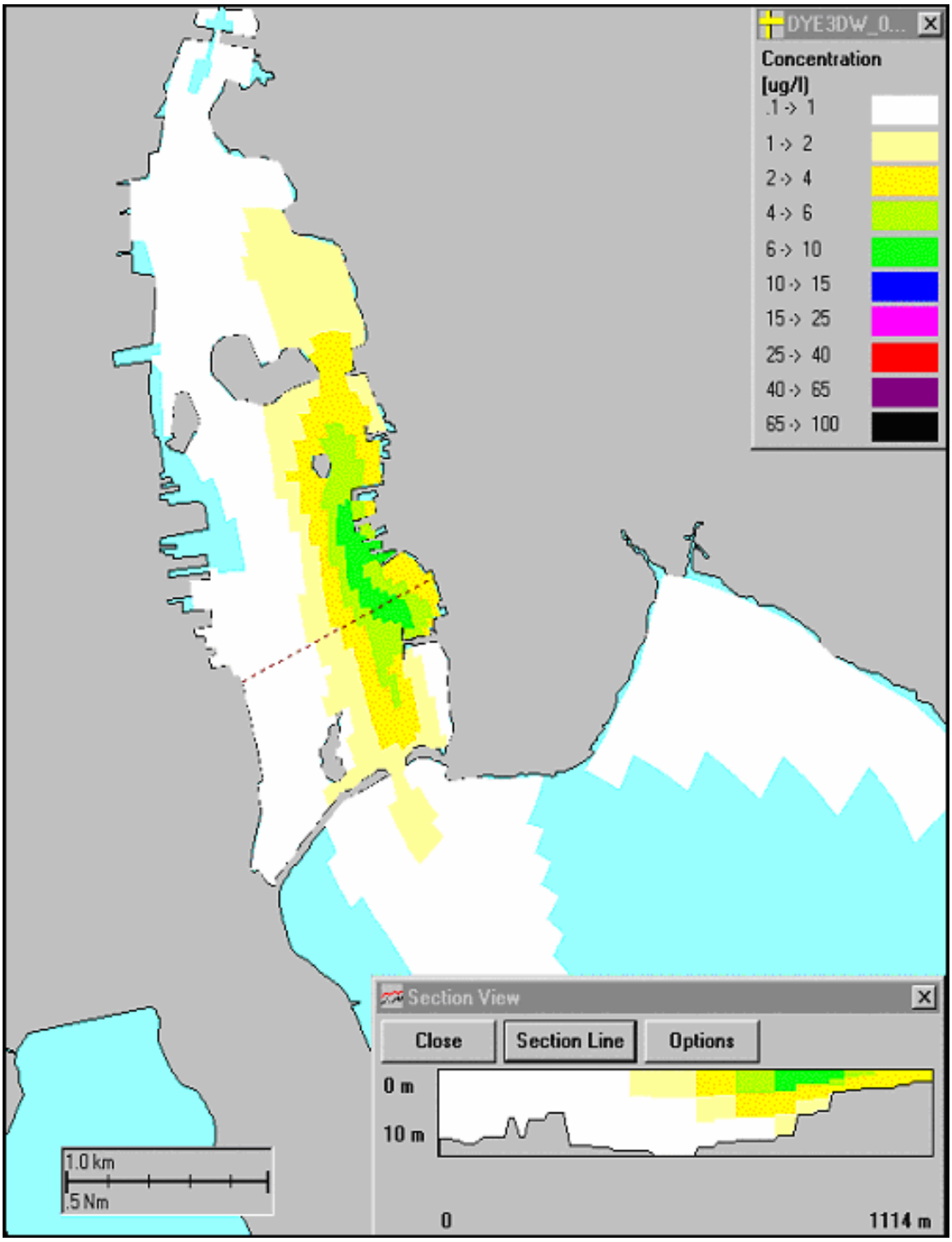

Figure 4-7c. Simulated dye field at 9:00PM 23 October. Inset exhibits vertical distribution across the outfall along a dashed line.

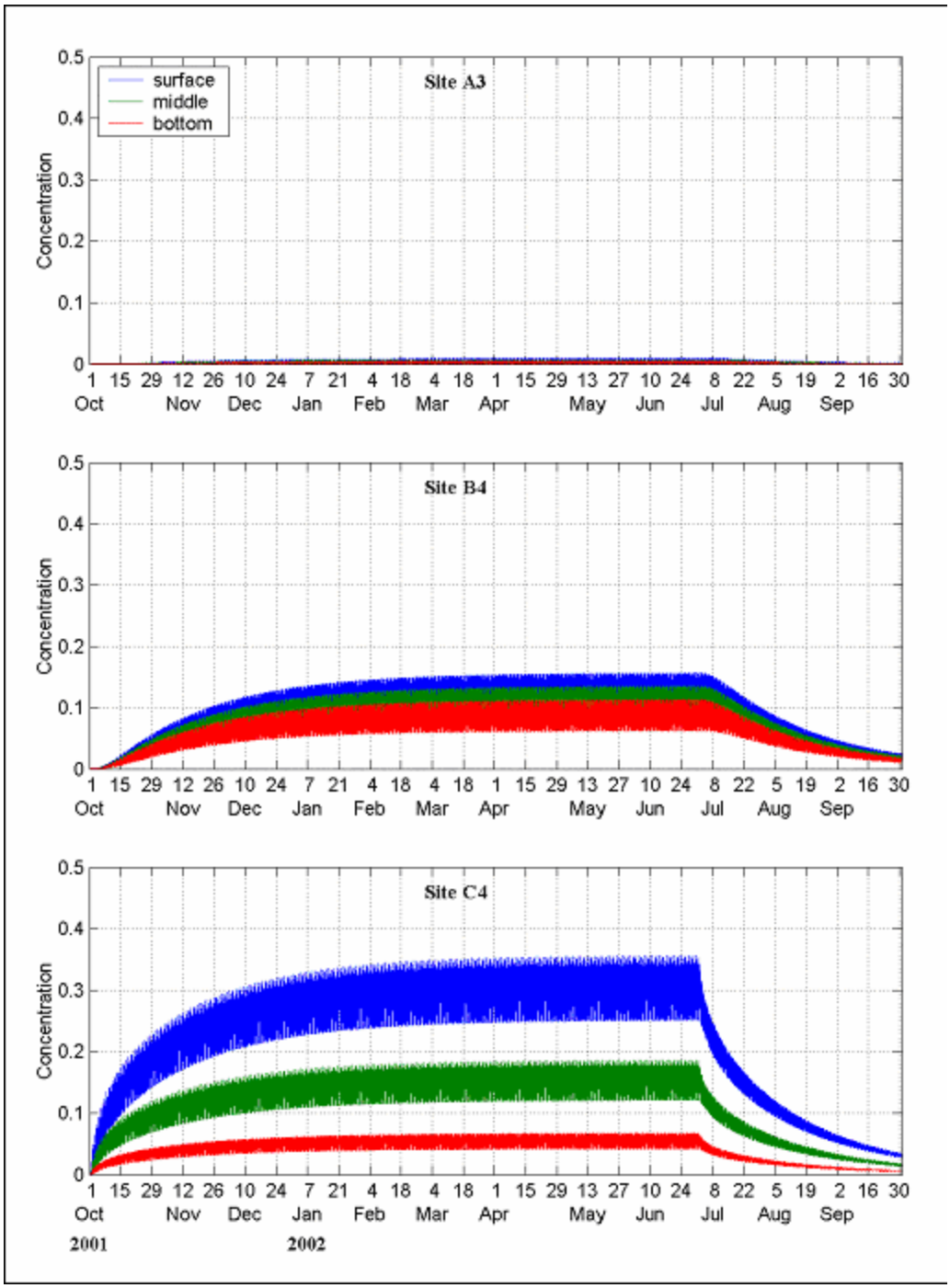

Figure 4.8. Simulated dye concentrations for the surface, middle and bottom layers at sites A3, B4 and C4 (see Figure 2.2).

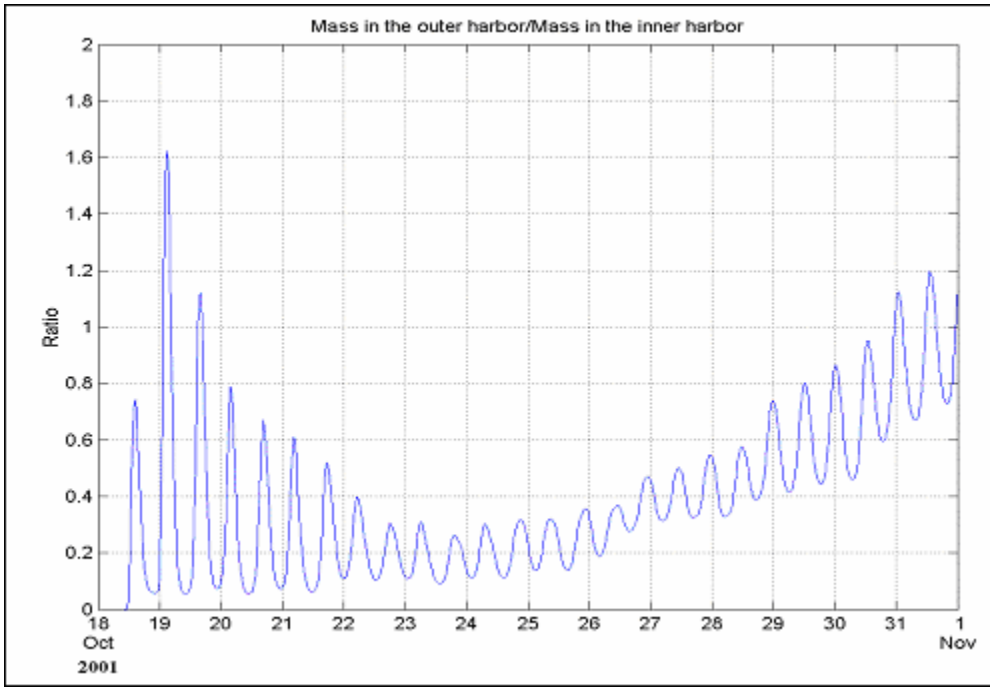

Figure 4.9. Ratio of total simulated dye mass in the outer harbor to the inner harbor.

4.3.2. Flushing Time Simulation

The third approach to estimate flushing time for the Acushnet River estuary is using a 3-layer BFMASS model was employed. The flushing time simulation was based on assumptions that the source strength is unit and the source type is an instantaneous, by distributing a unit load evenly over the entire volume of the study area and releasing at once at the initial time. The strength of freshwater uses the river flow observed on 1 November. Similar to the residence time simulation, coefficients used for horizontal and vertical dispersions were $0.02 m^2/s$ and 1×10^{-7} m^2/s, respectively.

In addition to the entire Acushnet River estuary, numerical simulations were separately performed to estimate flushing times for the upper (zone-A), middle (zone-B) and lower (zone-C) estuaries shown in Figure 2-2. Results yield 10.6 days of flushing time for the whole estuary, and between 3.5 days and 4.6 days for the individual zones (4.3 days for zone-A, 3.5 days for zone-B and 4.6 days for zone-C). When the river flow volume on 24 October ($1.14 m^3/s$) was used as the freshwater input, the estimates decreased to 7.1 days for the entire estuary, and 2.5 days, 2.9 days and 4.5 days for zone-A, zone-B and zone-C, respectively. Flushing times decrease less with downstream distance when the river flow increased. Reason is that greater advection takes place by large river flow in the upper estuary than other two areas.

4.4. Comparison with Previous Studies

According to definitions in ACI (1995), residence time is the average time that it takes to replace the mean volume of area of interest with the tidal prism volume. System residence time is defined by the volume of area of interest (either the entire estuary or zone) divided by the tidal prism of the entire estuary, while local residence time is defined by the volume of an area divided by its tidal prism (ACI, 1995).

Table 5-2 lists estimates of system and local residence times for the Acushnet River estuary. Also presented in the table are dimensions of the area of interest.

Table 4-5. System and local residence times for the Acushnet River estuary.

	Surface Area ($\times 10^6$ m^2)	Length (km)	Volume ($\times 10^6$ m^3)	Tidal prism (m^3/tidal cycle)	System residence time (day)	Local residence time (day)
Whole estuary	3.98	6.1	16.01	4,477,500	1.85	1.85
Zone A	0.82	2.4	1.36	930,924	8.90	0.76
Zone B	1.15	1.8	4.24	1,293,408	6.41	1.70
Zone C	2.00	1.9	10.37	2,213,285	3.74	2.42

For the whole estuary, both system and local residence times are obviously same (1.85 days). This estimate agreed with the value determined for the upper Acushnet River in ACI (1995). However, this residence time estimate is substantially different from the value determined using the modified tidal prism method, 1.85 days vs. 18.8 days. This is because the modified prism method counted in the hydrological characteristics of the estuary such as tidal excursion and river flow as well as its morphology, whereas the method employed in the ACI was based on complete mixing over the entire area of interest and complete removal of the water volume existing in ebb tide.

Compared to the flushing time estimate from the BFMASS simulation, the estimate from the previous dye study (2.5 days) conducted in 1986 (ASA, 1987) is more than four times shorter. The reason is that the simulation yields the length of time to replace its e-folding volume of the entire estuary with fresh water, whereas the estimate from the dye study is based on the time required to flush dye mostly existing in the upper layer.

5. Discussion and Conclusions

The objectives of this work were to estimate the residence time of wastewater effluent from the Fairhaven WWTP in the lower New Bedford Inner Harbor and flushing time for the Acushnet River estuary. As part of the work, an intensive field study was attained to collect dye concentrations and salinity data, including currents and surface elevations. While the current and elevation data were used for the hydrodynamic model calibration, the dye and salinity data were ultimately applied to the estimation of residence time and flushing time.

A dye study was conducted as part of the field program in the lower estuary, at the Fairhaven WWTP discharge outfall. This study was designed with three parts. The first was a survey to measure background level of fluorescence at eleven stations, and the second was the dye release study by pumping at the Fairhaven WWTP at a rate of 21 mg/s for a 5-day period from 9:00 18 October to 9:00 23 October. The last was three surveys to monitor dye distribution once before and twice after the termination of dye injection. The survey observations exhibited that dye rose to the surface as soon as it was discharged through the outfall, and it immediately spread out forming a localized plume mostly residing near the outfall. There was no significant vertical distribution of dye observed during the observation. Four hours after the cessation of dye injection, the spatial coverage of dye distribution became much smaller than the survey six hours earlier. Twenty-two hours later, the dye concentration became at the same level as background fluorescence concentration, indicating that the residence time of dye was less than 22 hours.

Also performed was a long-term dye release simulation in the Acushnet River estuary, having a unit source strength at the Fairhaven WWTP outfall. The results suggested that the estuary system took six months to reach steady state. Estimated residence time was on the order of 15 days. A comparison of estimated residence time between the 5-day and long-term dye simulations implied that the reason for the shorter residence time from the 5-day simulation was due to the dye lost by not only dispersion in the inner harbor but also transport to the outer harbor. Therefore, the actual dye study was unable to determine an accurate estimate of residence time since the amount of dye pumped into the system was not sufficient for the system to reach steady state.

Flushing time for the entire Acushnet River estuary was estimated using three independent approaches, under 1 November hydrologic condition. Estimated flushing times from the freshwater ratio and modified tidal prism methods were 15.6 days and 18.8 days, respectively. The BFMASS simulation used a fixed river flow on 1 November but time-varying hydrodynamics that were ambient currents and played an important role for the pollutant advection. The simulation results yielded 10.6 days of flushing time. As the freshwater budget increased to 2.5 times of the 1 November river flow (24 October), estimated flushing times decreased to 6.4 days, 17.8 days and 7.1 days for the freshwater exchange and modified tidal prism methods, and numerical simulation, respectively.

Flushing times estimated from three methods are different. This is due to the differences in theoretical approaches and assumptions of each method. The freshwater ratio method is based on assumptions that salinity is uniform, no net flux exists within each segment, and variables are steady state. The method also assumes complete and instantaneous mixing in a segment before and after the exchange of water with adjacent segments. On the other hand, the modified tidal prism method assumes that the amount of water to exchange with adjacent segments is equal to the tidal prism of the segment. The modified tidal prism method assumes the steady-state condition per each segment, the same as the freshwater ratio method. In addition, the prism method allows only freshwater budget and its location at the head of the estuary and it is only applicable to a system where the flow is unidirectional. Hence, this method is sensitive to the morphology of the estuary and

tidal conditions. Unlike the freshwater ratio and modified tidal prism methods, the BFMASS numerical simulation requires a steady state at initial time only, and takes into account variations of hydrologic condition over the turnover time.

In addition, the difference in the flushing time estimates is related to representing different types of flushing time. In Costa et al. (1999), there are three terms commonly used for a measure of flushing time (used as “hydraulic turnover time” in Costa et al., 1999). They are “flushing time”, turnover time and residence time. According to the definitions in Costa et al. (1999), the estimates from the freshwater ratio and modified tidal prism methods are “flushing time”, and the estimate from the BFMASS simulation is turnover time.

The ultimate application of flushing time is to establish nitrogen-loading limits for the estuary. While a portion of nitrogen is flushed out of the estuary, the remains and returned nitrogen stay in the estuary available to assimilate. Hence flushing time is important to determine the load limits. In this work, we provide flushing times from various methods including differences in theories and assumptions for each method in order to make a better decision for the maximum loading in the estuary.

6. References

Abdelrhman, M.A. and E.H. Dettmann, 1995. Modeling of current circulation, residence time, and salinity distribution in New Bedford Harbor, MA. U.S. Environmental Protection agency, Environmental Research Laboratory, Narragansett, RI.

Abdelrhman, M.A., 2002. Modeling How a Hurricane Barrier in New Bedford Harbor, Massachusetts, Affects the Hydrodynamics and Residence Times. Estuaries, Vol. 25, No. 2, p177-196.

Ambrose, R.B. et al, 1993. The Water Quality analysis Simulation Program, WASP5 Part a: Model Documentation, Part B: The WASP5 Input Data Set. U.S. Environmental Protection agency, Athens, Ga.

ASA, 1987. Selected studies of PCB transport in New Bedford Harbor. Applied Science associates, Inc., Narragansett, RI. 193 pp.

ASA. 1990. Measurements of PCB Transport from upper New Bedford Harbor. April 18, 1990. Narragansett, RI, ASA 89-27. 127 pp.

ACI (Aubrey Consulting, Inc.), 1995. Estimation of flushing rates in selected Buzzards Bay Embayments. Aubrey Consulting, Inc., Cataumet, MA.

Battelle, 1990. Modeling of the transport, distribution and fate of PCBs and heavy metals in the Acushnet River / New Bedford Harbor / Buzzards Bay system. Battelle Memorial Institute, Duxbury, MA.

Cape Cod Commission, 1998. The Cape Cod embayment project, Interim final report. Cape Cod Commission, Water Resources Office, Barnstable, MA.

Costa, J.E., B.L. Howes, D. Janik, D. Aubrey, E. Gunn and a.E. Giblin, 1999. Managing anthropogenic nitrogen inputs to coastal embayments: Technical basis and evaluation of a management strategy adopted for Buzzards Bay. Buzzards Bay Project National Estuary Program, East Wareham, MA.

Costa, J.E., 2000. A preliminary evaluation of nitrogen loading and water quality of New Bedford Inner Harbor (Acushnet River) as it relates to the Fairhaven Wastewater Treatment Facility. Buzzards Bay Project National Estuary Program, East Wareham, MA.

Geyer, W. R. and W. D. Grant. 1986. Final Report: A Field Study of the Circulation and Dispersion in New Bedford Harbor. Woods Hole Oceanographic Institution. pp250.

Guo, Qizhong and George P. Lordi. 2000. Mehtod for Quantifying Freshwater Input and Flushing Time in Estuaries. Journal of Environmental Engineering, July. p. 675 – 683.

Howes, B.L. and D.D. Goehringer, 1996. Ecology of Buzzards Bay: An Estuarine Profile. Biolofical Report 31. National Biological Service, U. S. Department of the Interior.

Howes, B.L., T. Williams and M. Rasmussen, 1999. Baywatchers II, nutrient related water quality of Buzzards Bay embayments: A synthesis of Baywatchers monitoring 1992-1998. The Coalition for Buzzards Bay, New Bedford, MA.

Ketchum, B.H., 1951. The exchanges of fresh and salt waters in tidal estuaries. J. Mar. Res. 10:18-38.

Madala, R.V. and S. A. Piacsek, 1977. A semi-implicit numerical model for Baroclinic Oceans. *Journal of Computational Physics,* 23, p. 167-178.

McCutcheon, S. C., Z. Dongwei, and S.Bird, 1990. Model calibration, validation, and use, Chapter 5 in Technical Guidance Manual for Performing Waste Load allocations. In: Book III: Estuaries, Part 2: application of estuarine waste load allocation models, J.J., Martin, R.B. Ambrose, and S. C. McCutcheon (eds.), US Environmental Protection agency, Office of Water, March 1990.

Mendelsohn, D, T. Isaji and H. Rhines, 1995. Hydrodynamic and water quality modeling of Lake Champlain. *Report to Lake Champlain Management Conference*, Burlington, Vt, ASA Report 92-034.

Mills, W.B., D.B. Porcella, M.J. Ungs, S. A. Gherini, K.V. Summers, L. Mok, G.L. Rupp, G.L. Bowie, 1985. Water quality assessment: a screening procedure for toxic and conventional pollutants. EPA/600/6-85/002b, U.S. Environmental Protection agency, Office of Research and Development, Athens, Ga.

Muin, M. 1993. A Three-Dimensional Boundary Fitted Circulation Model in Shperical Coordinates. *Ph. D. Dissertation*, Department of Ocean Engineering, University of Rhode Island, Kingston, RI.

Muin, M. and M. L. Spaulding, 1996. Two-dimensional boundary fitted circulation model in spherical coordinates. In: *Journal of Hydraulic Engineering*, Vol. 122, No. 9, September 1996, p. 512-521.

Muin, M. and M. L. Spaulding, 1997a. Application of Three-dimensional boundary fitted circulation model to Providence River. *ASCE Journal of Hydraulic Engineering.* Vol. 123, No. 1.

Muin, M. and M. L. Spaulding, 1997b. Three-dimensional boundary fitted circulation model. In: *Journal of Hydraulic Engineering*, Vol. 123, No. 1, January 1997, p.2-12.

Officer, C. B., 1976. Physical oceanography of estuaries (and associated coastal waters). John Wiley & Sons. pp 465.

Signell, R. 1987. Tide- and Wind-Forced Currents in Buzzards Bay, Massachusetts. WHOI-87-15 Technical Report. pp 86.

U. S. Geological Survey (USGS), 1995. Streamflow, Ground-Water Recharge and Discharge, and Characteristics of Surficial Deposits in Buzzards Bay, Southeastern Massachusetts. U. S. Geological Survey, Water-Resources Investigations Report 95-4234. 61 pp.

Appendix A

Salinity Data

The salinity survey was designed to collect data at high and low tidal conditions each day for four consecutive days from 30 October to 2 November. The strategy for the survey was to synoptically measure salinity over the entire estuary at each tidal condition. The goal of the salinity survey was to provide data for the flushing time estimate using a freshwater ratio method (Ketchum, 1951). It was expected that the measurements at a low tide provide the best indication of flushing as they provide the largest longitudinal gradient in salinity. The high slack measurements would offer some indications on the variability of the salinity gradient and be a useful check on the predicted range of flushing times for the estuary.

The entire estuary was divided into 21 sub-zones mainly in the longitudinal direction, which extends over 6.1 km distance from the head to the mouth of the estuary. A difficulty in the survey was to collect data over the 21 sections. To minimize the problem of non-synopticity, two boats were operated at the same time but in different sections of the estuary.

Vertical casts were taken at between 2 and 3 stations each section, using SEACAT or YSI instruments. Each cast started at 6 inches below the surface and then every foot (0.3 m) to the bottom. The stations are shown in Figures A-1 and A-2 for 30-31 October, Figures A-6 and A-7 for high and low tides on 1 November, and Figures A-11 and A-12 for high and low tides on 2 November, respectively. Original schedule for salinity sampling was set-up so that measurements would take place at two consecutive tidal stages per day. However, due to instrument malfunctioning on 30 October and a broken shifter cable on 31 October measurements were collected twice on high tide and four times on low tide over a 4-day period (Table 2-1).

Figures A-3, A-8 and A-13 exhibits the surface and near surface salinity distributions, and Figures A-4, A-5, A-9, A-10, A-14 and A-15 presents salinity profiles.

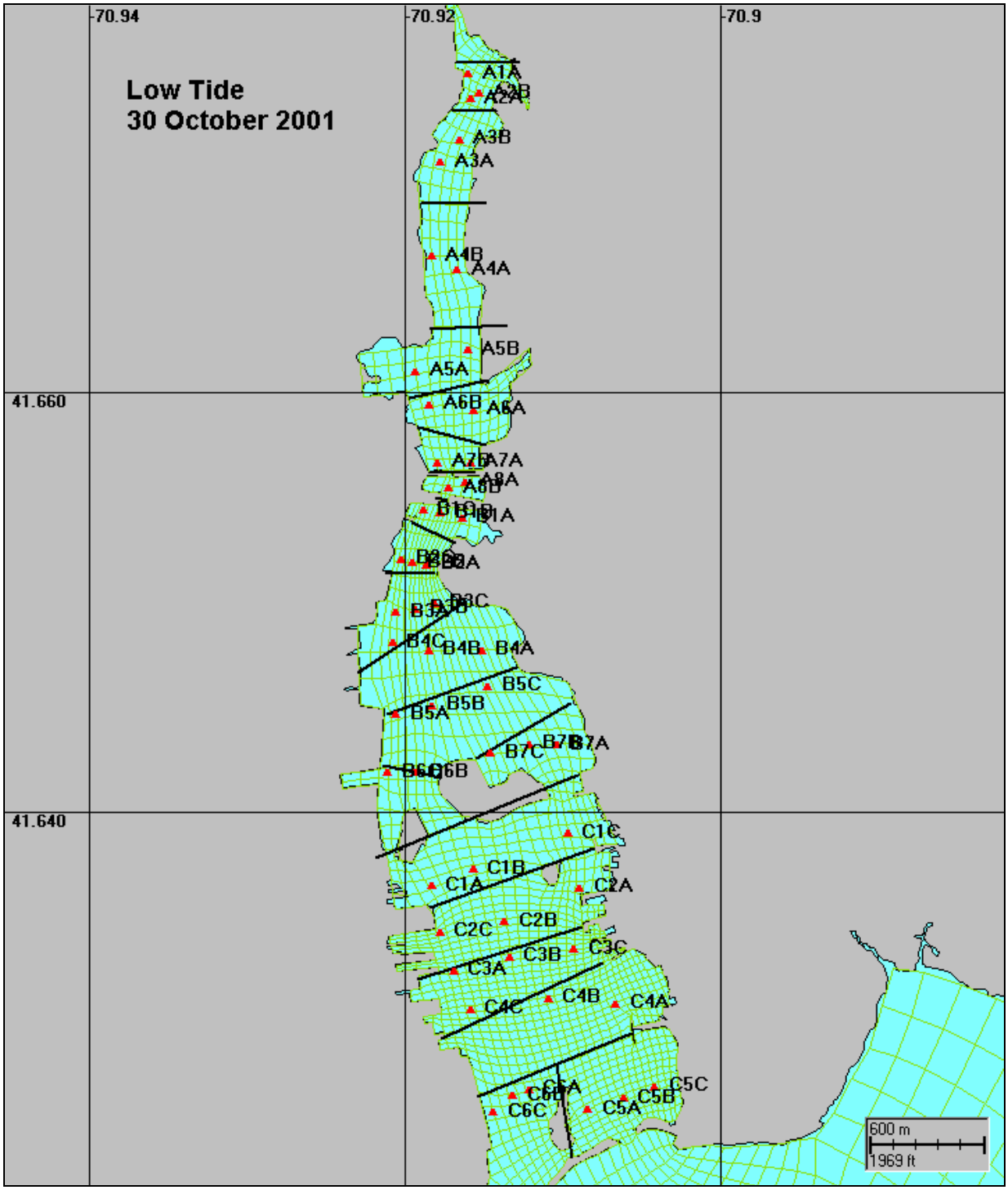

Figure A-1. Salinity sampling stations during low tide (13:48 am) 30 October 2001.

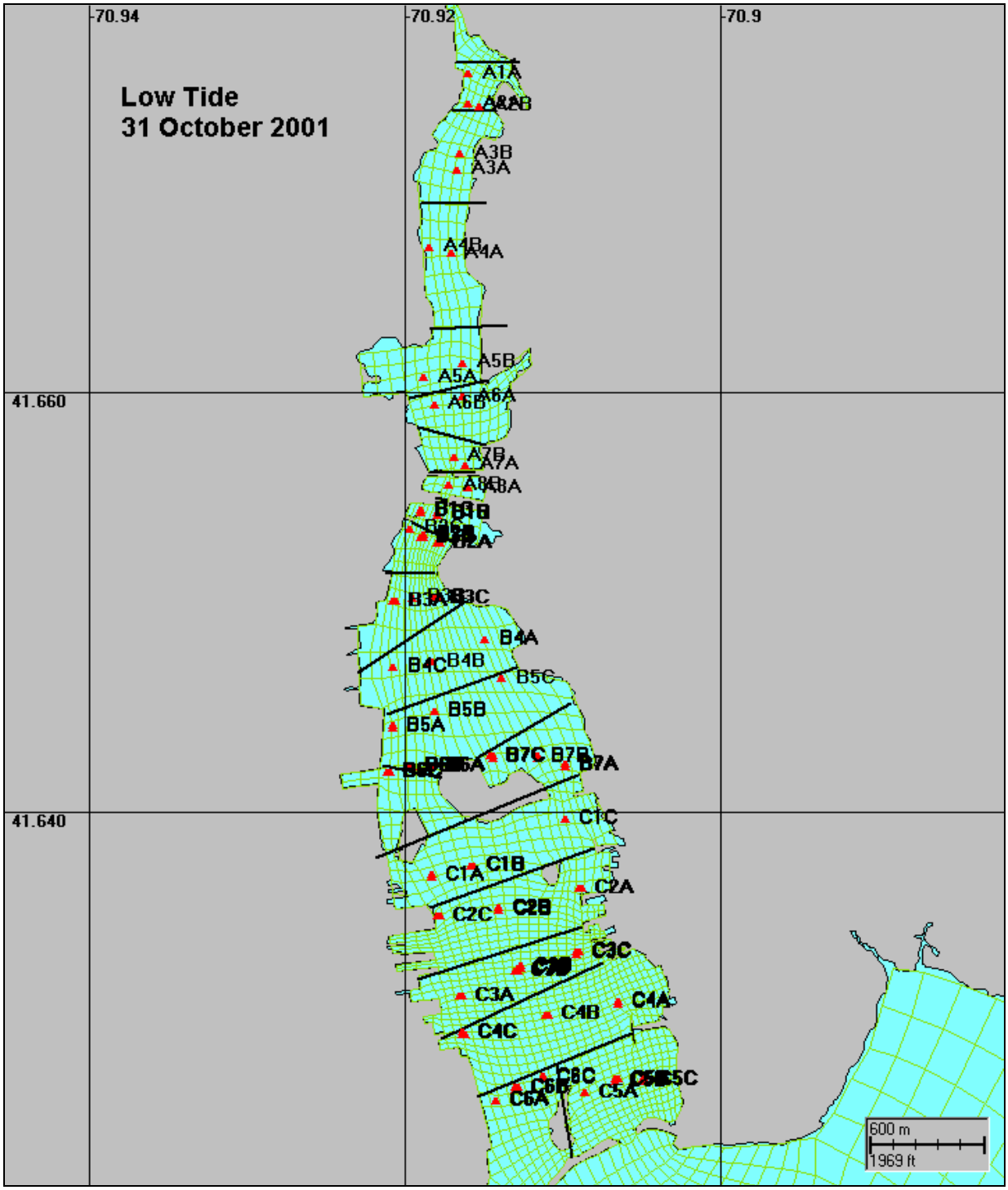

Figure A-2. Salinity sampling stations during low tide (11:41 am) 31 October 2001.

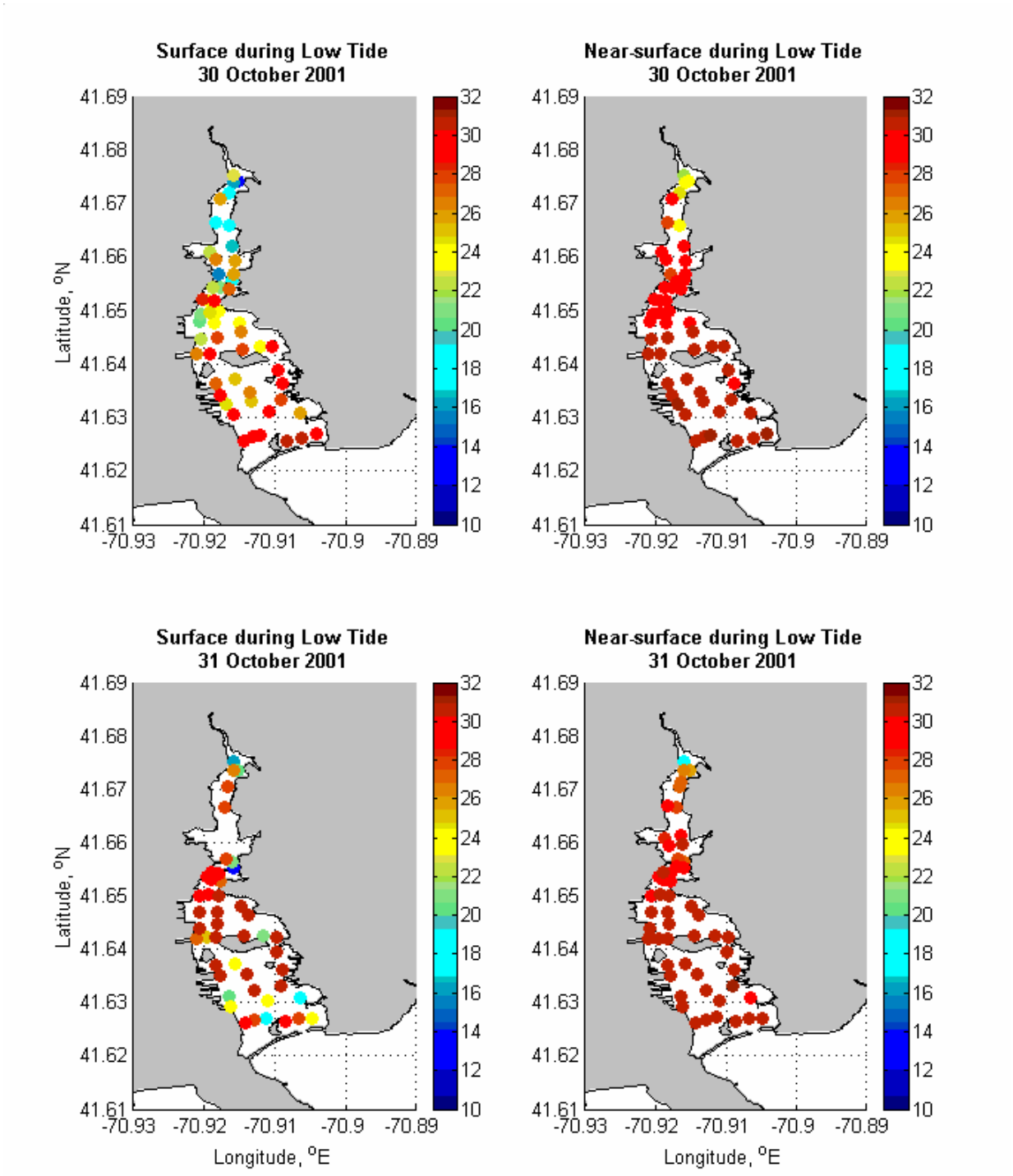

Figure A-3. Scatter plots of salinity at surface (~18 cm) and next the surface (~38 cm) during low tide on 30 and 31 October 2001.

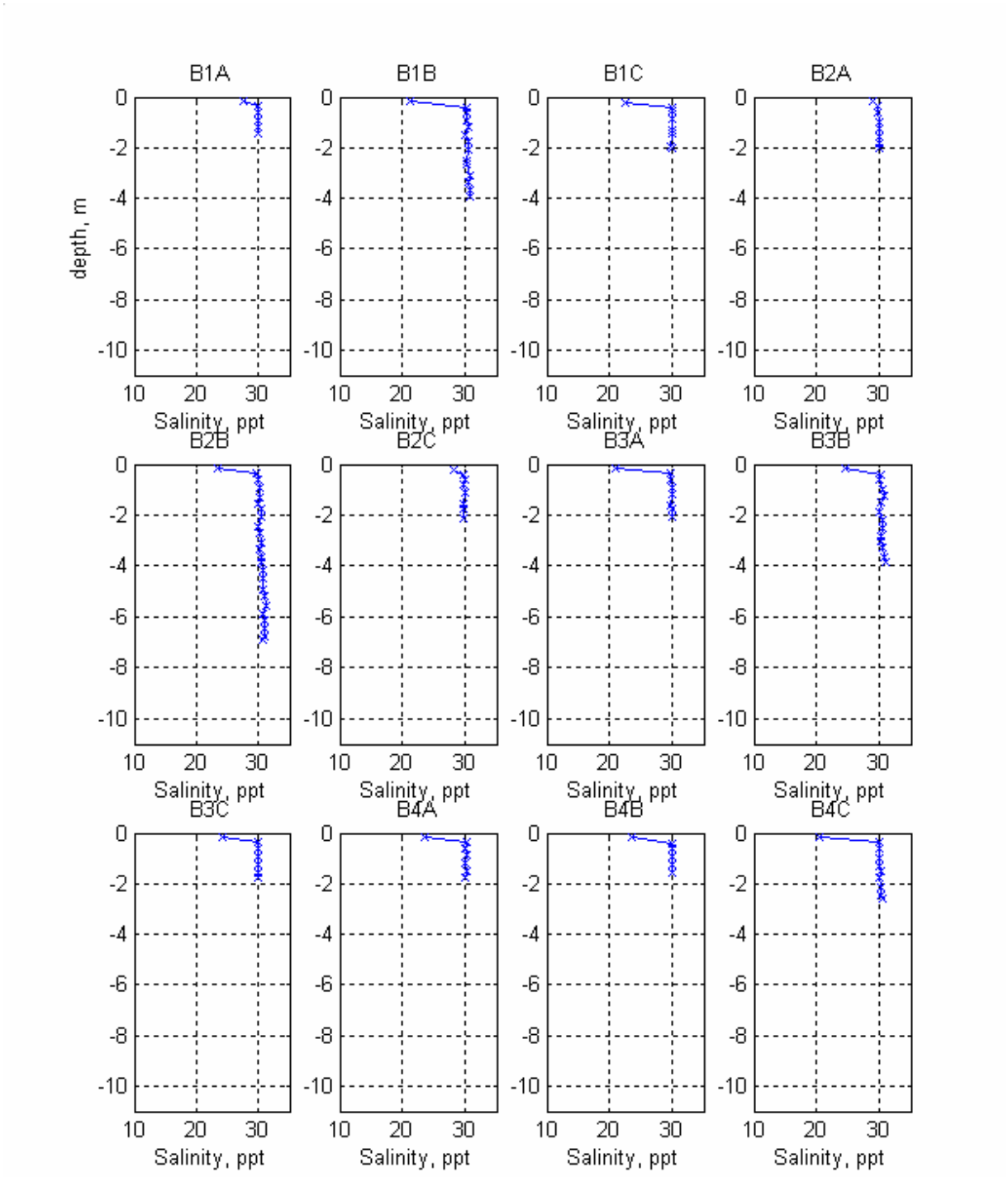

Figure A-4a: Salinity profile each sampling station collected during low tide on 30 October 2001.

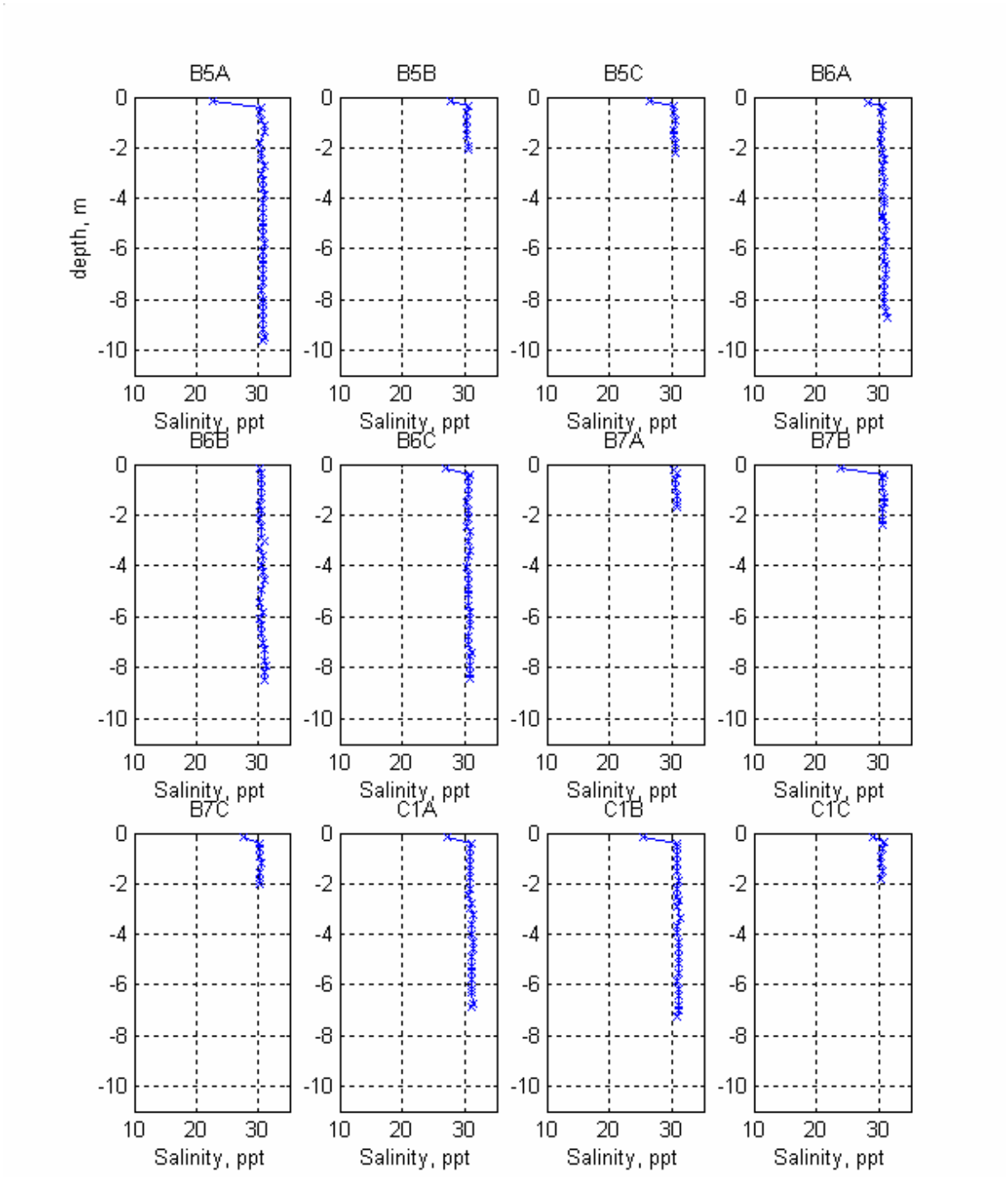

Figure A-4b: Salinity profile each sampling station collected during low tide on 30 October 2001.

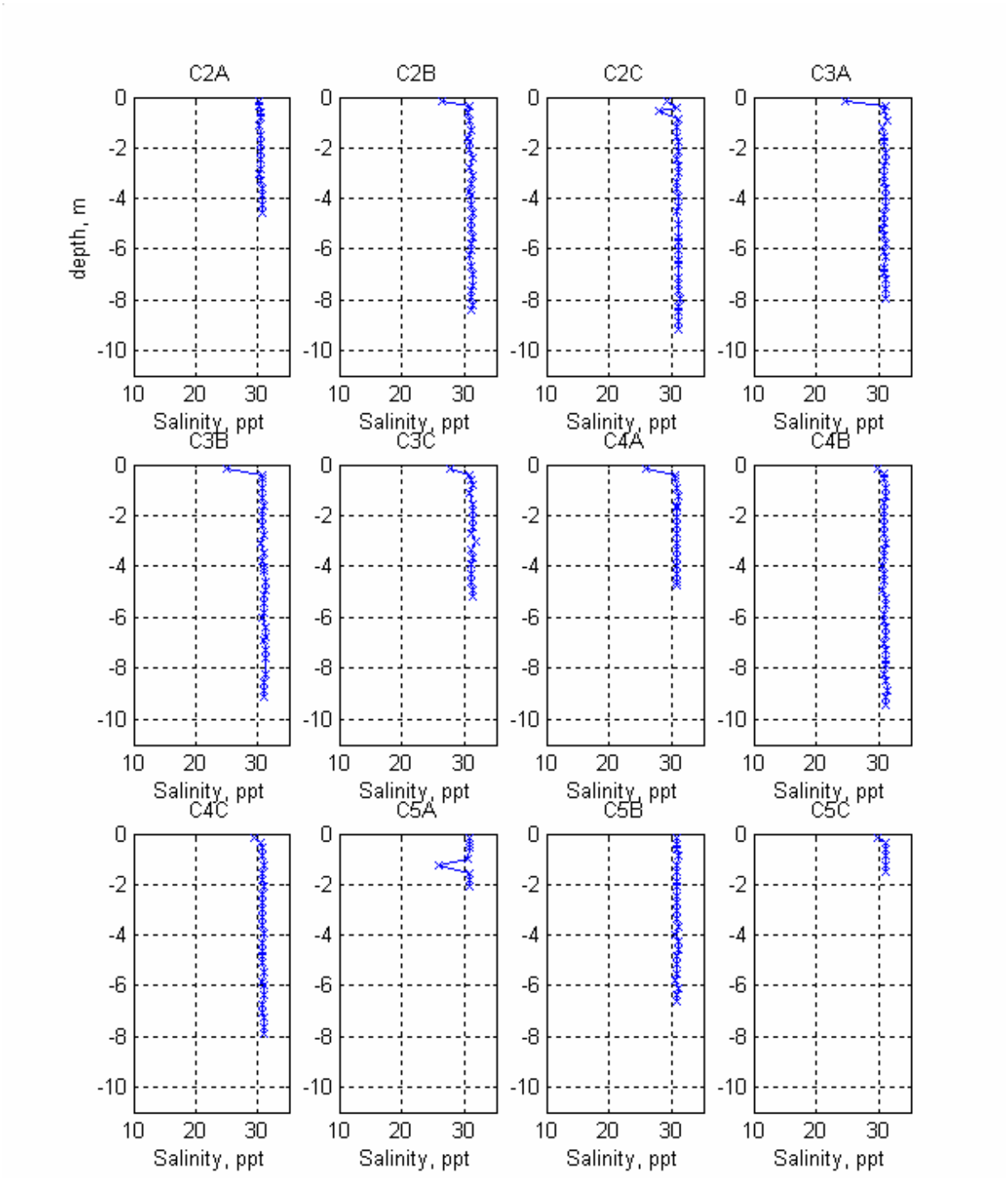

Figure A-4c. Salinity profile each sampling station collected during low tide on 30 October 2001.

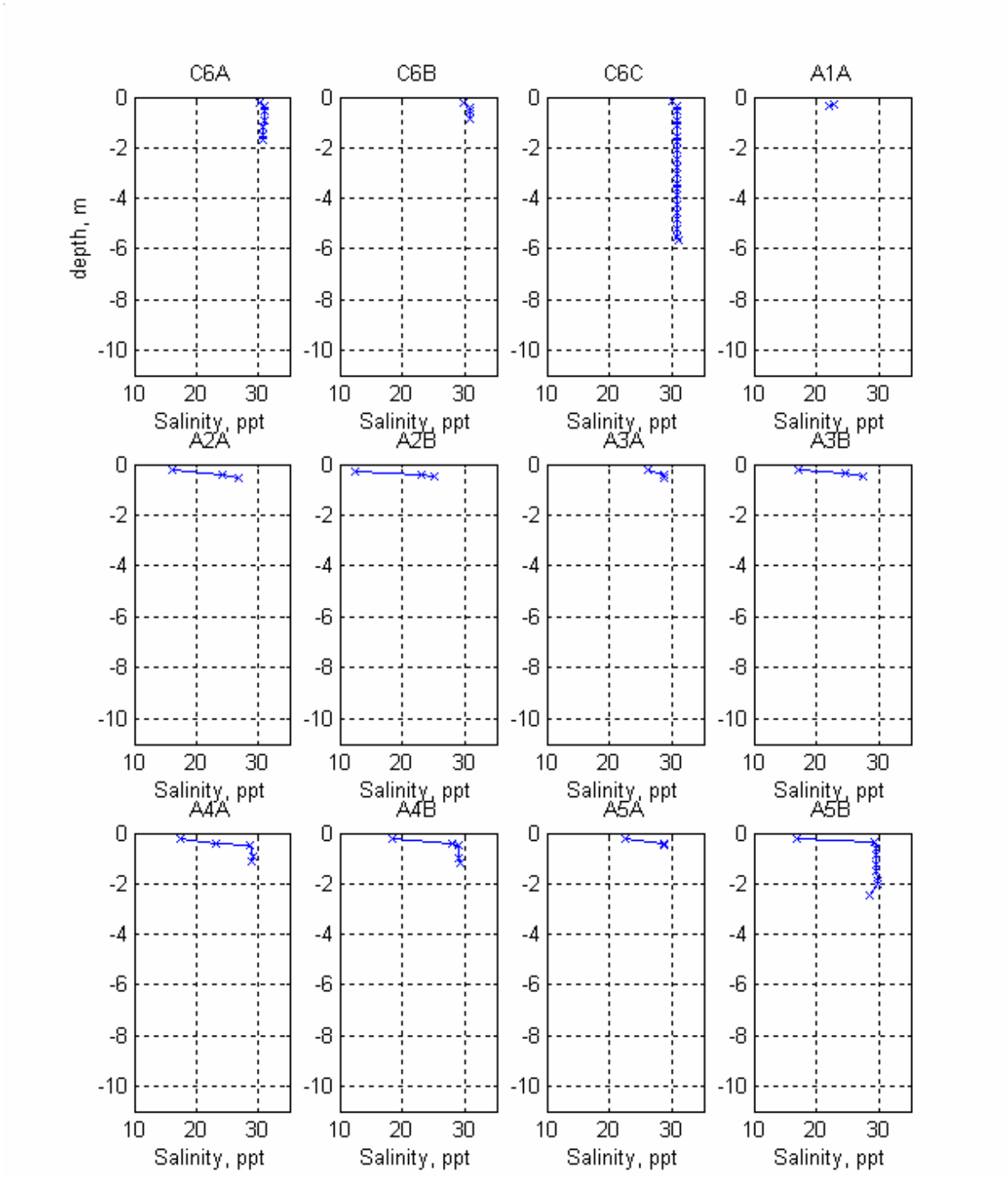

Figure A-4d. Salinity profile each sampling station collected during low tide on 30 October 2001.

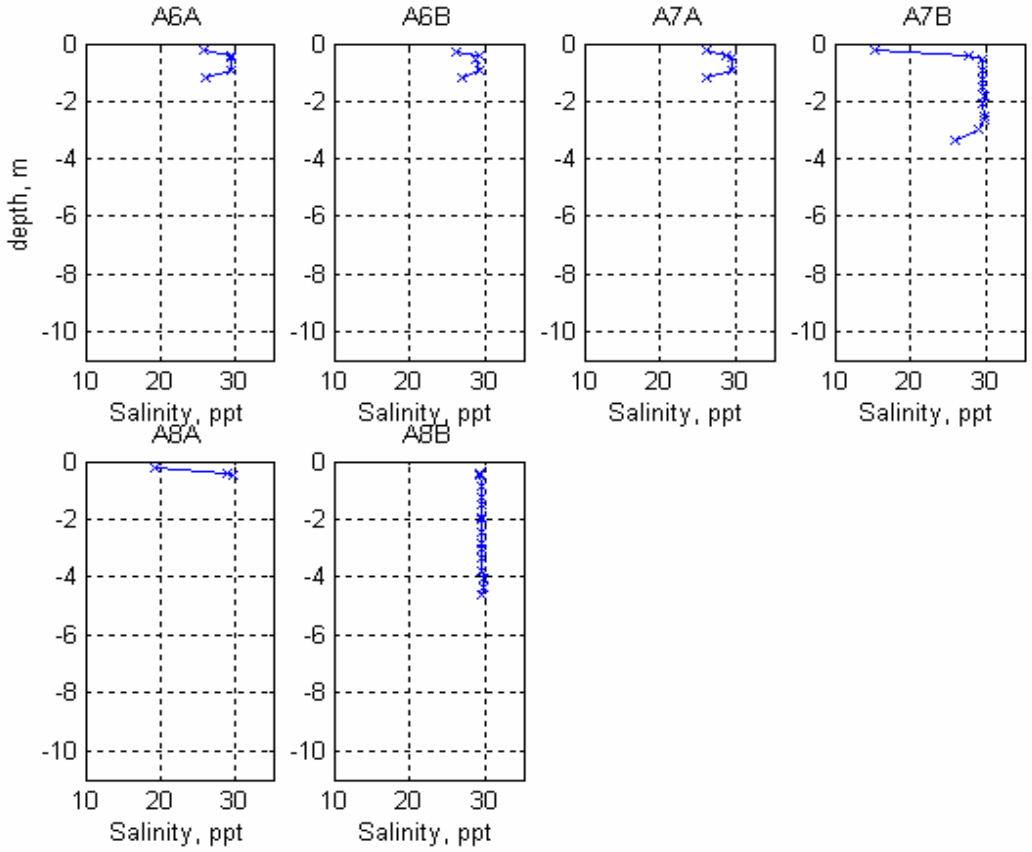

Figure A-4e. Salinity profile each sampling station collected during low tide on 30 October 2001.

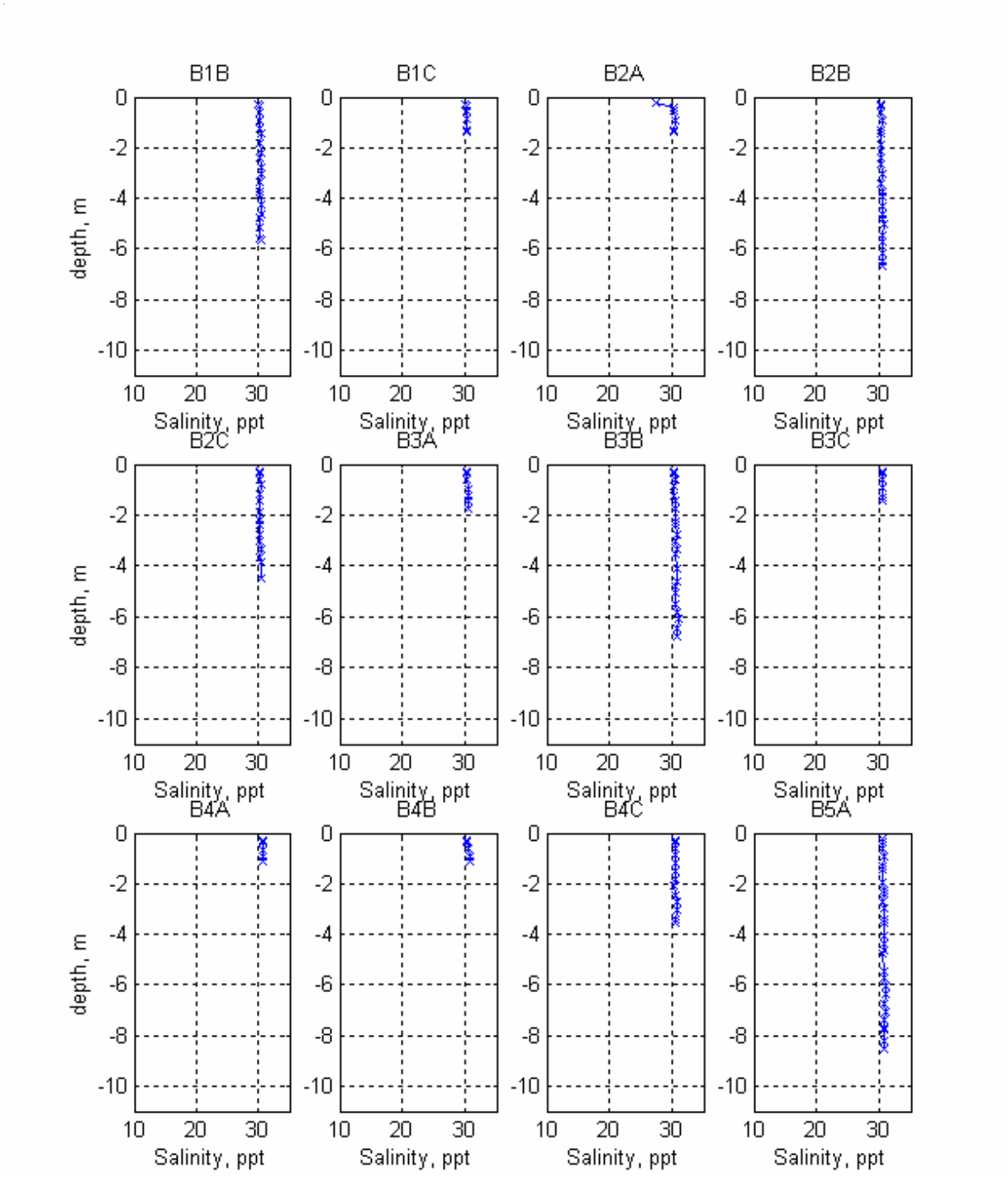

Figure A-5a. Salinity profile each station collected during low tide on 31 October 2001.

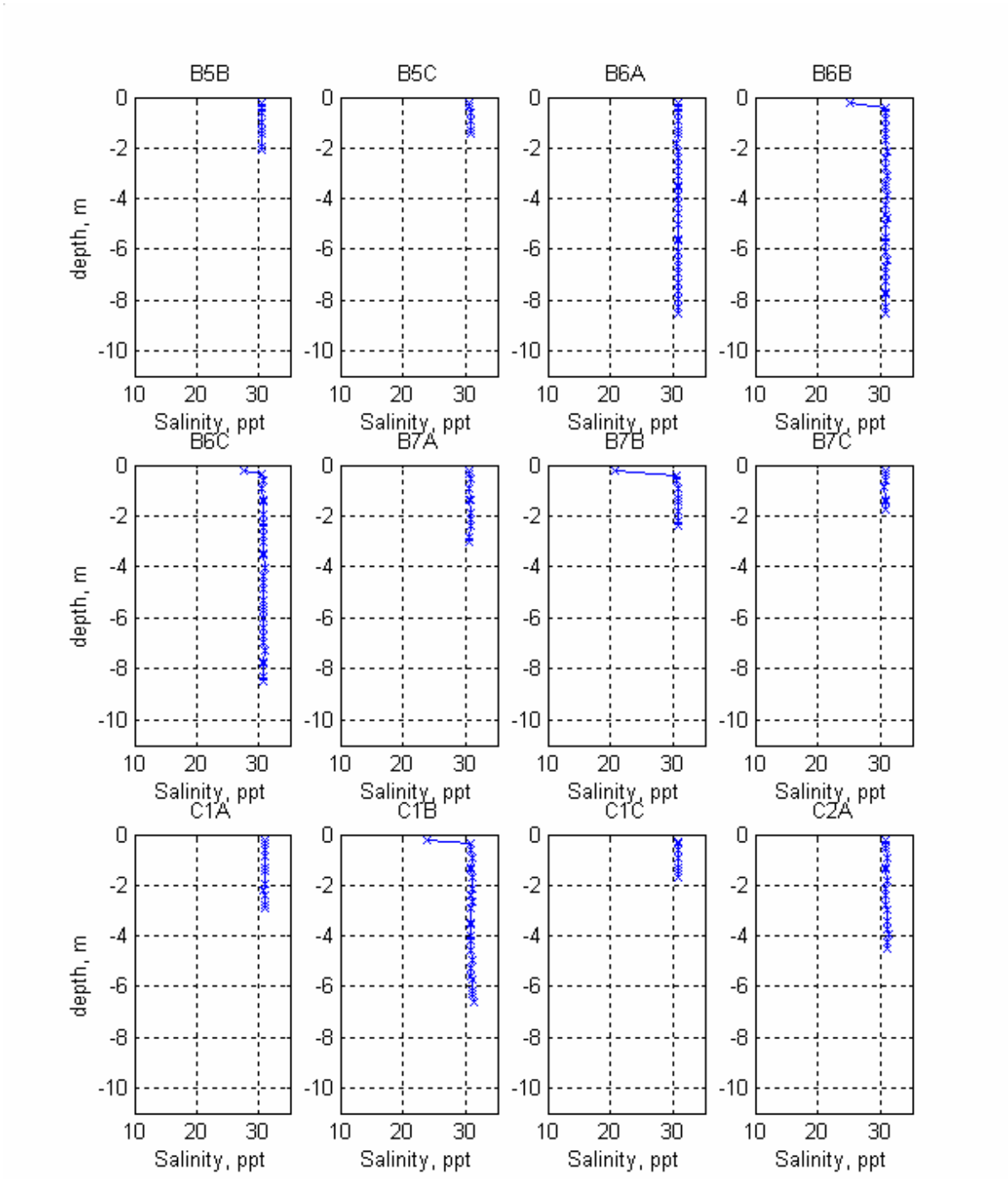

Figure A-5b. Salinity profile each station collected during low tide on 31 October 2001.

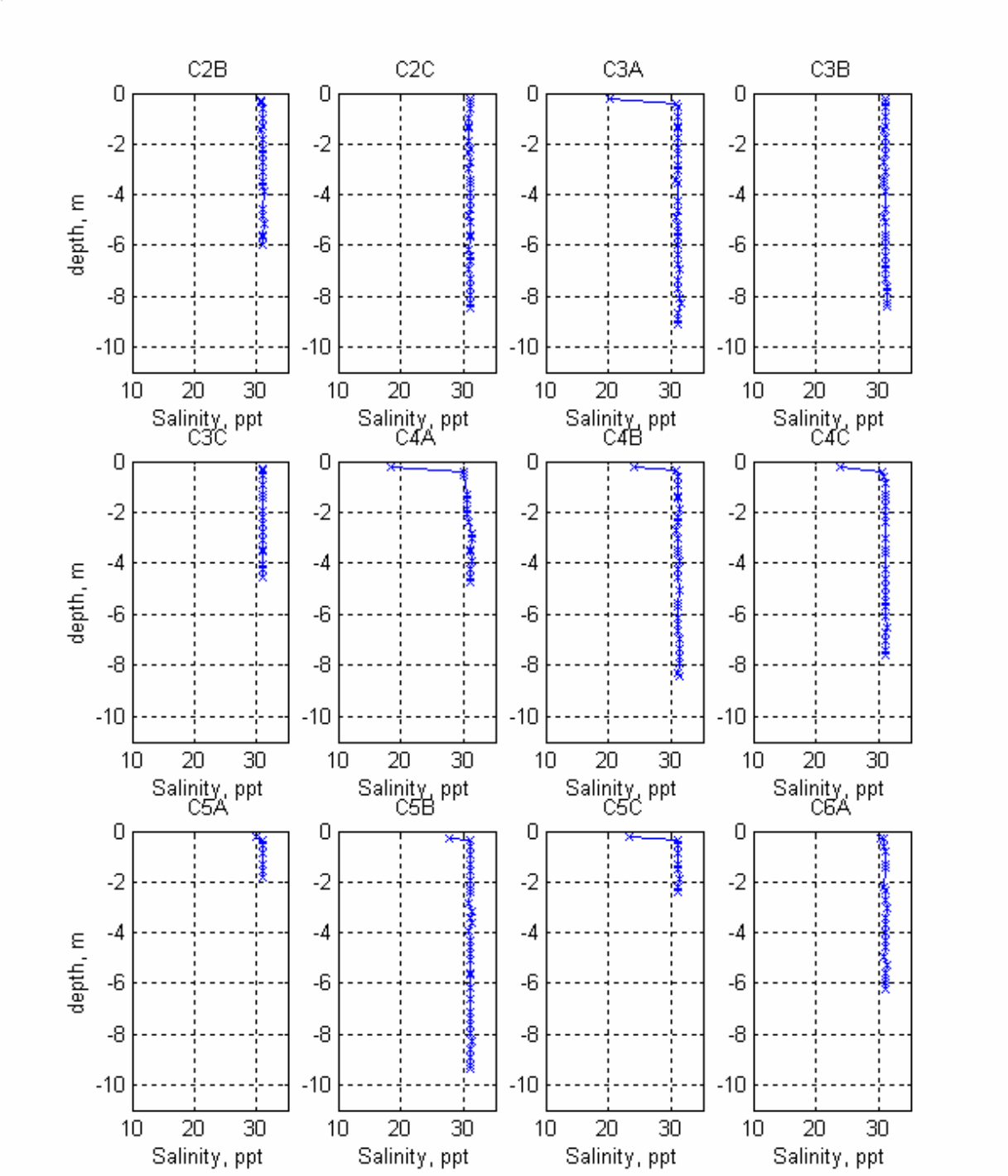

Figure A-5c. Salinity profile each station collected during low tide on 31 October 2001.

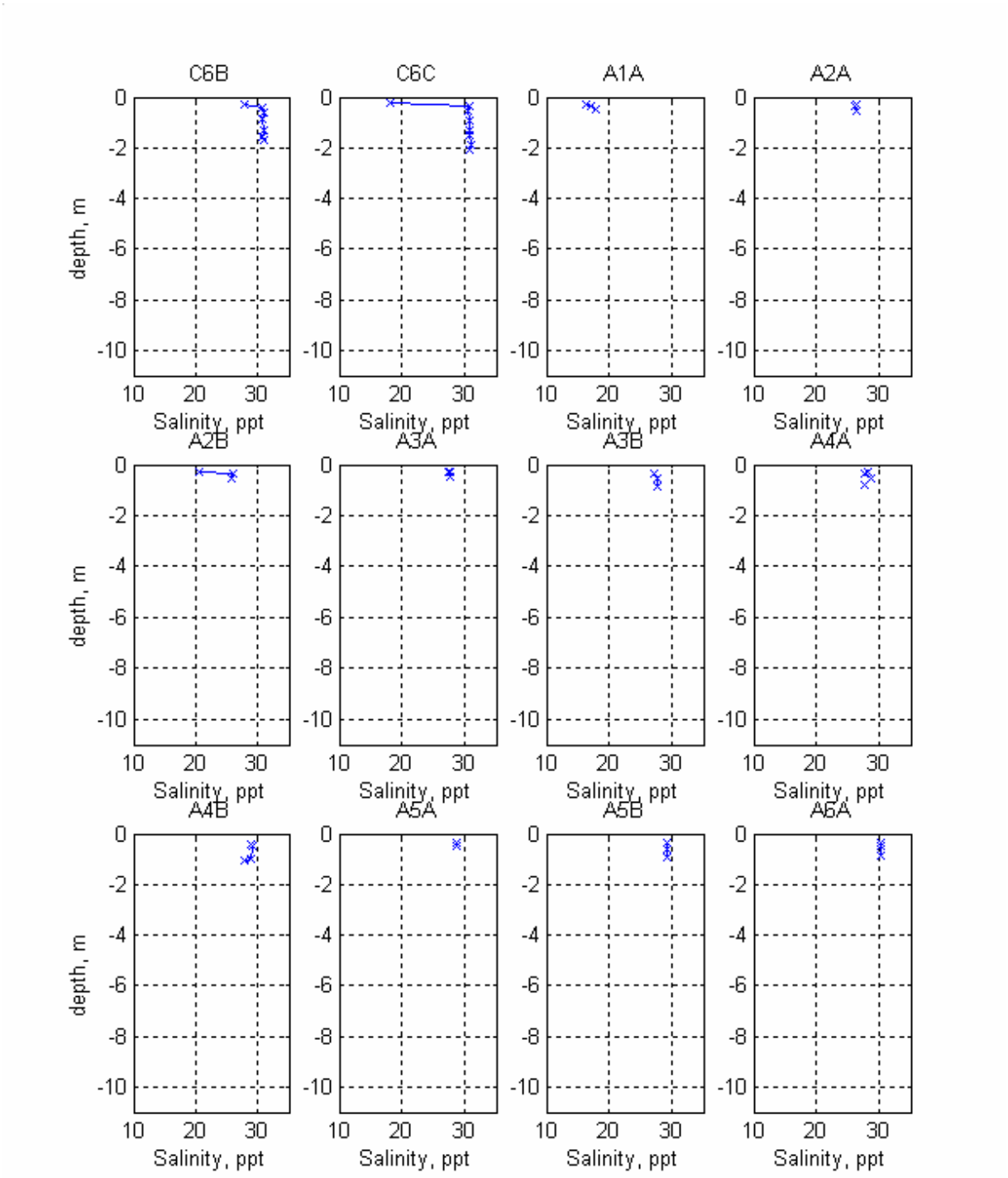

Figure A-5d. Salinity profile each station collected during low tide on 31 October 2001.

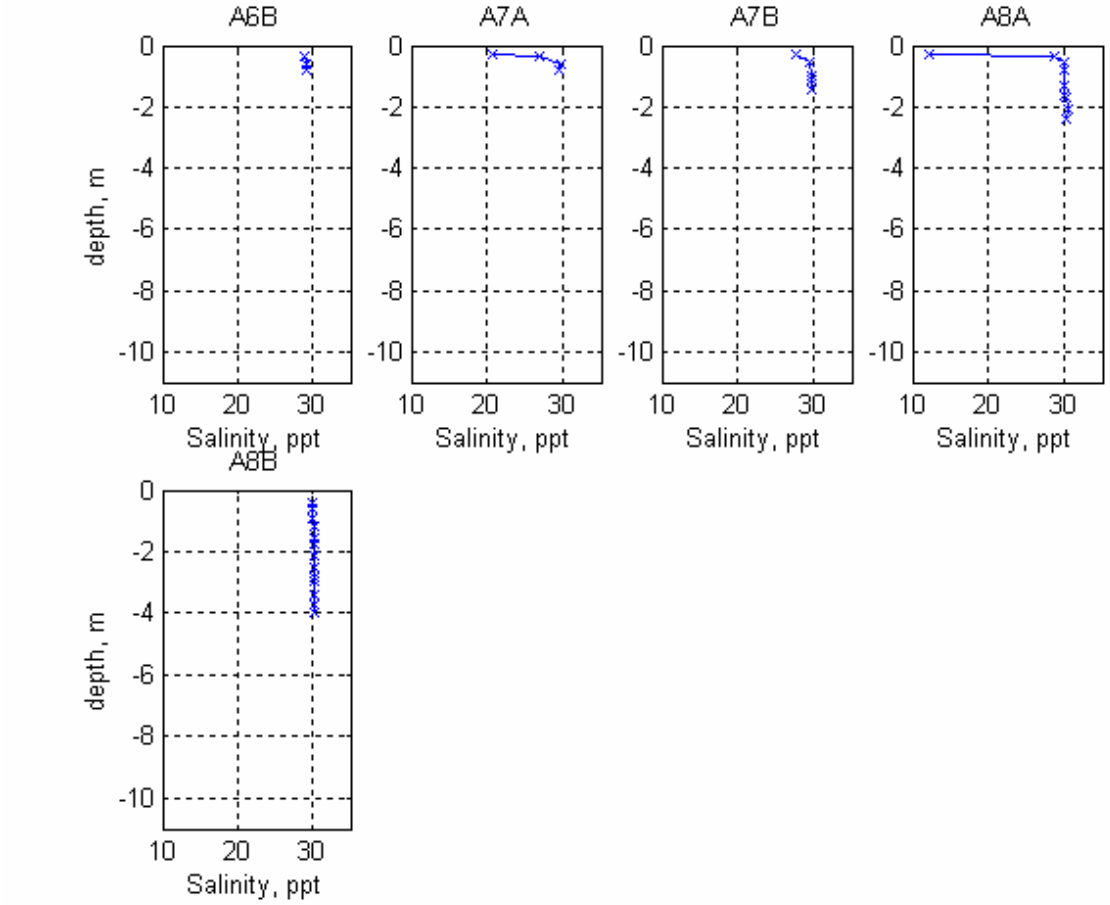

Figure A-5e. Salinity profile each station collected during low tide on 31 October 2001.

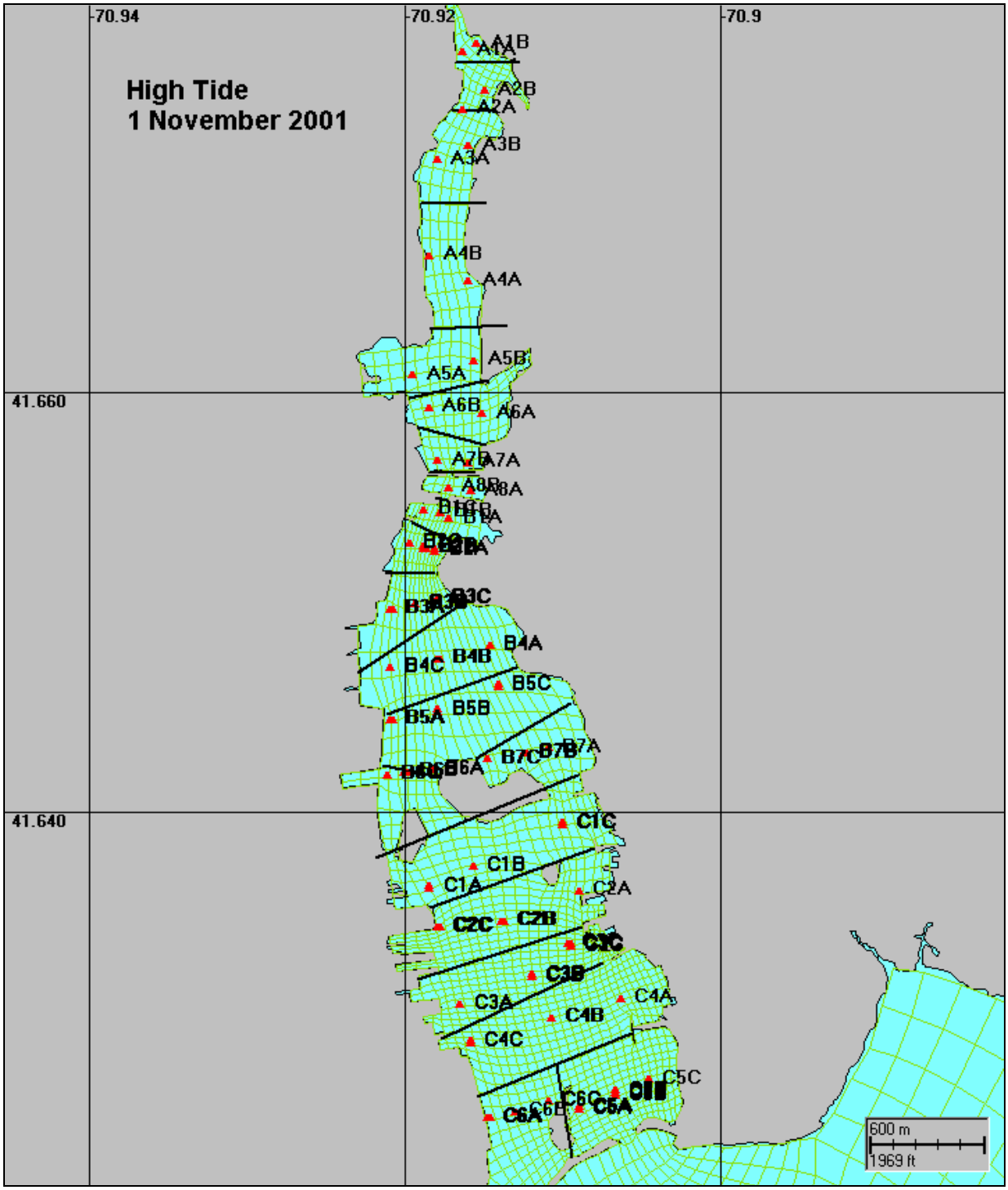

Figure A-6. Salinity sampling stations during high tide (06:27 am) on 1 November 2001.

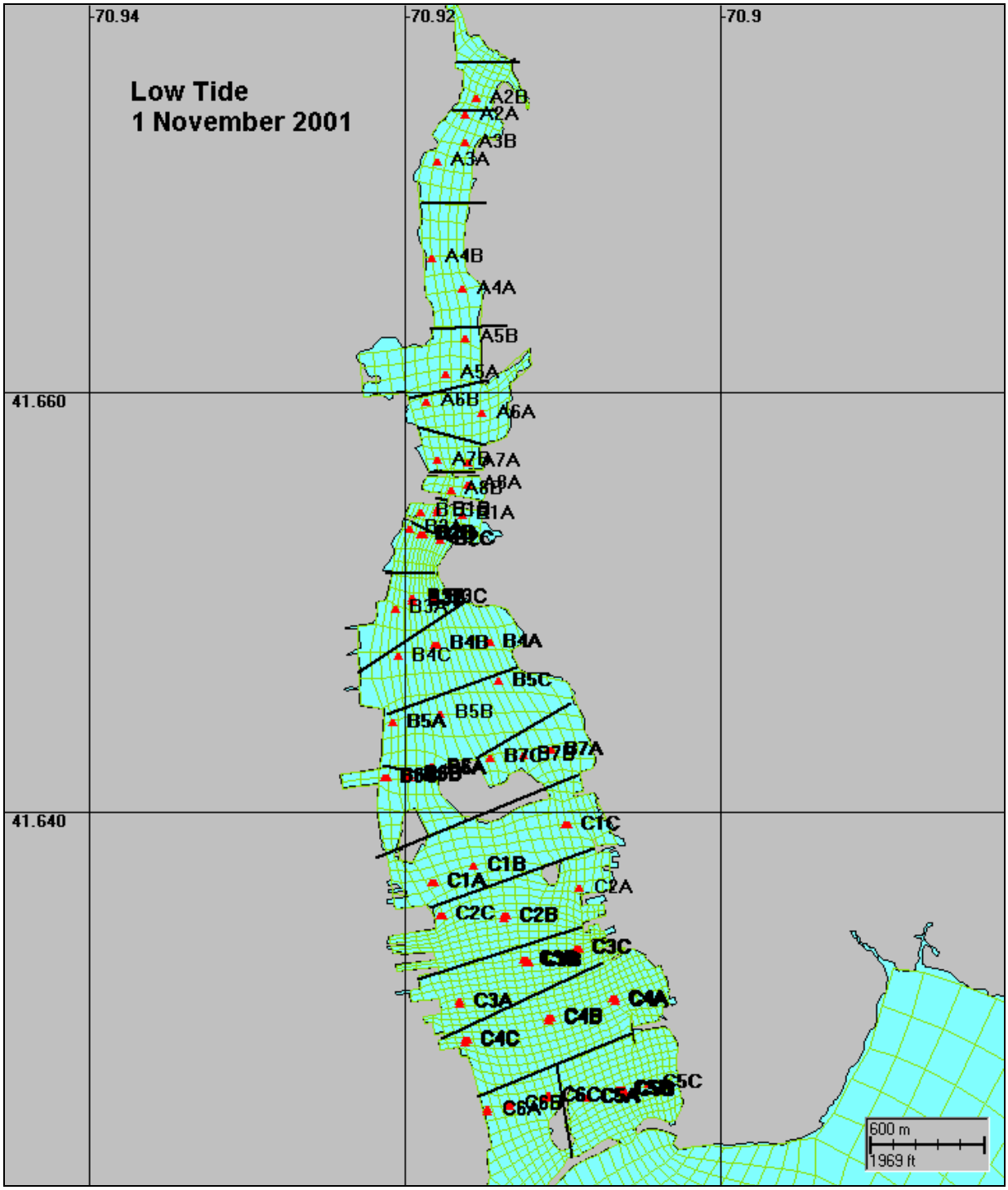

Figure A-7. Salinity sampling stations during low tide (12:09 pm) on 1 November 2001.

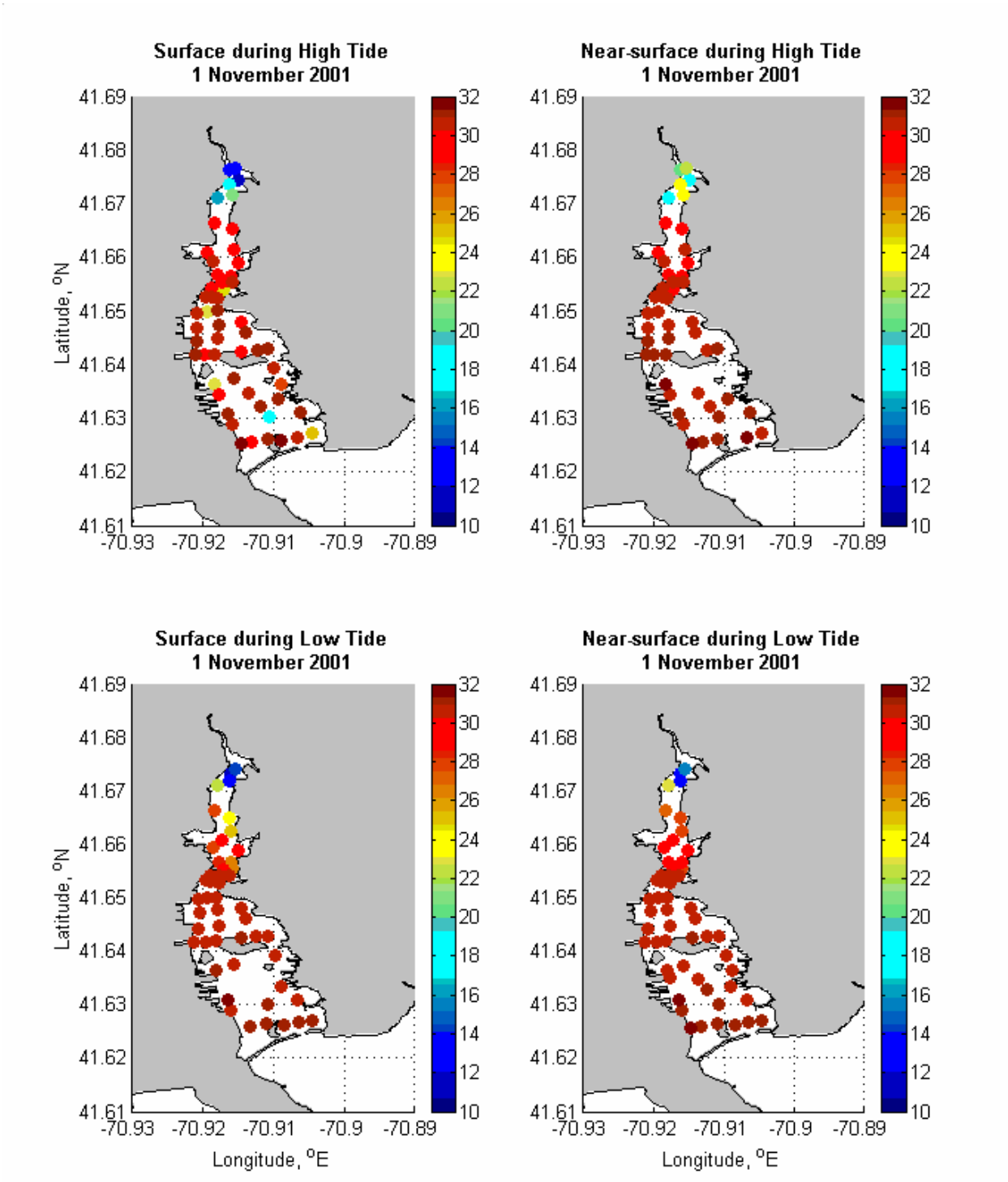

Figure A-8. Scatter plots of salinity at surface (~18 cm) and next the surface (~38 cm) during low tide on 30 and 31 October 2001.

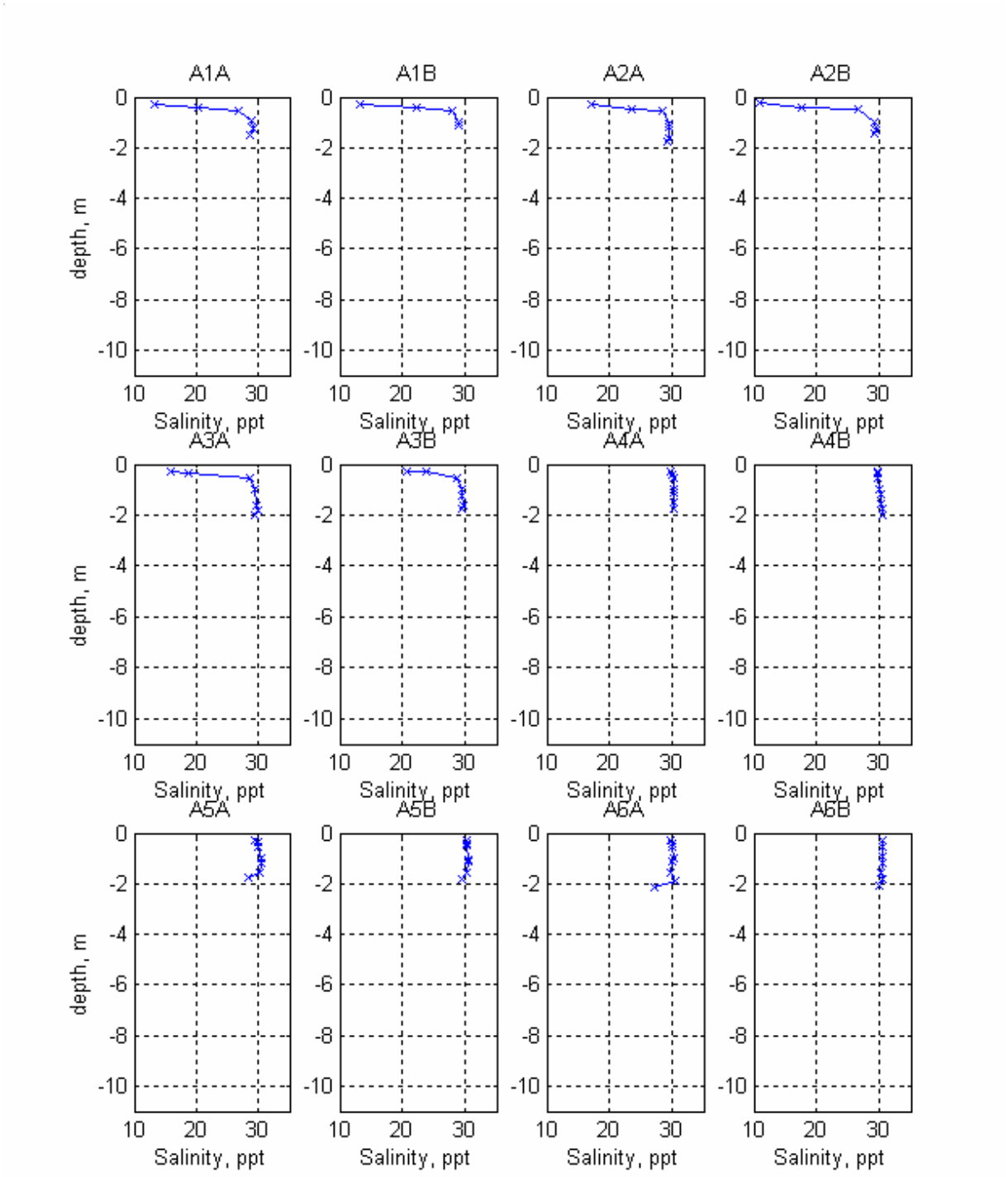

Figure A-9a. Salinity profile each sampling station collected during high tide on 1 November 2001.

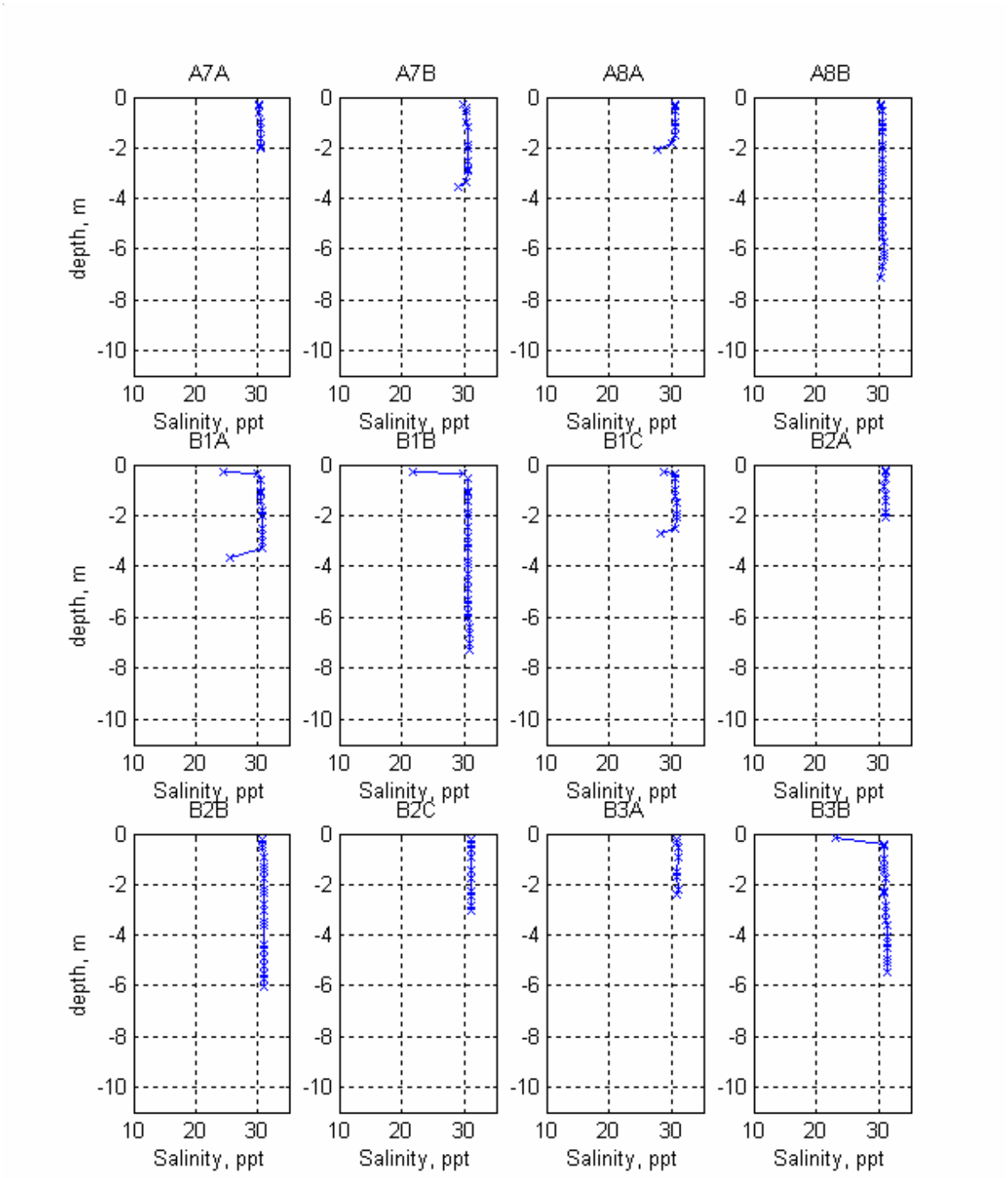

Figure A-9b. Salinity profile each sampling station collected during high tide on 1 November 2001.

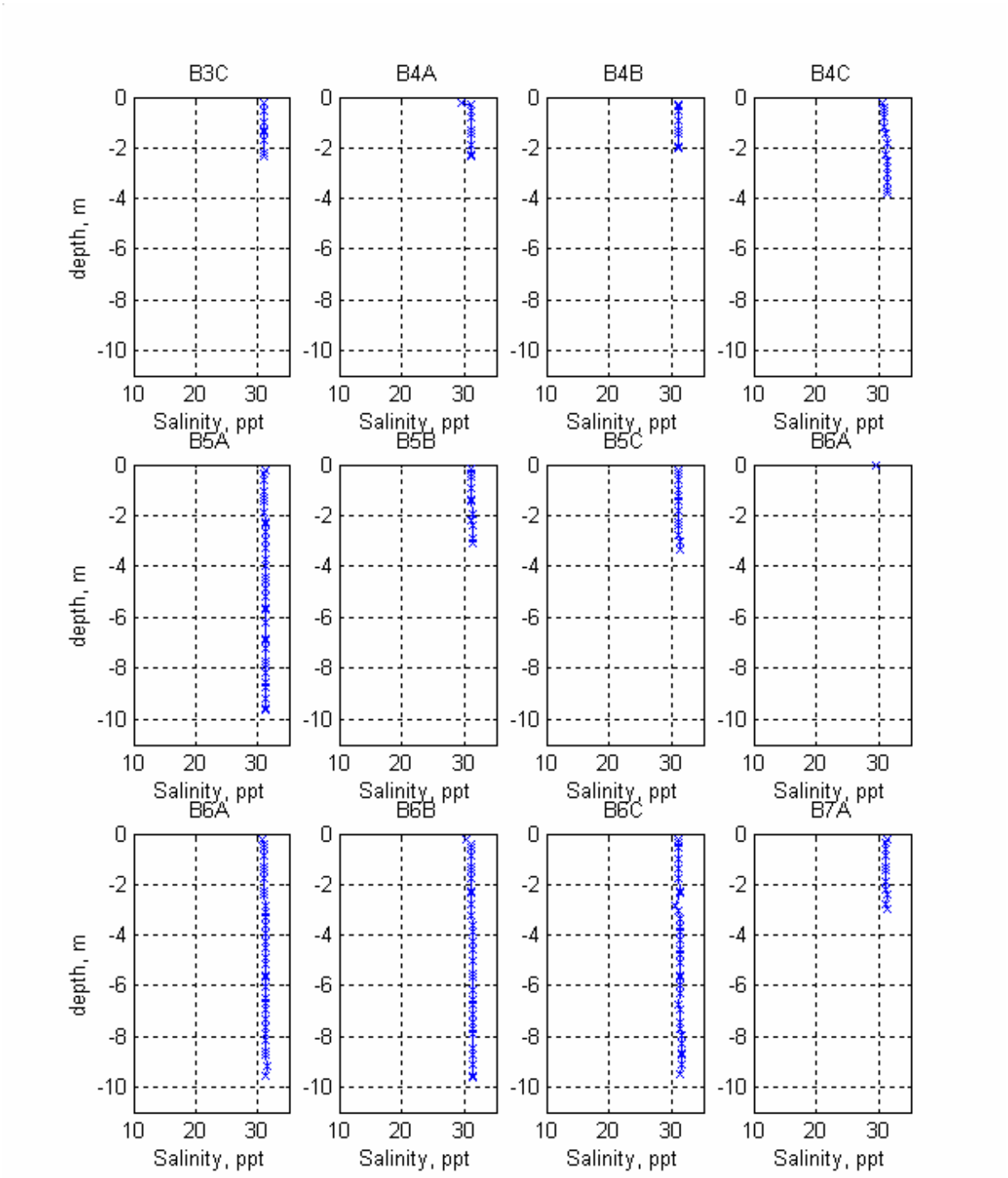

Figure A-9c. Salinity profile each sampling station collected during high tide on 1 November 2001.

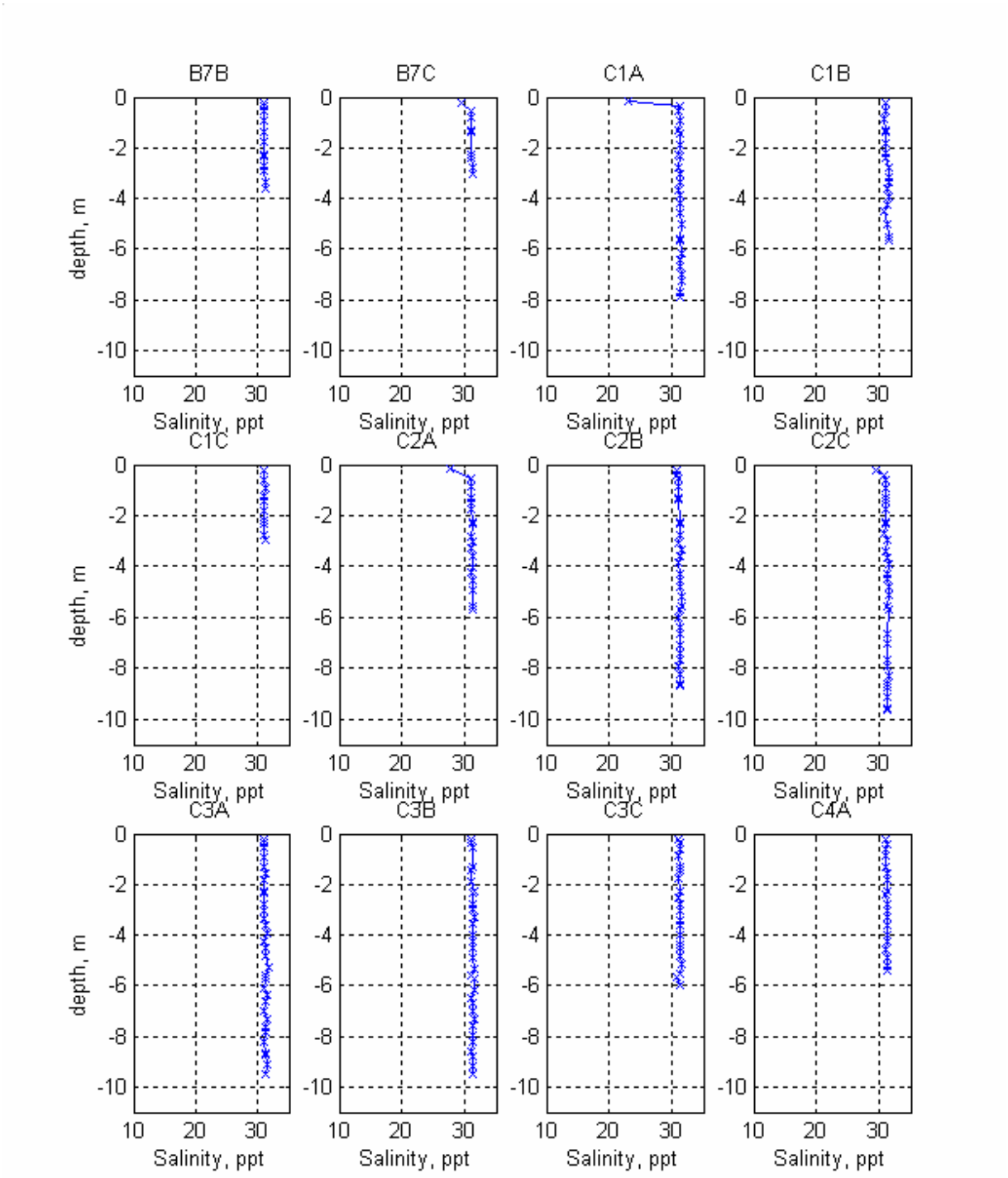

Figure A-9d. Salinity profile each sampling station collected during high tide on 1 November 2001.

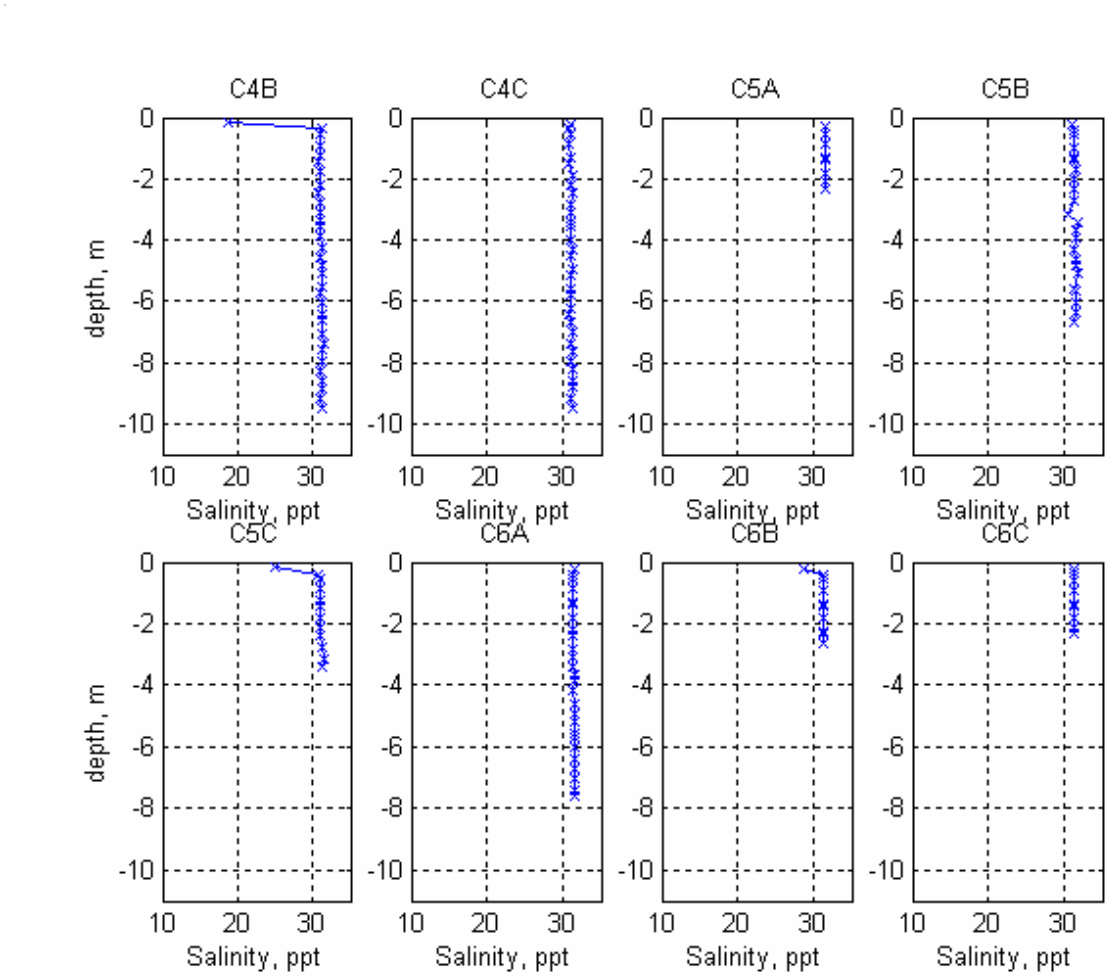

Figure A-9e. Salinity profile each sampling station collected during high tide on 1 November 2001.

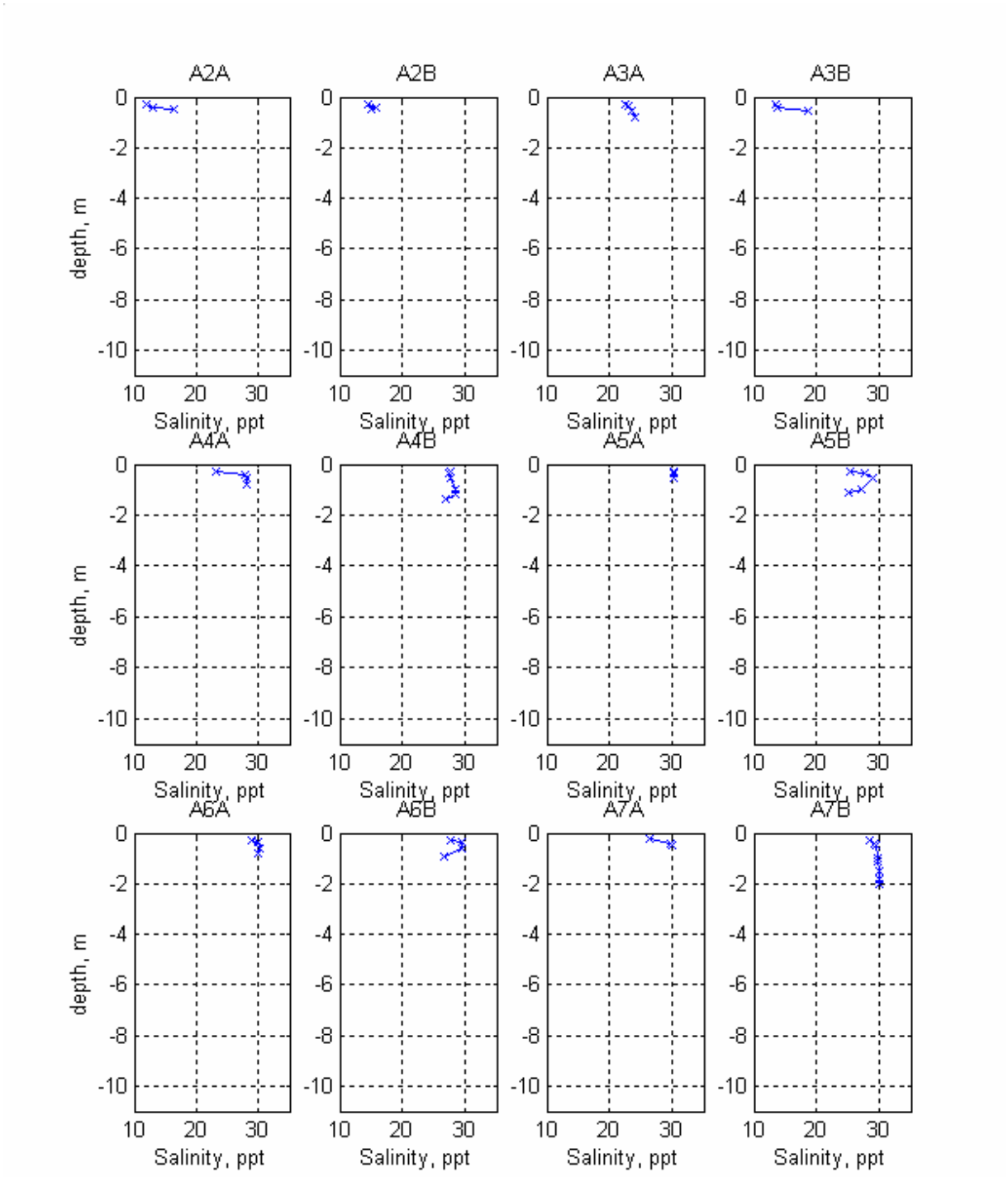

Figure A-10a. Salinity profile each station collected during low tide on 1 November 2001.

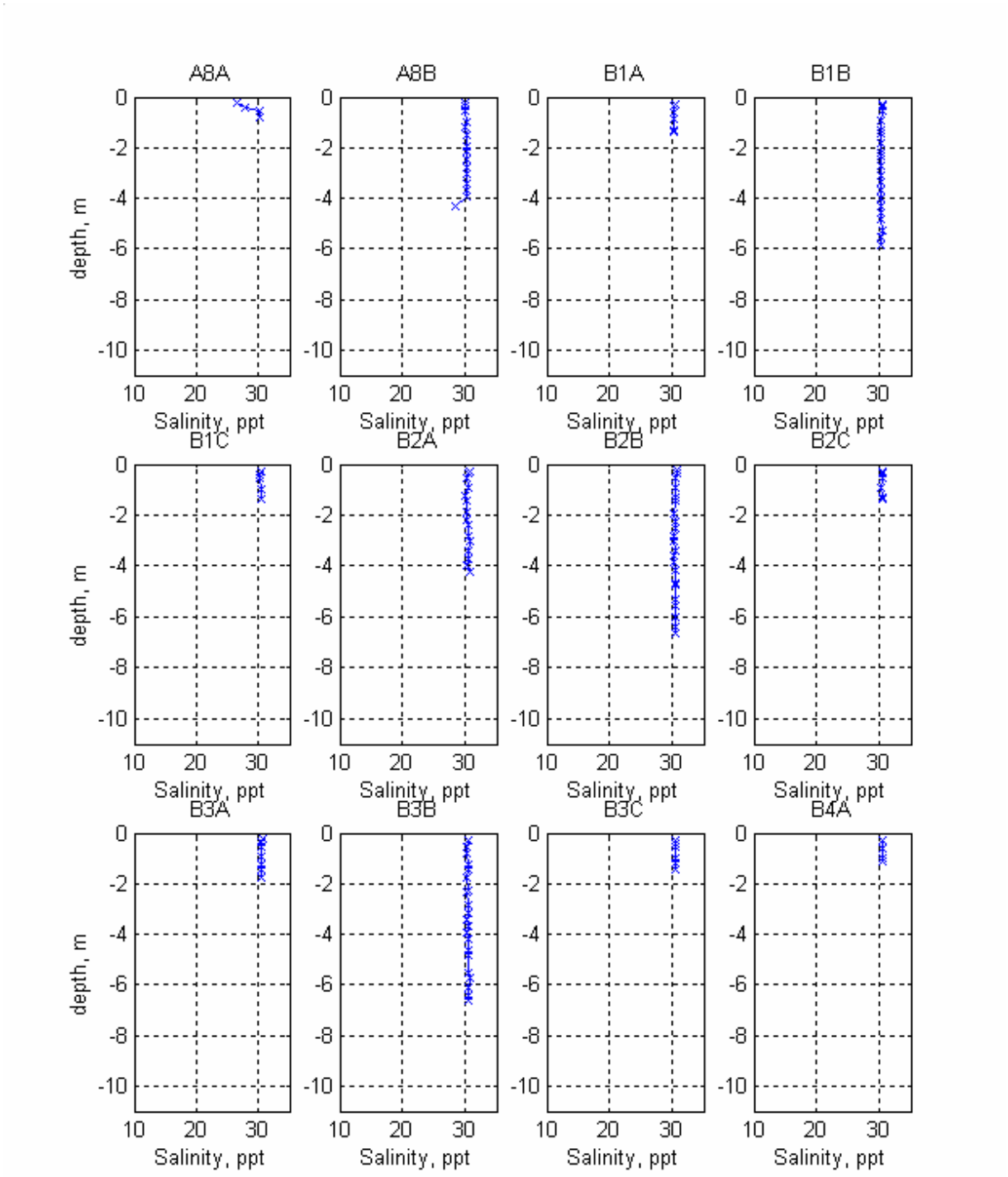

Figure A-10b. Salinity profile each station collected during low tide on 1 November 2001.

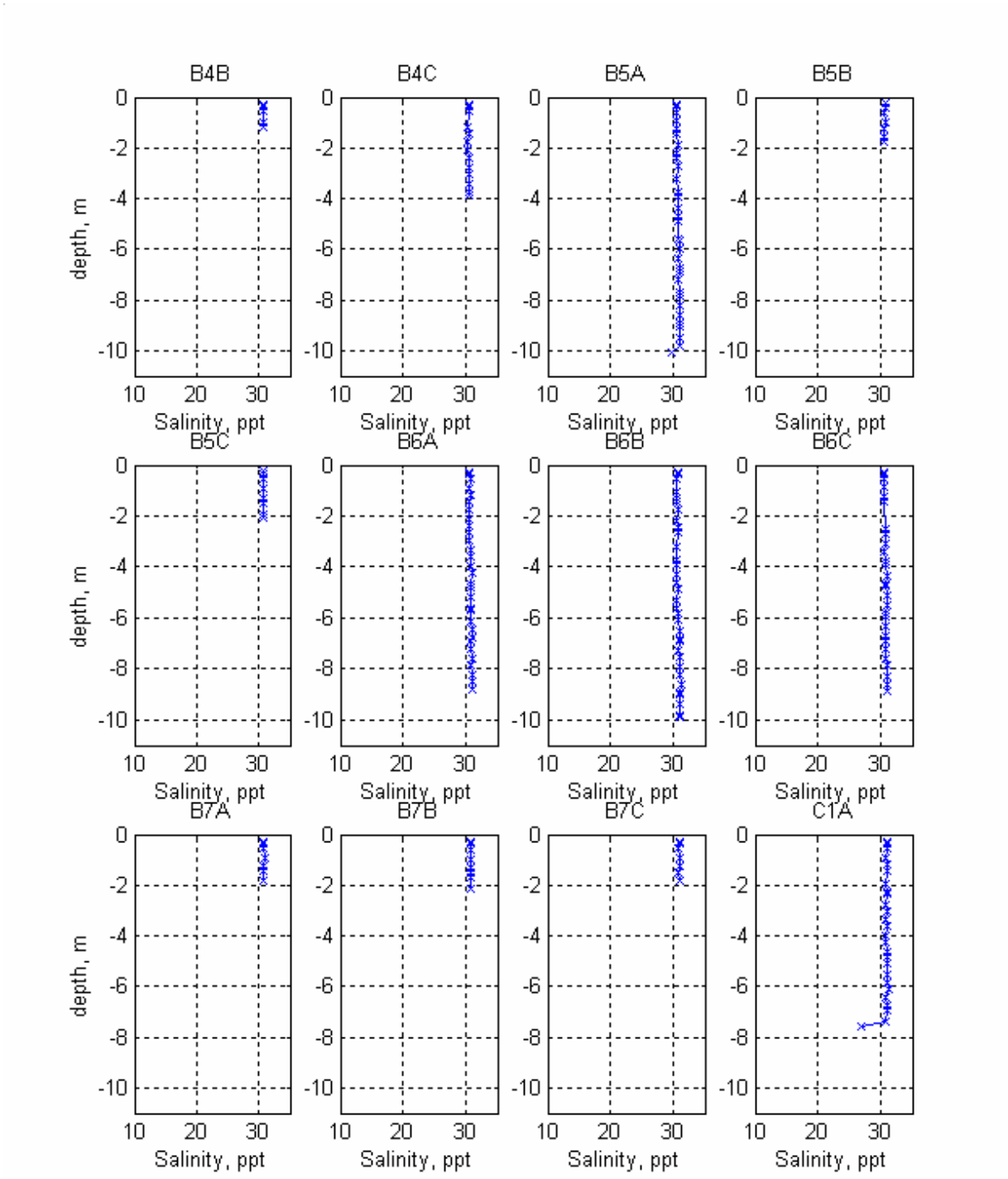

Figure A-10c. Salinity profile each station collected during low tide on 1 November 2001.

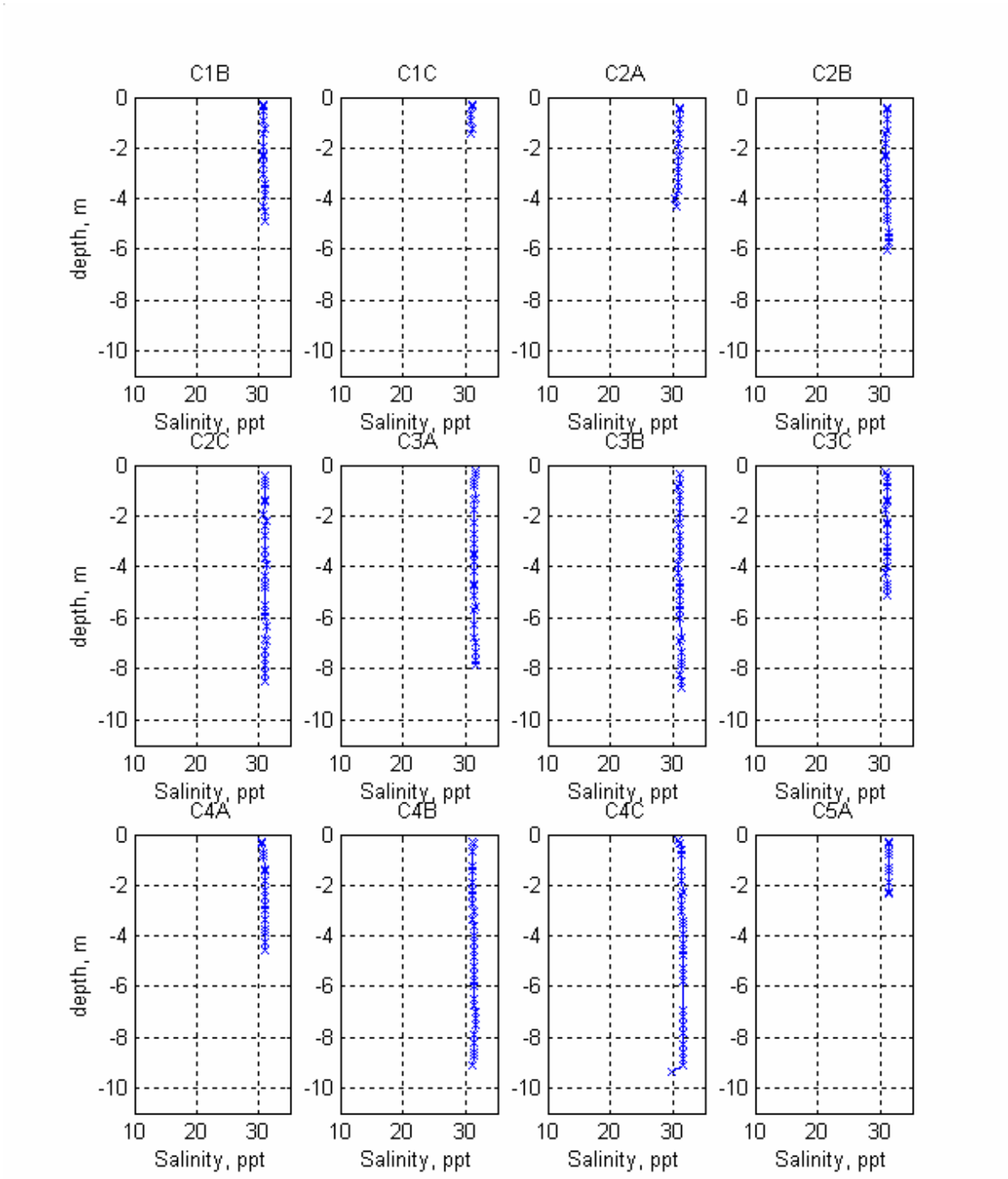

Figure A-10d. Salinity profile each station collected during low tide on 1 November 2001.

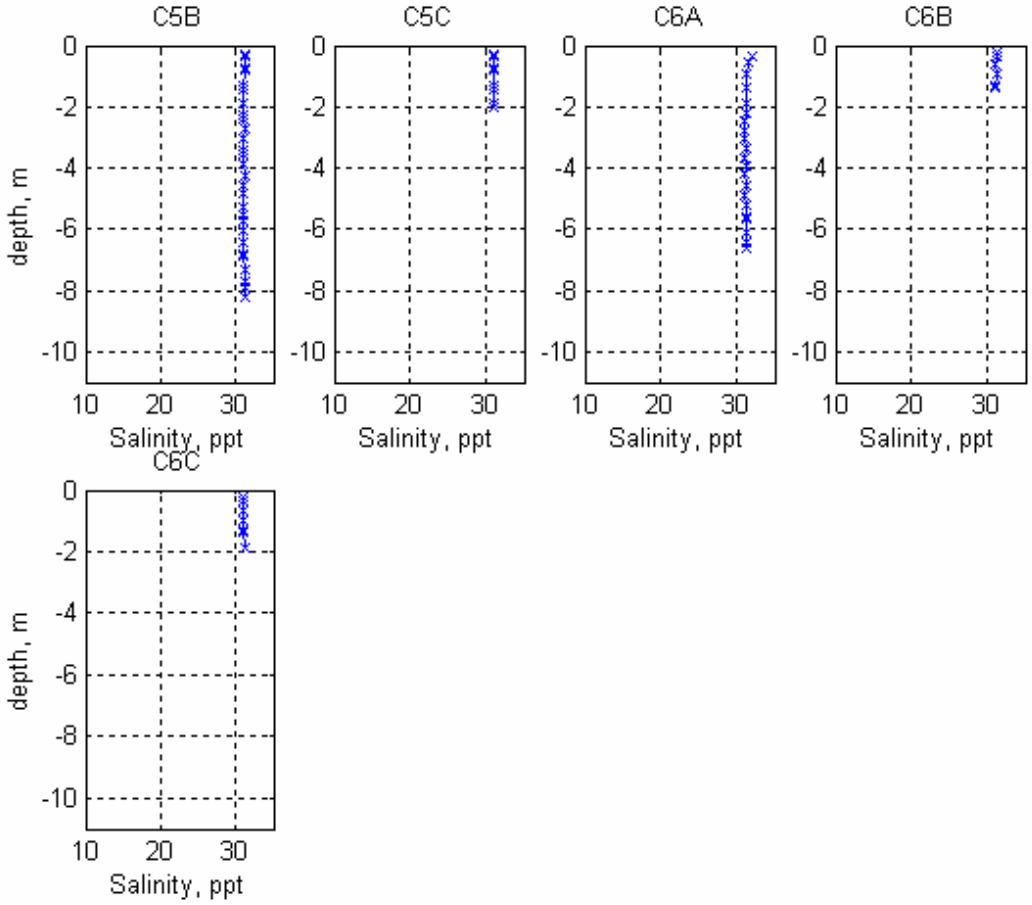

Figure A-10e. Salinity profile each station collected during low tide on 1 November 2001.

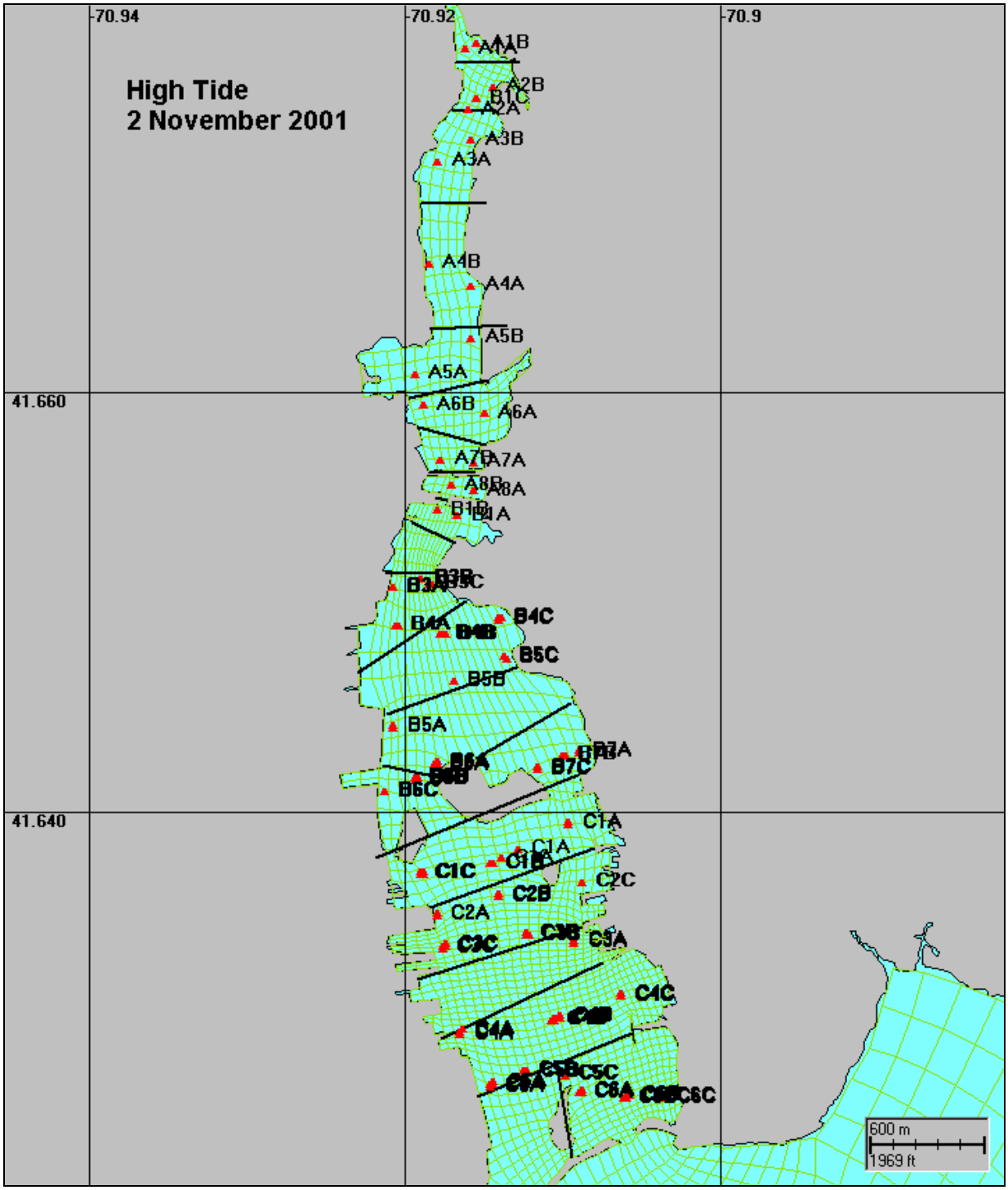

Figure A-11. Salinity sampling stations during high tide (07:07 am) on 2 November 2001.

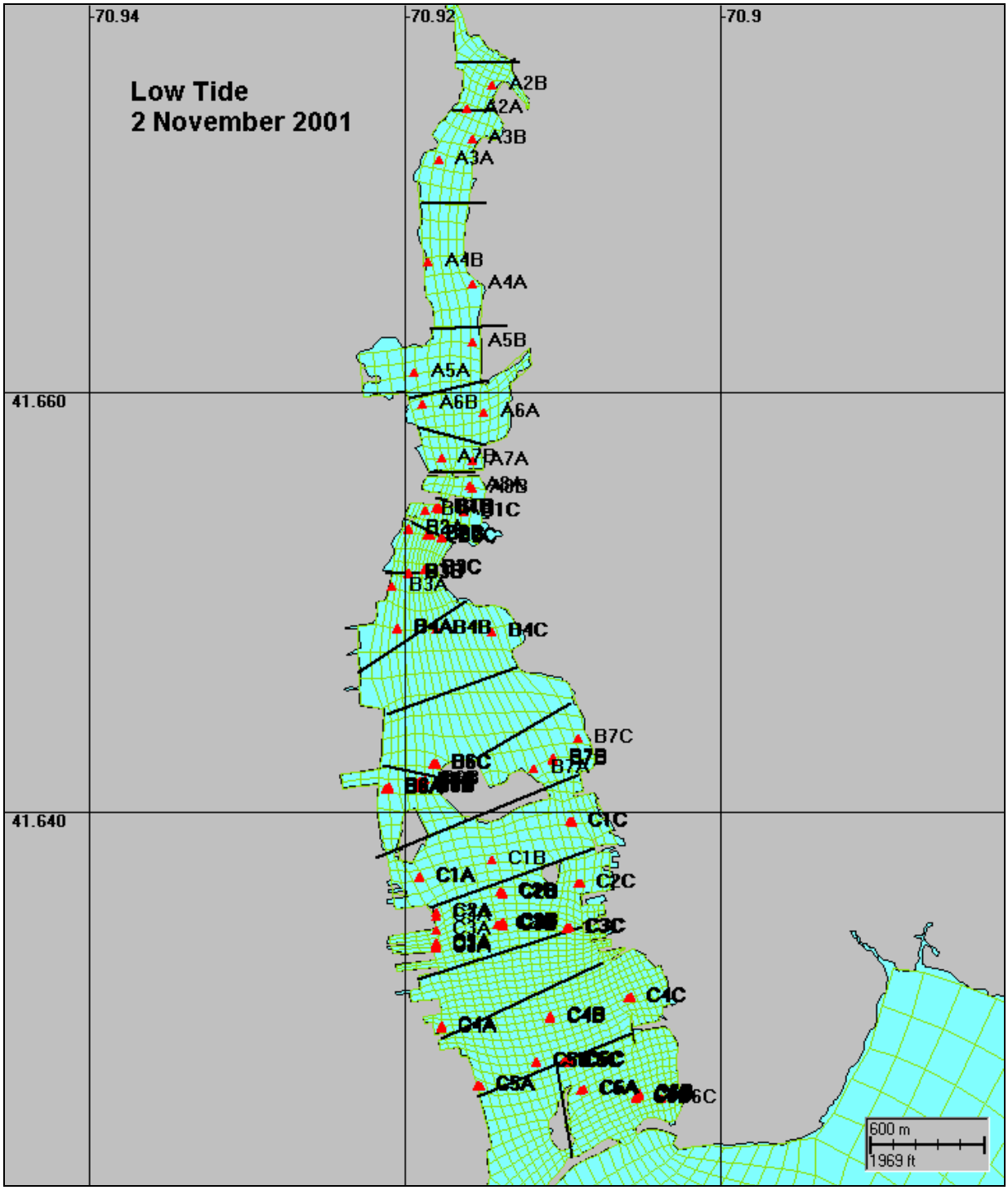

Figure A-12. Salinity sampling stations during low tide (01:14 pm) on 2 November 2001.

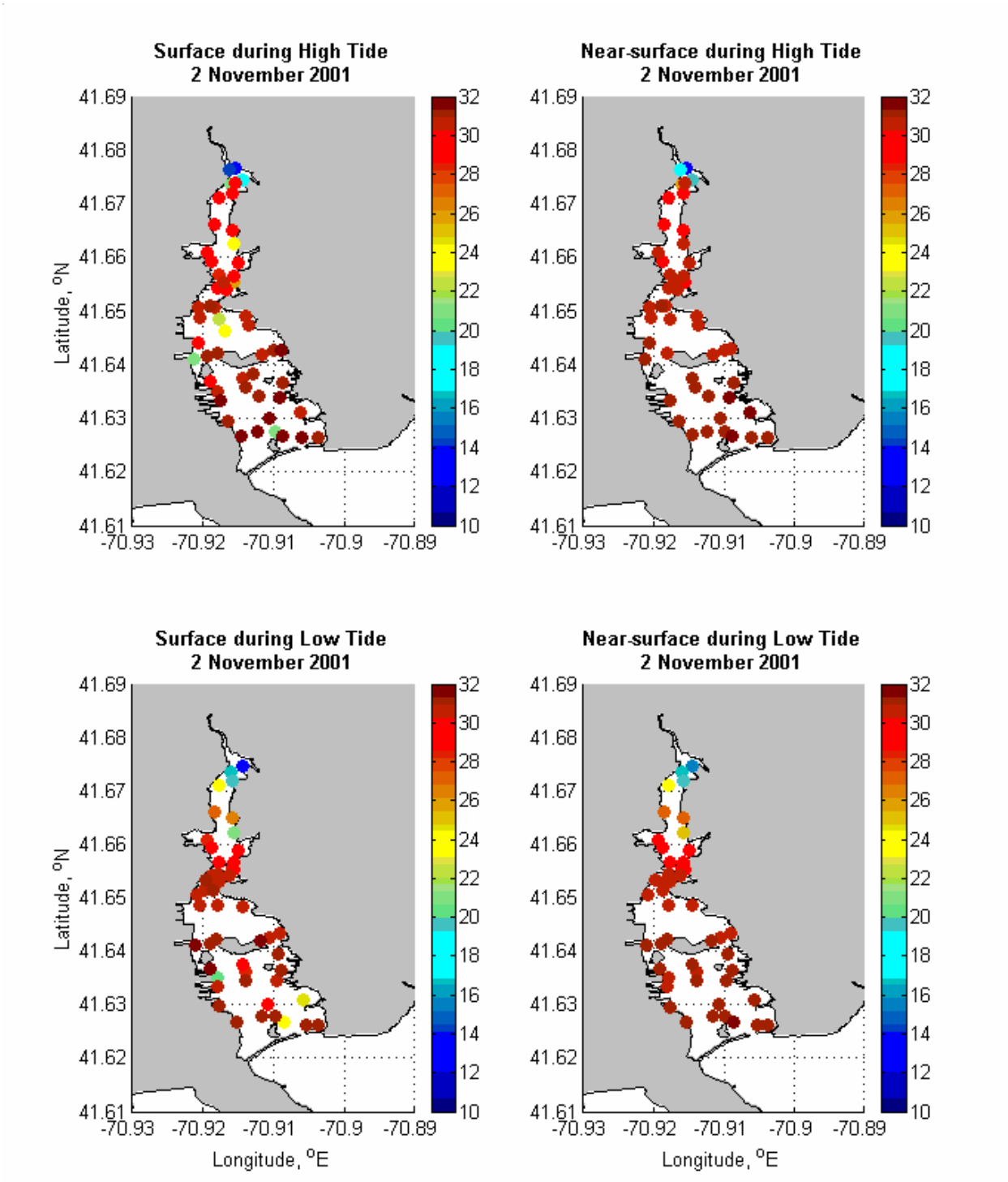

Figure A-13. Scatter plots of salinity at surface (~18 cm) and next the surface (~38 cm) during high and low tides on 2 November 2001.

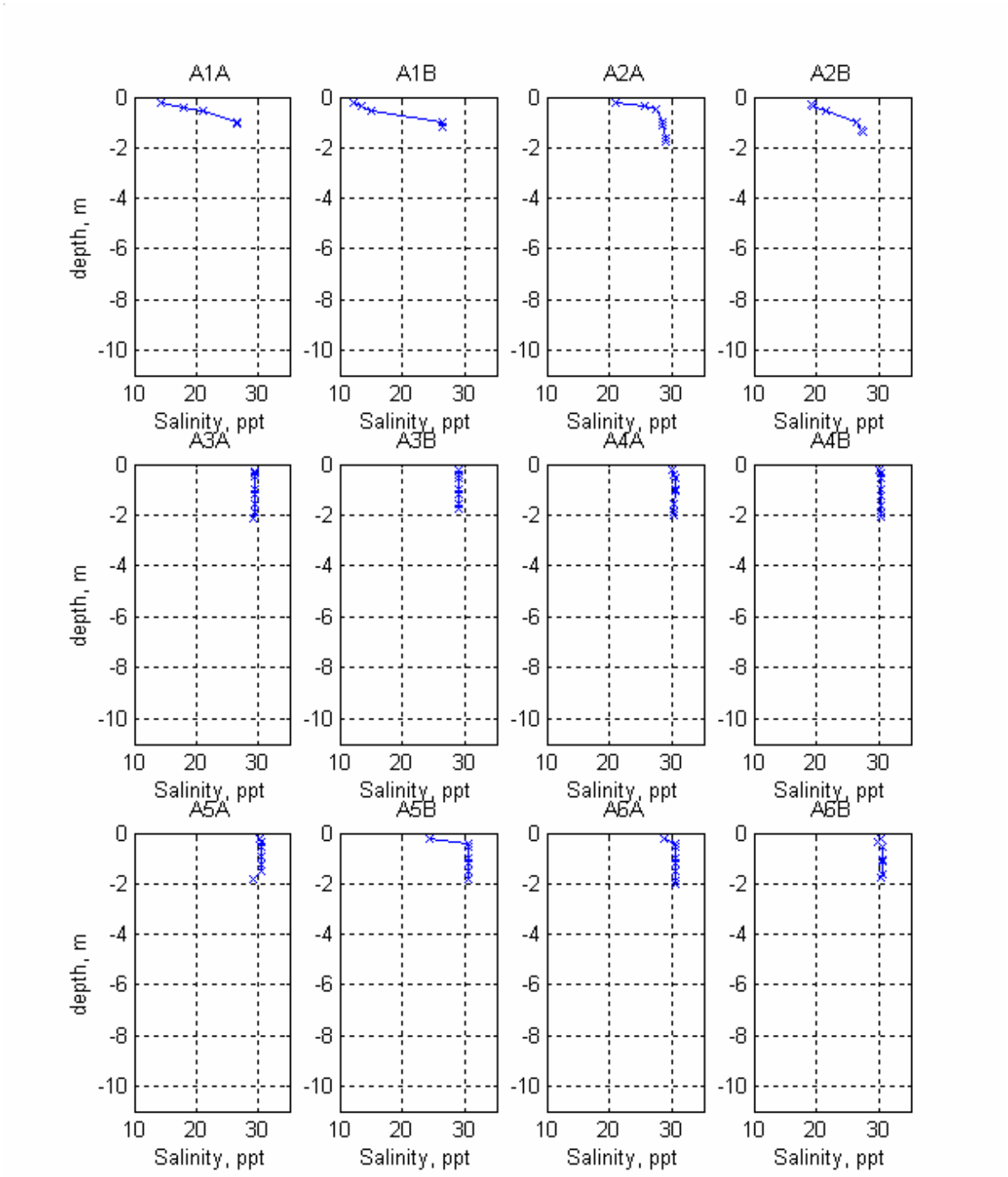

Figure A-14a. Salinity profile each station collected during high tide on 2 November 2001.

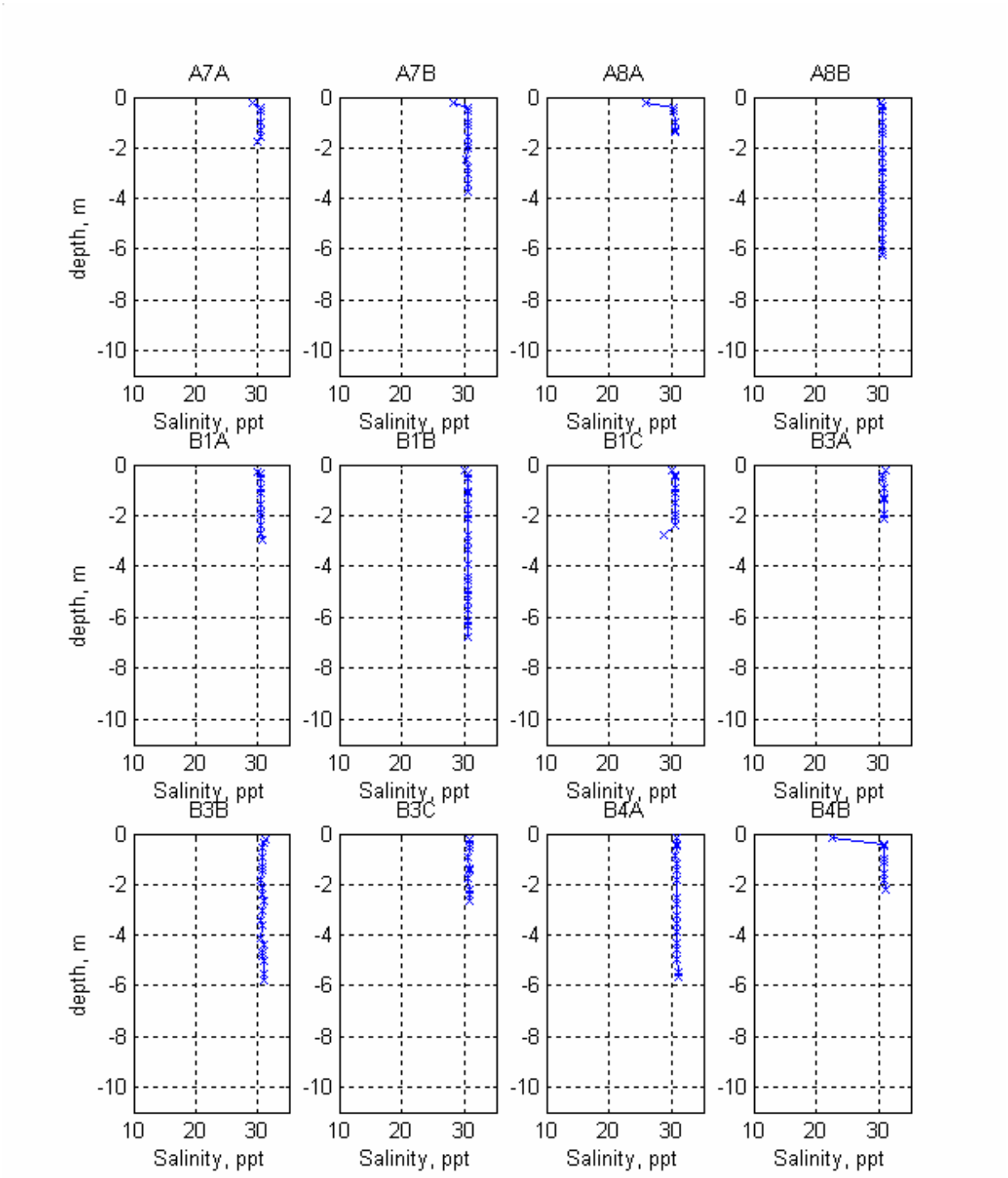

Figure A-14b. Salinity profile each station collected during high tide on 2 November 2001.

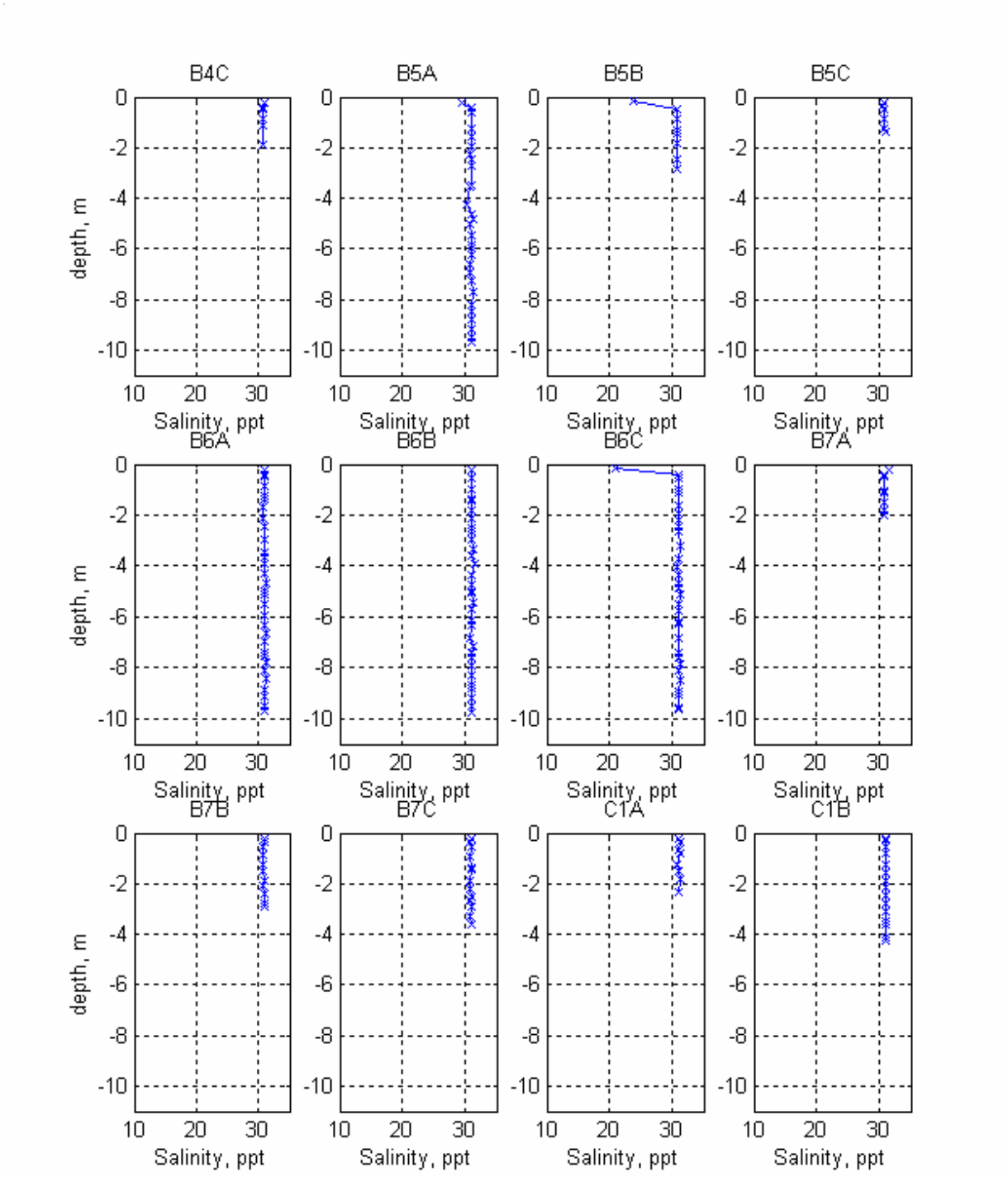

Figure A-14c. Salinity profile each station collected during high tide on 2 November 2001.

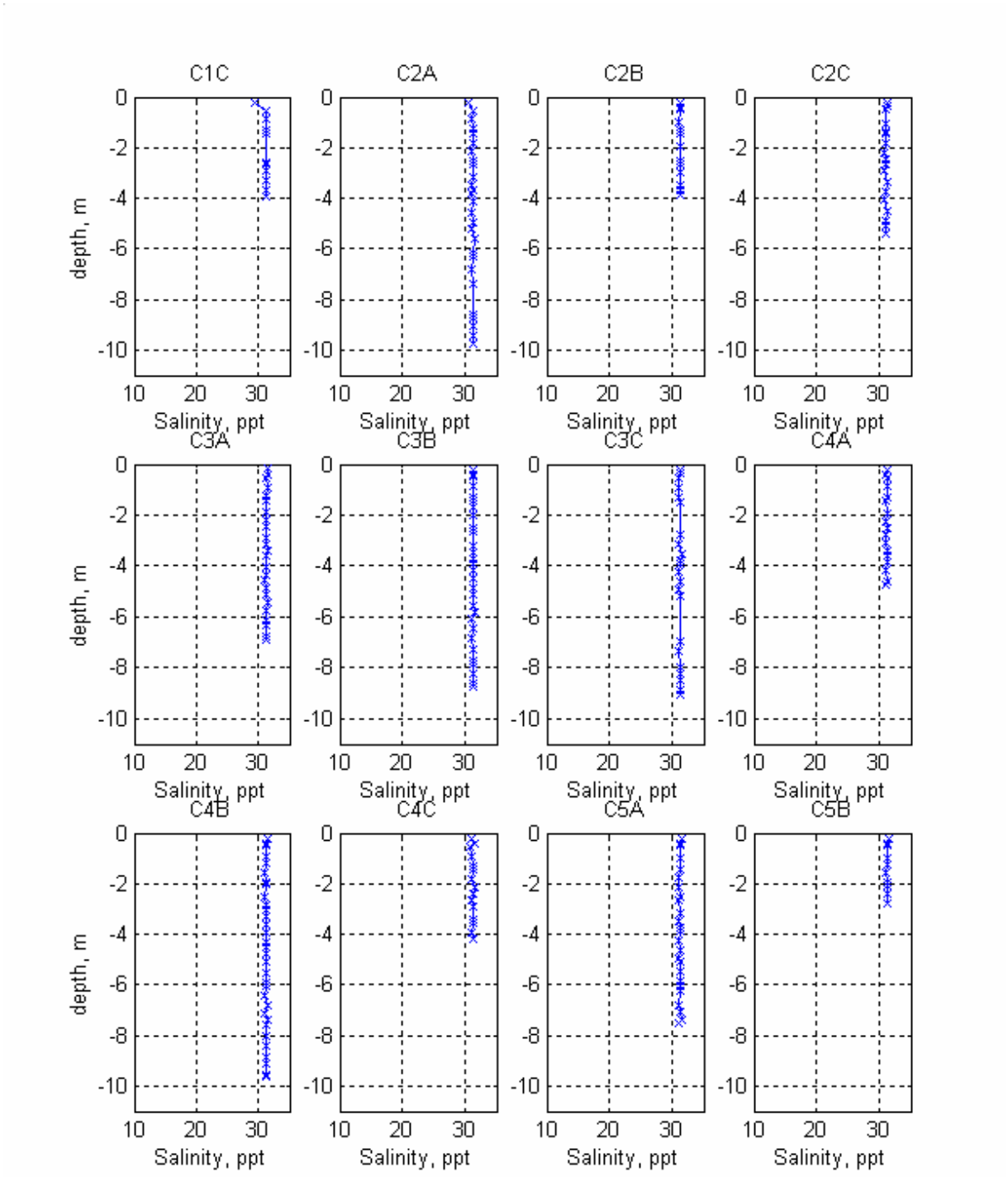

Figure A-14d. Salinity profile each station collected during high tide on 2 November 2001.

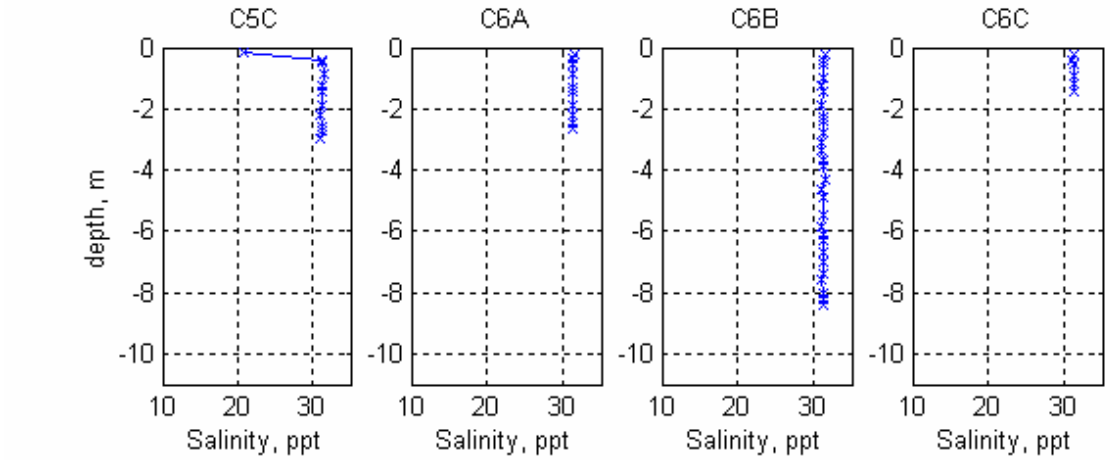

Figure A-14e. Salinity profile each station collected during high tide on 2 November 2001.

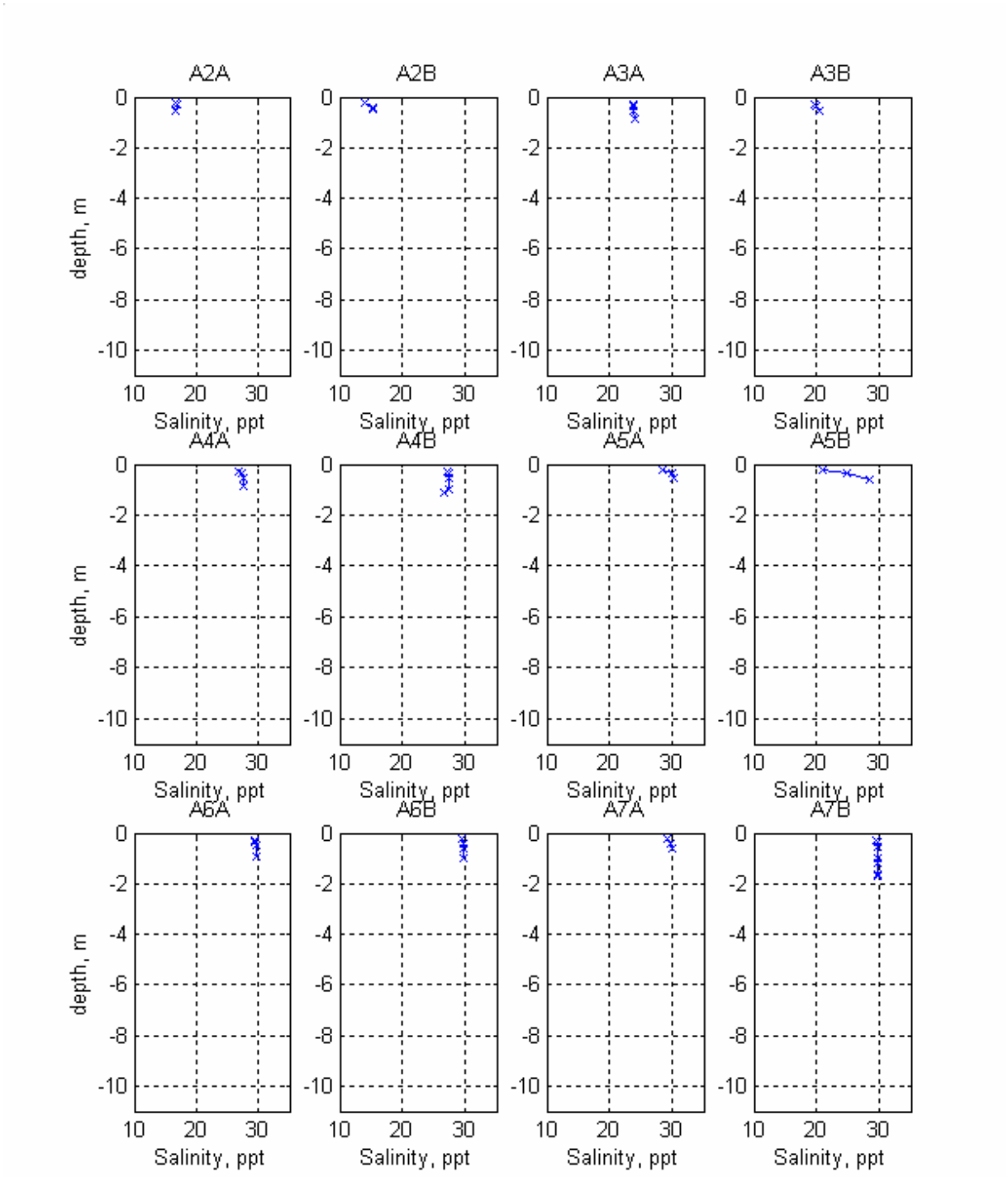

Figure A-15a. Salinity profile each station collected during low tide on 2 November 2001.

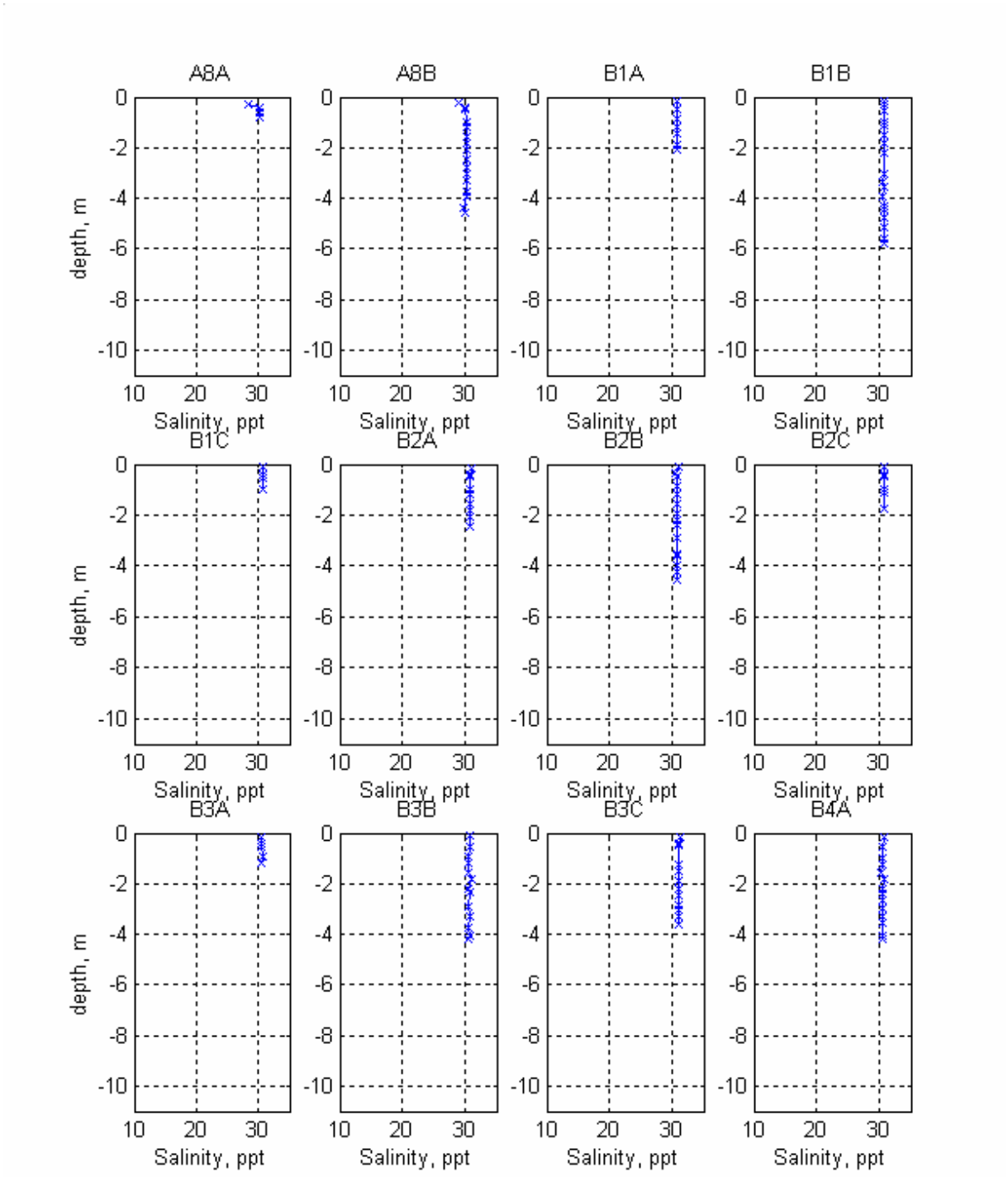

Figure A-15b. Salinity profile each station collected during low tide on 2 November 2001.

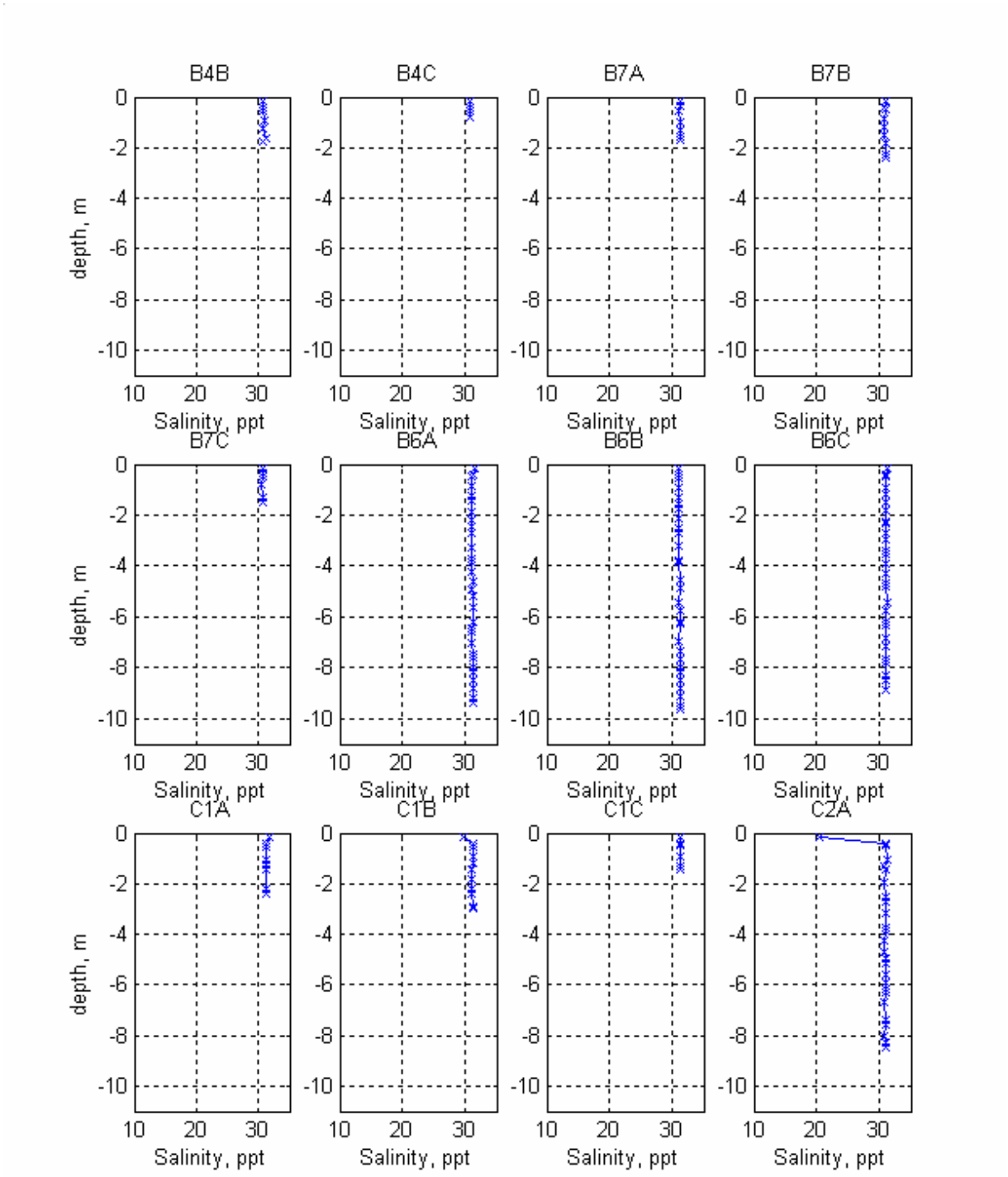

Figure A-15c. Salinity profile each station collected during low tide on 2 November 2001.

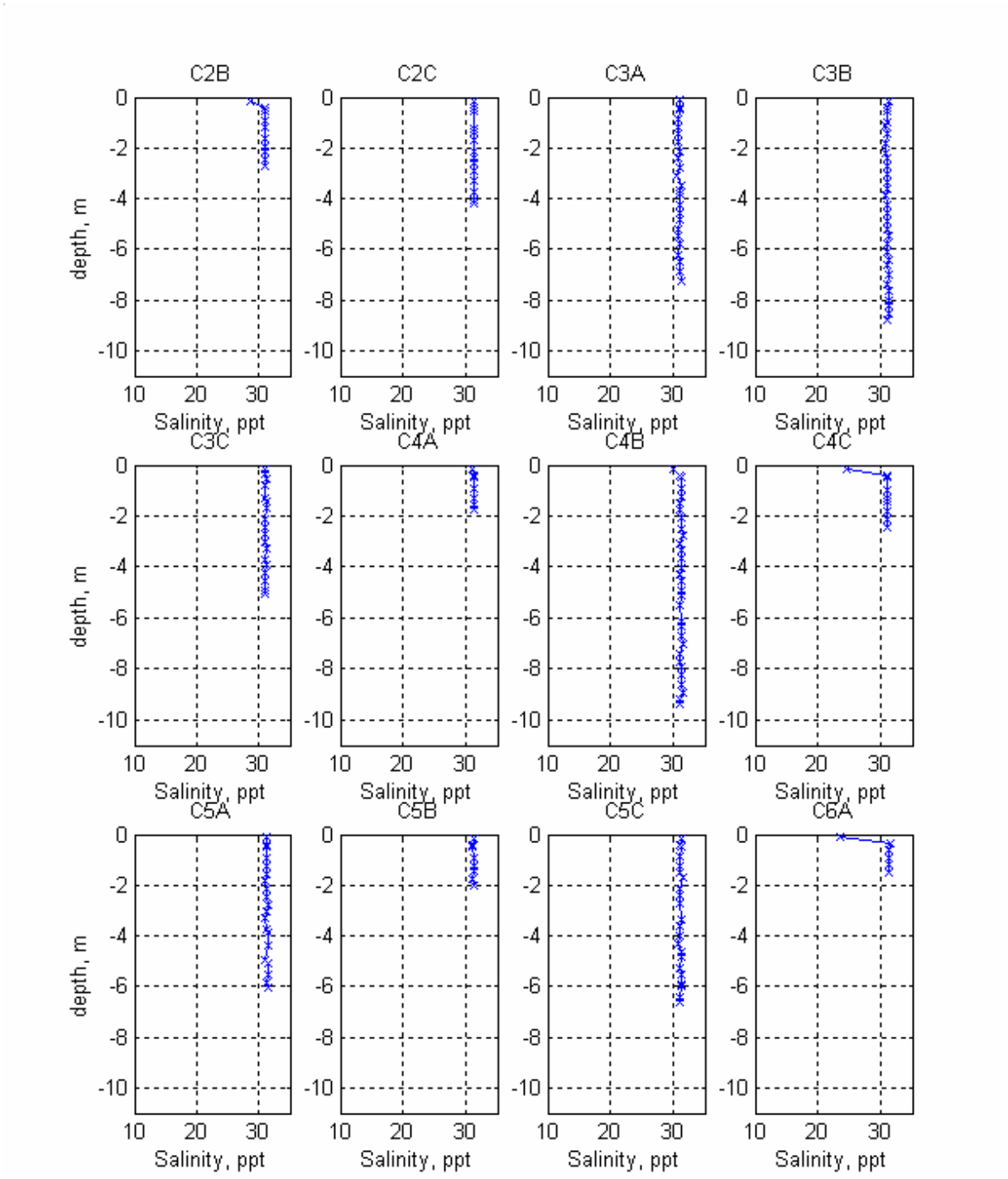

Figure A-15d. Salinity profile each station collected during low tide on 2 November 2001.

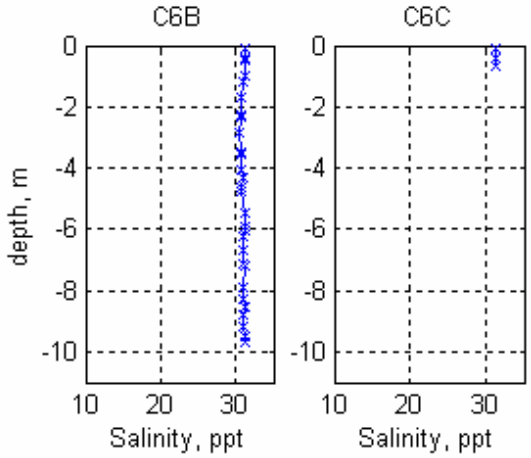

Figure A-15e. Salinity profile each station collected during low tide on 2 November 2001.

Appendix B

Dye Study

The dye study was conducted from 18 to 24 October 2001 in the area centered at the Fairhaven Wastewater Treatment Plant (WWTP) discharge outfall in the lower Inner Harbor. The goal of the study was to determine the residence time of the discharged wastewater from the outfall.

Rhodamine WT dye was chosen for the study. A total of 100 lb solution was continuously released at the Fairhaven WWTP from 0900 18 October to 0900 23 October. Average daily flow of the discharge effluent at the plant for the period was 1.8 million gallons per day (MGD). A precision laboratory pump (Fluid Metering Inc. Positive Displacement Drive Pump) metered 2 gallons of a 20% dye solution into the effluent to produce the 1100 parts per billion (ppb) concentration of the dye solution. This equals a 0.088 ml/s pumping rate of solution or a 21 mg/s dye release rate.

Due to rain on 16 October, the injection of dye did not start until 9:00 AM 18 October and the pumping continued through 9:00 AM on 23 October. There were two types of surveys related to the study: One was to monitor dye concentration level at 11 stations before and during the release period in order to observe the background fluorescence level and the rise to steady state. These discrete sample locations are listed in Table B-1, and are shown in Figure B-1 except New Bedford Reservoir (B4) and 1 mile point (#5). The other type of survey was conducted on-board for a 25-hour period following the cessation of dye release.

Table B-1. Position information for discrete sampling stations.

Station #	Location	Position	
		Latitude, °N	Longitude, °W
1	Hurricane Barrier Fairhaven	41.62561	70.90451
2	Seaport Inn	41.62566	70.91491
3	Bridge Street	41.64040	70.90816
4	Howland St. Bridge	41.65517	70.91685
5	1 mile point	41.63547	70.89630
6	Popes Is. Bridge East	41.64129	70.91051
7	Popes Is. Bridge West	41.64045	70.91785
9	WWTP Outfall East	41.63252	70.90460
B1	Above Main St. Bridge	41.63547	70.89629
B2	Hamlin St. Bridge	41.68414	70.91895
B4	New Bedford Reservoir	41.69636	70.91426

The dye survey showed that there was no vertical dye distribution, and hence the measurements were taken at or near the water surface. The observed background fluorescence level varied from –4.7 ppb east of the outfall to –4.2 ppb at the mouth of the

Acushnet River, showing an average of –4.36 ppb. All the measurements were corrected accordingly by offsetting them with the lowest level.

Table B-2 shows a complete set of discrete observations. The observed dye concentration level was below 7 ppb, except a location at 1 mile point from the WWTP. The concentration level at the 1 mile point station varied between 734 ppb and 1149 ppb (Figure B-2a), with a daily average of 880 ppb. This implied that the injection concentration was not always constant as it was designed (1100ppb).

The dye concentration east of the Fairhaven WWTP outfall (Figure B-2b) slowly increased over the 5-day period, with the maximum concentration 6.46 ppb at 0850 22 October. However, the concentration level appeared to vary depending on a tidal stage. Although the concentration level was much lower than the observations at a station east of the outfall, a similar temporal increase in the level was found at the Hurricane Barrier Fairhaven (Figure B-2c). At a site about 1.12 km north from the outfall, observed dye concentration level was less than 0.5 ppb for the first four days of the pumping, and increased to 2.6 ppb at 0930 22 October (Figure B-2d).

Figures B-3 to B-5 show the synoptic survey results before and after the cessation of dye pumping. The data were collected near the surface for the most of time (Normandeau personnel, 2001). Two surveys on 23 October were conducted at low and high tides, and one survey on 24 October was during low tide.

Two-and-half hours before the dye termination (Figure B-3), maximum concentration was found at the outfall with 46 ppb. The distribution was asymmetric, whose front extends further northwest than other directions. This is because the measurements were taken at different times. The concentration level hour after the injection cessation drastically decreased (Figure B-4) in an area away from the outfall, although the maximum value was about 46 ppb. The distribution was very localized and was centered at the outfall. About 18 hours later, the dye concentration decreased to on the order of 4.7 ppb and it was about the same as the background level (Figure B-5).

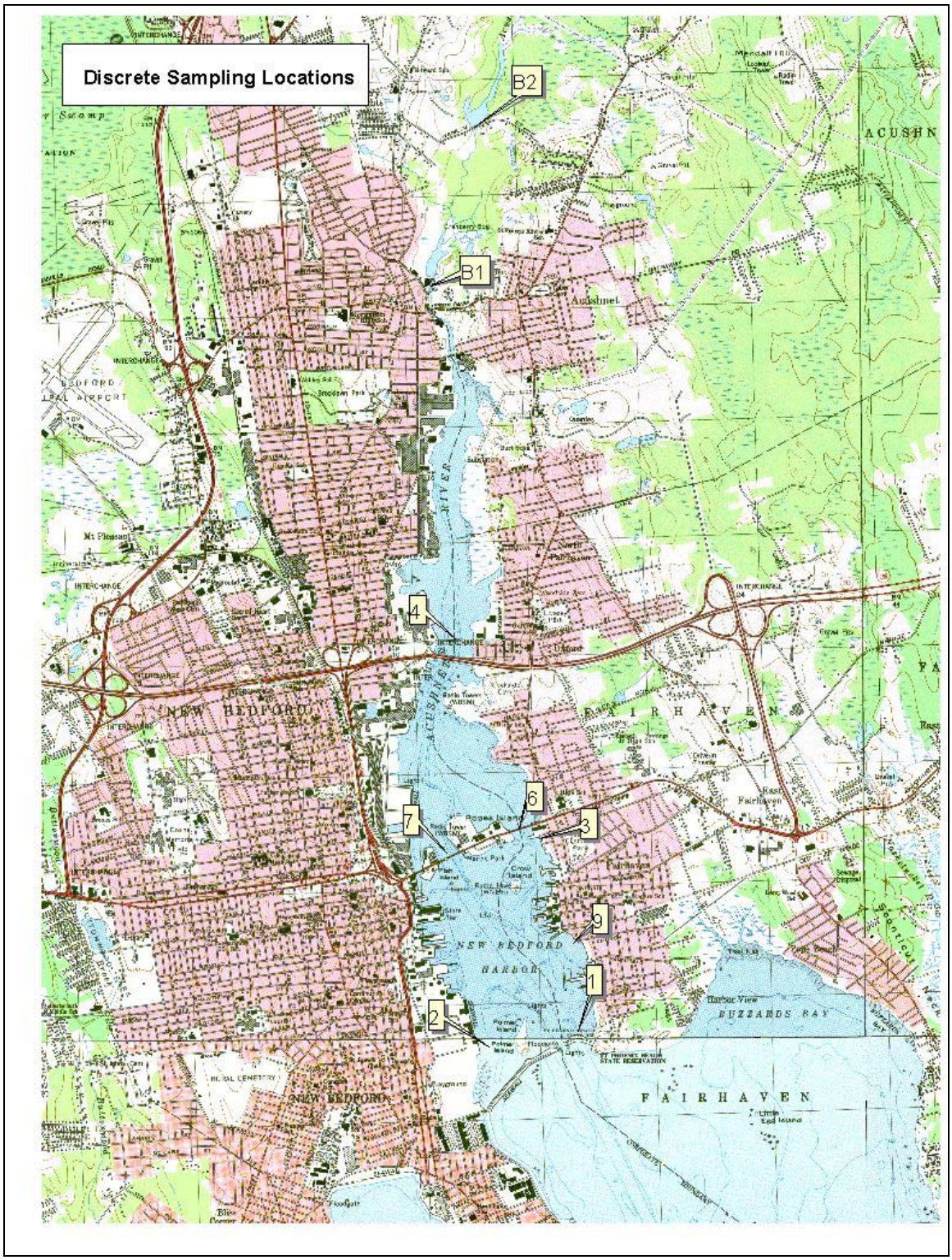

Figure B-1. Discrete sampling locations.

Table B-2. Dye concentration levels before and during dye pumping period.

Date	Time	Location	ppb	Location #
18-Oct-01	1200	1 mile point	1148.7	5
18-Oct-01	1415	WWTP Outfall East	0.3	9
18-Oct-01	1730	Barrier Fairhaven	0.4	1
18-Oct-01	1800	Pope Is. Bridge East	0.2	6
19-Oct-01	0800	1 mile point	742.7	5
19-Oct-01	0945	Pope Is. Bridge East	0.2	6
19-Oct-01	1000	WWTP Outfall East	2.6	9
19-Oct-01	1015	Hurricane Barrier Fairhaven	1.4	1
19-Oct-01	1645	WWTP Outfall East	0.4	9
19-Oct-01	1700	Hurricane Barrier Fairhaven	1.8	1
19-Oct-01	1715	Pope Is. Bridge East	0.4	6
19-Oct-01	1720	Pope Is. Bridge West	5.584	7
19-Oct-01	1740	Howland St. Bridge	0.3	4
20-Oct-01	1120	Pope Is. Bridge West	0.0	7
20-Oct-01	1135	Pope Is. Bridge East	0.2	6
20-Oct-01	1145	WWTP Outfall East	6.11	9
20-Oct-01	1155	Hurricane Barrier Fairhaven	0.4	1
20-Oct-01	1210	Howland St. Bridge	0.5	4
20-Oct-01	1330	1 mile point	733.7	5
20-Oct-01	1650	Bridge street	0.2	3
20-Oct-01	1705	WWTP Outfall East	5.4	9
20-Oct-01	1730	Hurricane Barrier Fairhaven	1.2	1
20-Oct-01	1735	Howland St. Bridge	0.0	4
20-Oct-01	1800	Pope Is. Bridge West	0.1	7
21-Oct-01	0755	WWTP Outfall East	4.2	9
21-Oct-01	0815	Hurricane Barrier Fairhaven	0.9	1
21-Oct-01	0830	Pope Is. Bridge West	0.2	7
21-Oct-01	0845	Seaport Inn	0.5	2
21-Oct-01	0855	Pope Is. Bridge East	0.3	6
21-Oct-01	0905	Howland St. Bridge	0.2	4
21-Oct-01	0930	1 mile point	806.7	5
21-Oct-01	1740	Howland St. Bridge	0.2	4
21-Oct-01	1800	1 mile point	1001.7	5
21-Oct-01	1815	WWTP Outfall East	11.24	9
21-Oct-01	1820	Hurricane Barrier Fairhaven	1.3	1
21-Oct-01	1833	Pope Is. Bridge West	0.2	7
21-Oct-01	1840	Pope Is. Bridge East	0.4	6
22-Oct-01	0850	WWTP Outfall East	6.46	9
22-Oct-01	0915	Hurricane Barrier Fairhaven	2.4	1
22-Oct-01	0930	Pope Is. Bridge East	2.6	6
22-Oct-01	1000	Seaport Inn	0.8	2
22-Oct-01	1600	1 mile point	839.7	5

(a)

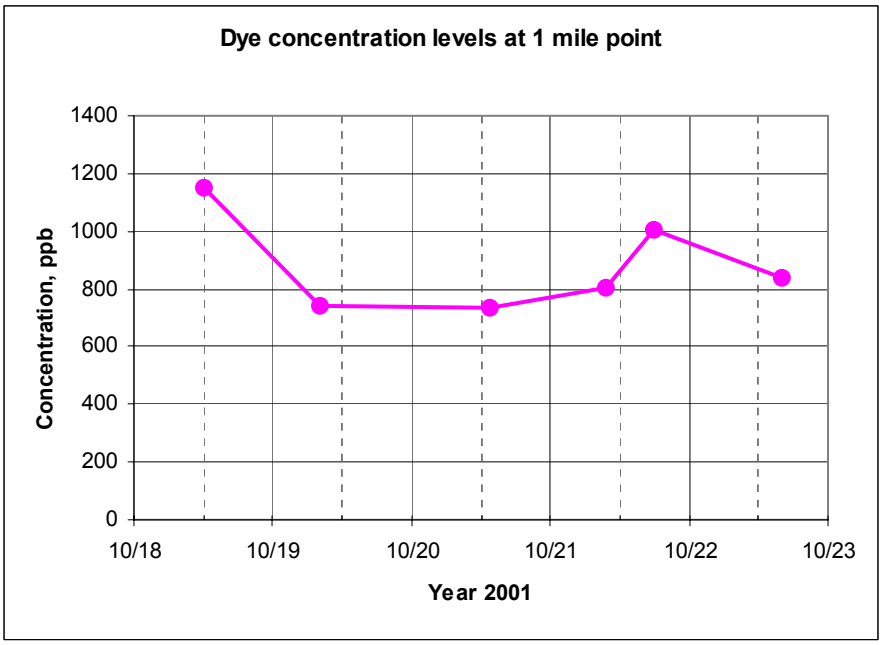

(b)

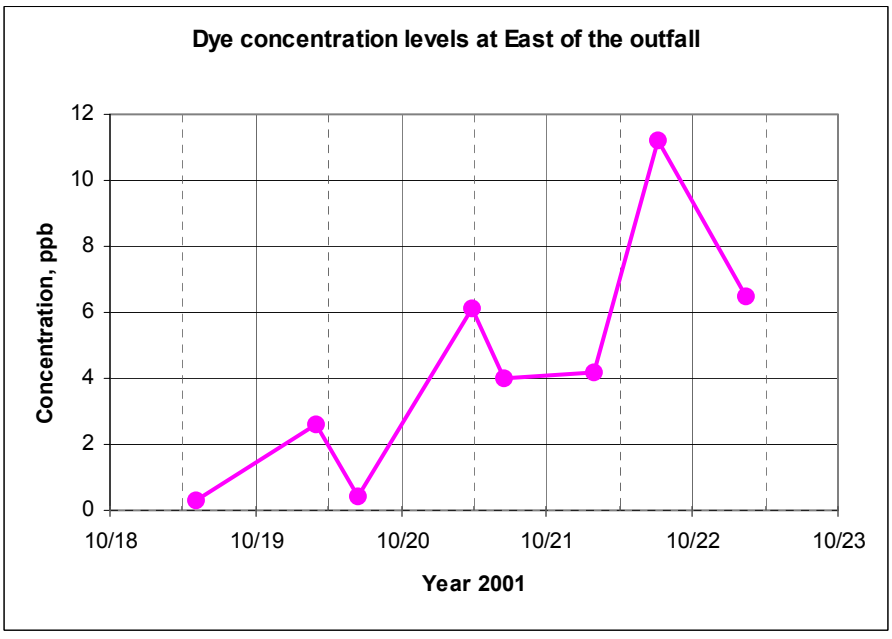

Figure B-2. Dye concentration levels in time at selected discrete sampling locations. Note that the y-axis range for (a) is larger than (b)-(d).

(c)

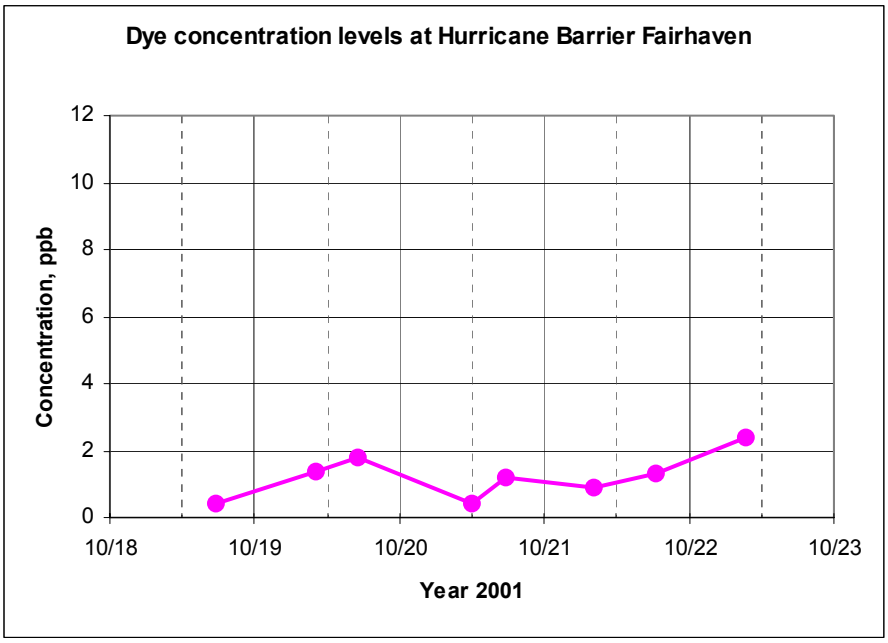

(d)

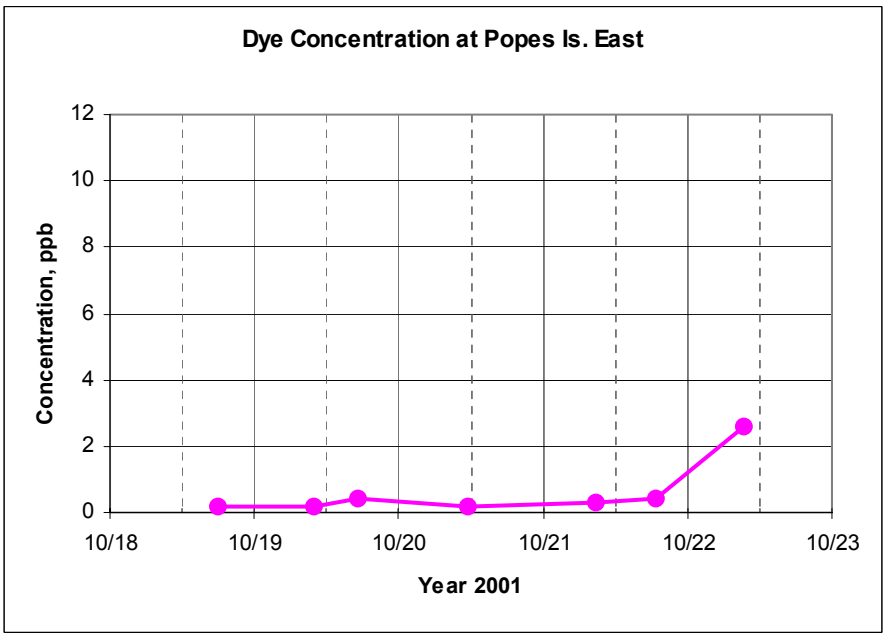

Figure B-2. Dye concentration levels in time at selected discrete sampling locations (continued).

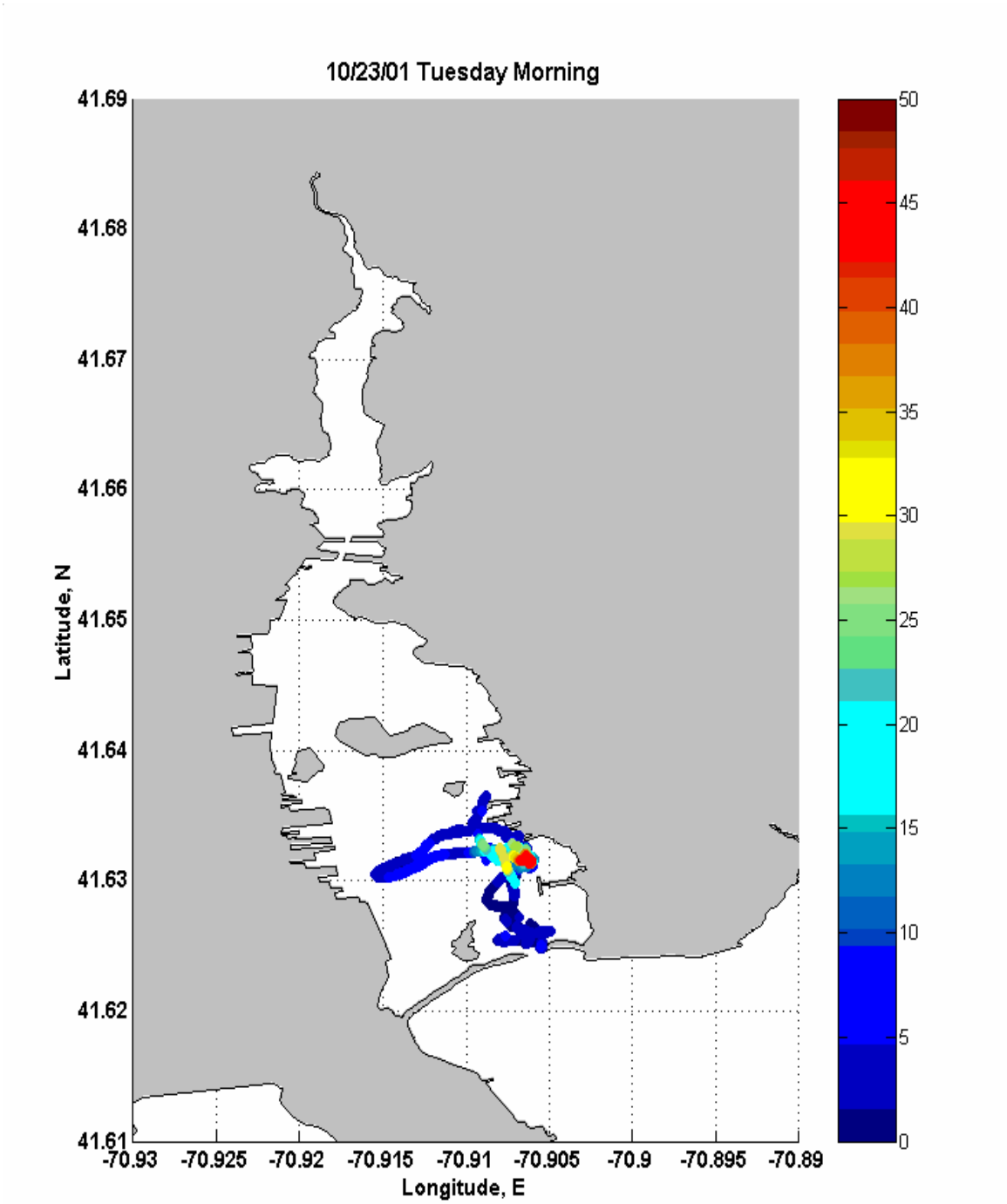

Figure B-3. Dye distribution observed from 6:44 to 9:22 on 23 October. Units are ppb.

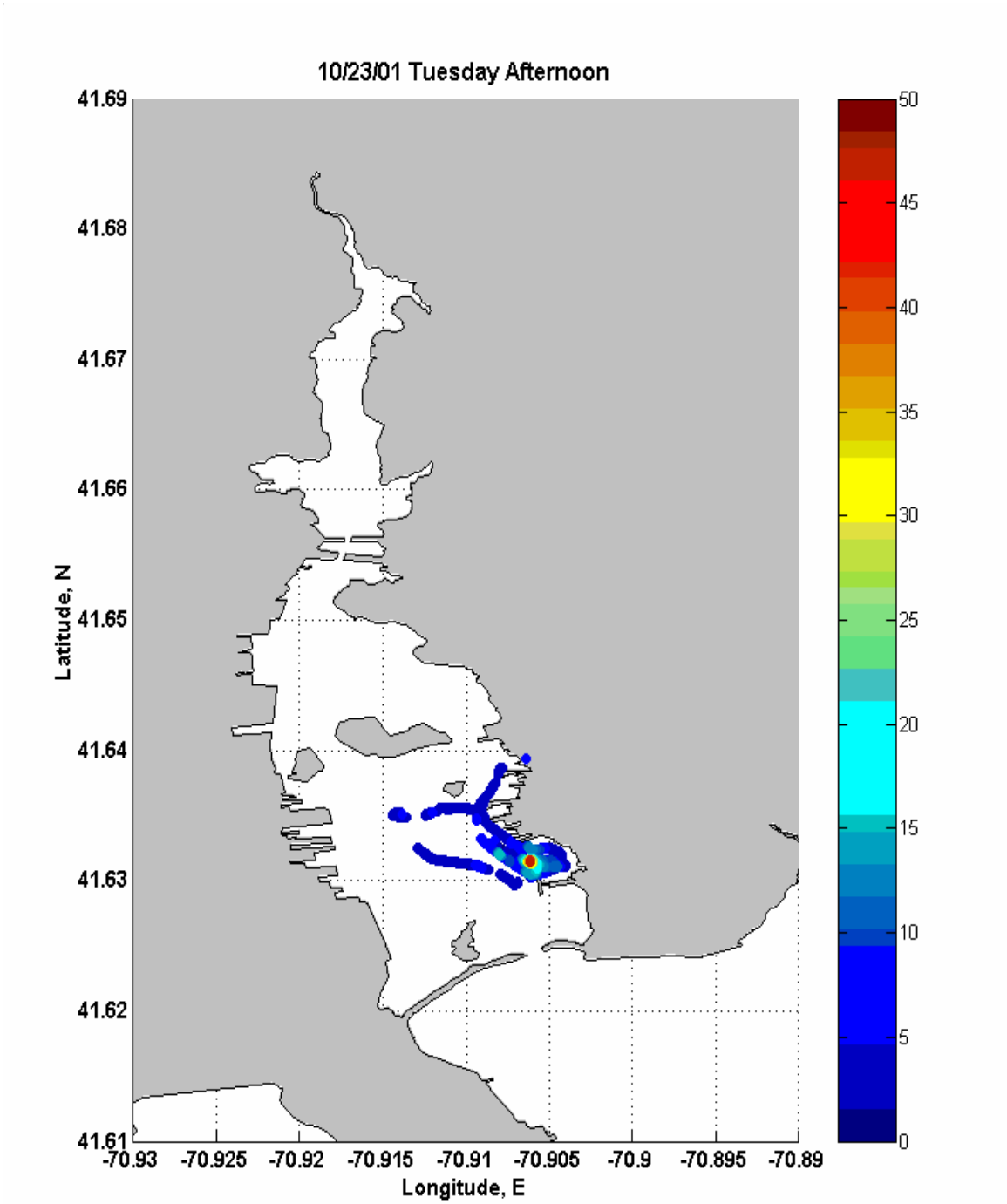

Figure B-4. Dye distribution observed from 13:00 to 14:13 on 23 October. Units are ppb.

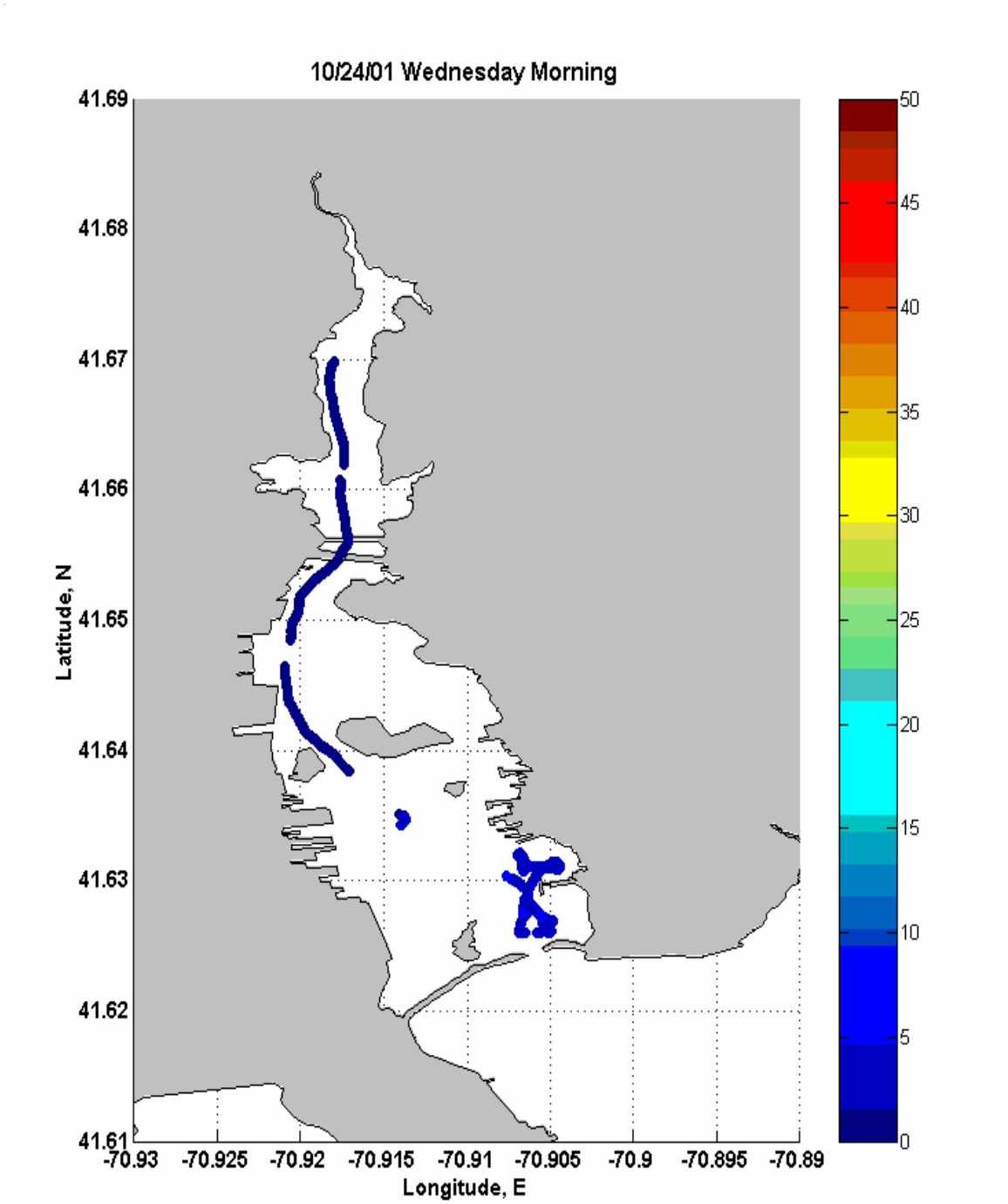

Figure B-5. Dye distribution observed between 7:00 and 10:00 on 24 October. Units are ppb.

Appendix C

Broad Band Acoustic Doppler Current Profilers Data

Velocity data were measured at a location (41° 37.808′N, 70° 54.643′W), west of the federal navigation channel in the lower Inner Harbor. The instrument used for the measurement was RDI 600 kHz convex BroadBand ADCP. It was moored at the bottom, where the mean water depth is about 10.4 m (34 ft), and it collected currents throughout the water column every 5 minutes at 0.5 m (1.6 ft) intervals (bins) in the vertical, for a period from 19 September to 7 November 2001.

The ADCP is set up so that it sends out a ping every 1.5 seconds. It collects a set of returning sound speeds for 200 pings over a 5 min ensemble period, and then converts the mean speed to a water velocity profile using the Doppler effect. Correlation and percent good profile data are collected together with the velocity component data, for use as a data quality check. The instrument used for this study is a convex 4-beam transducer. Each beam is oriented 20° from the vertical and is divided into 20 bins (depth-cells) in the vertical with a bin-size of 0.5 m (1.6 ft) with the first bin closest to the transducer.

General processing of ADCP data includes checking echo intensity, correlation and percent good profile data. For good ADCP data, for example, slow variation of echo intensity, and high correlation and high percent good profile with depth. Naturally all these profile data become smaller with distance in vertical from the transducer. However, quality of data collected in the channel was found consistently poor throughout the measurement period. Figures C-1, C-2 and C-3 show the three main profile data. Each figure is time series of the profile data for each beam. Figure C-1 shows the echo intensity measurement, Figure C-2 exhibits the correlation data and Figure C-3 shows the percent good data. Description for the status of each profile data is listed in Table C-1. From the status check, Beam 3 failed functioning for the most of the deployment period. The conclusion is that the velocity measurements were not good enough to use for simulation. The instrument was returned to the manufacturer who concurred that a major failure inexplicably occurred and replaced the instrument.

Table C-1. Status of profile data collection.

Echo Intensity	Beam 1 and 4 were fine, exhibiting the magnitude from 0 to 220, but Beam 3 failed functioning for the whole deployment period; Beam 2 was fine for the first about 5 days, went bad between 21 and 29 September and finally became functioning from 30 September.
Correlation	Beam 1 and 2 were fine; Data for Beam 3 showed erratic variation for the first few days after the deployment but the correlation for the rest of period was on the order of 115, relatively lower than values for other beams.
Percent Good	Beam 1 was working normally, but Beam 3 exhibited low values. Beams 2 and 4 collected zero percent good, implying that they did not pass quality criteria.
Heading, Pitching and Rolling	Heading was fine for the whole period. Pitching and Rolling showed large variation for the first days after the deployment, but they became steady.

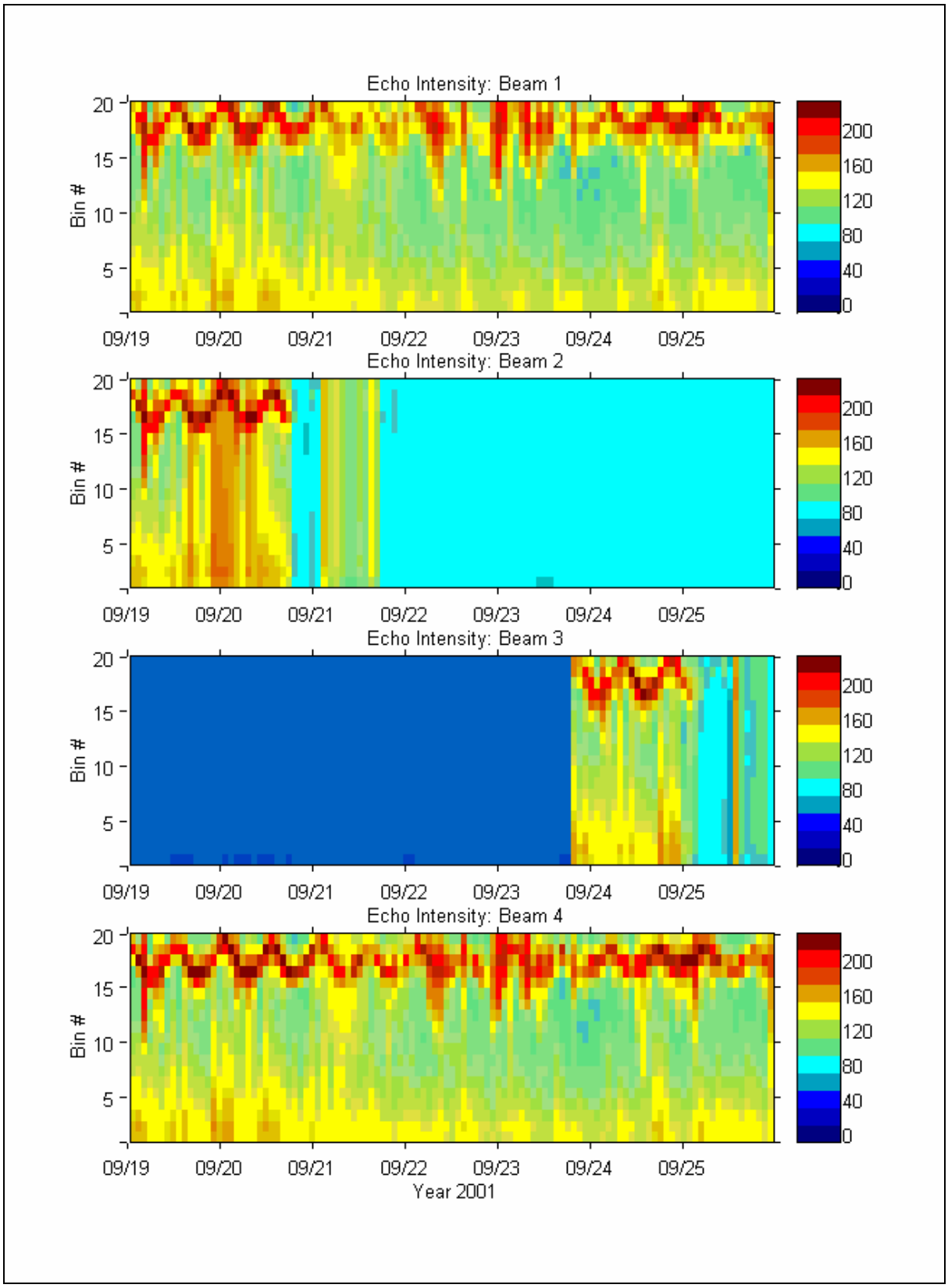

Figure C-1a. Time series of echo intensity profile data from 19 – 25 September.

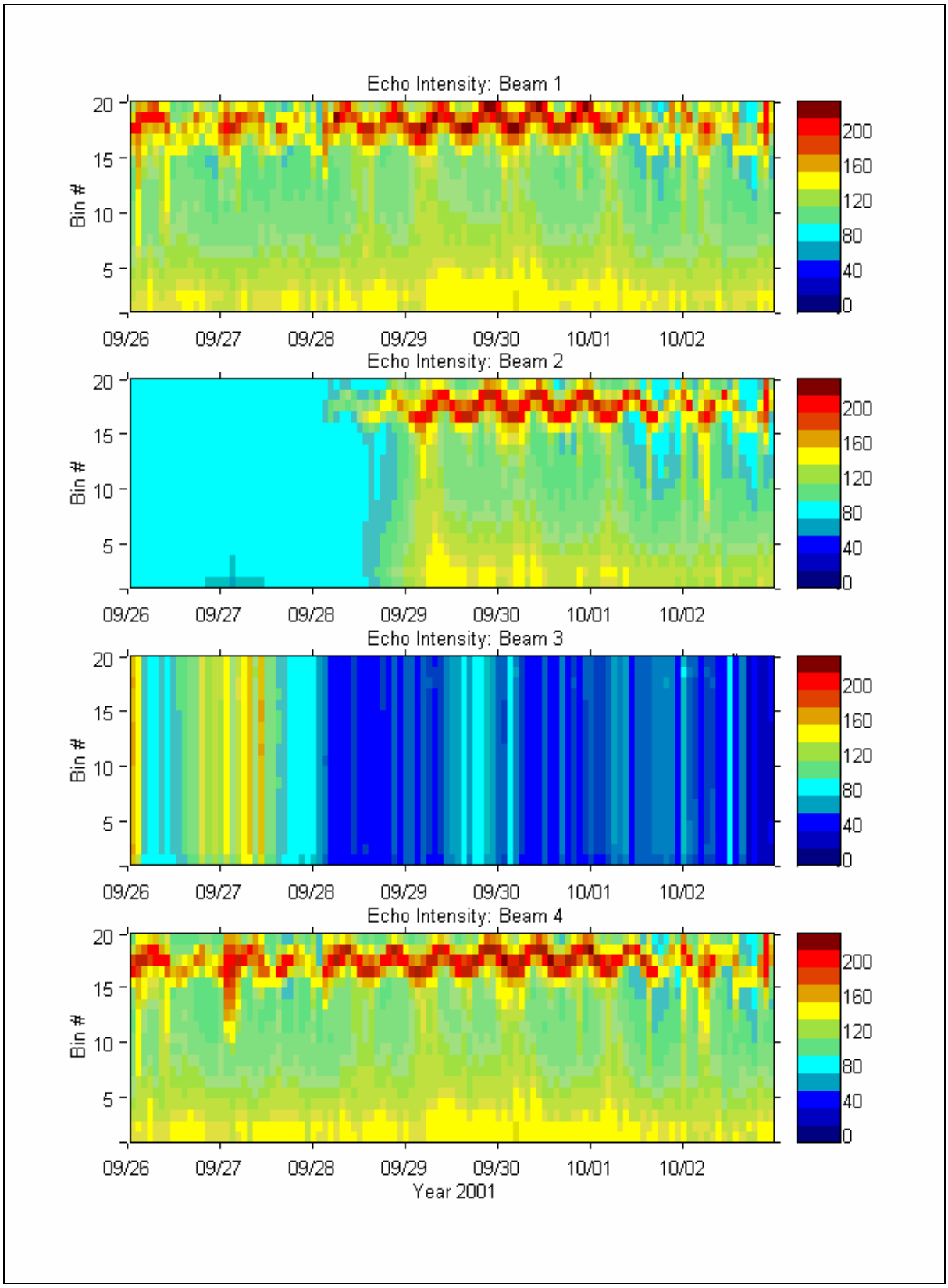

Figure C-1b. Time series of echo intensity profile data from 26 September to 2 October.

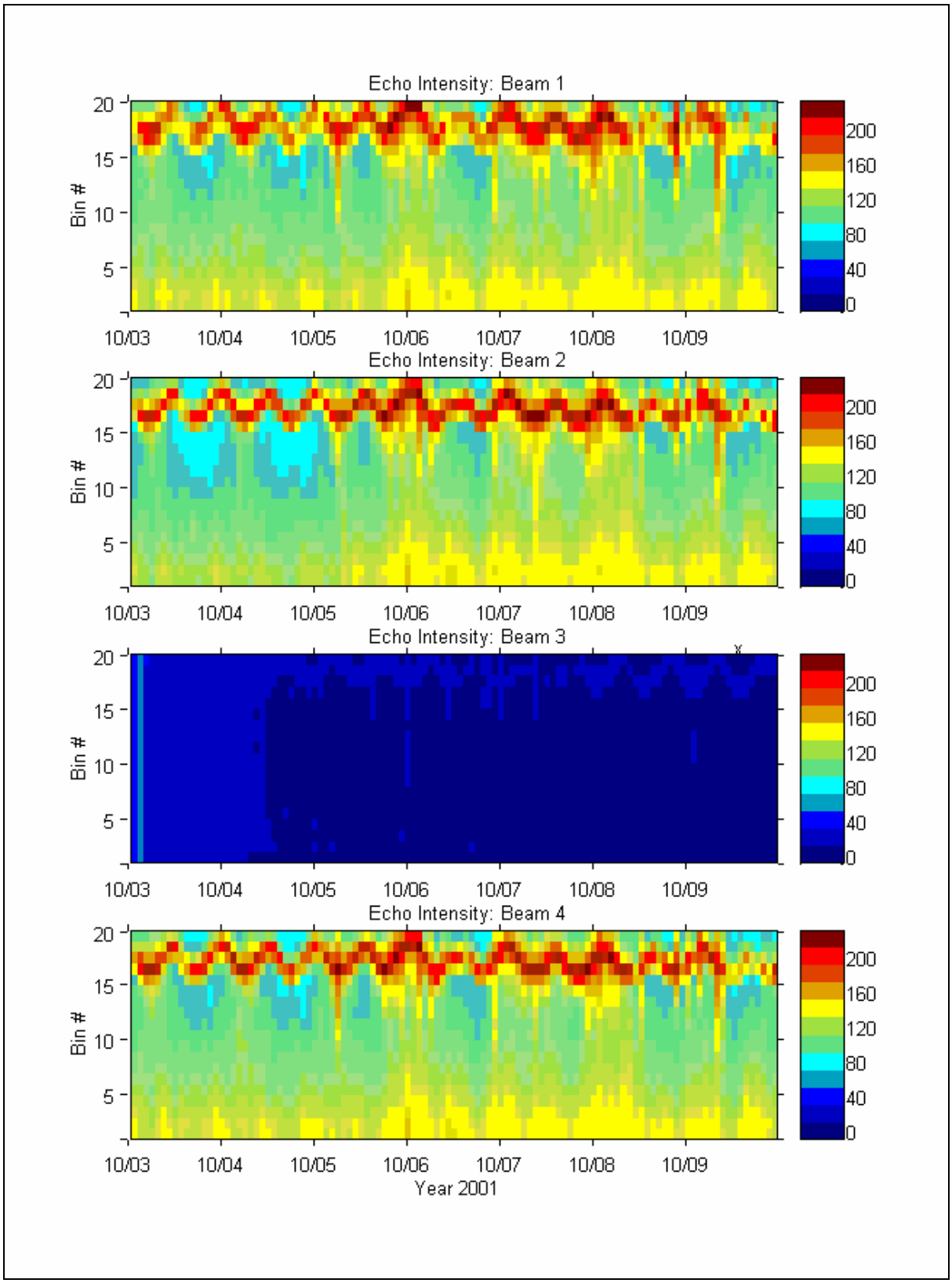

Figure C-1c. Time series of echo intensity profile data for 3 – 9 October.

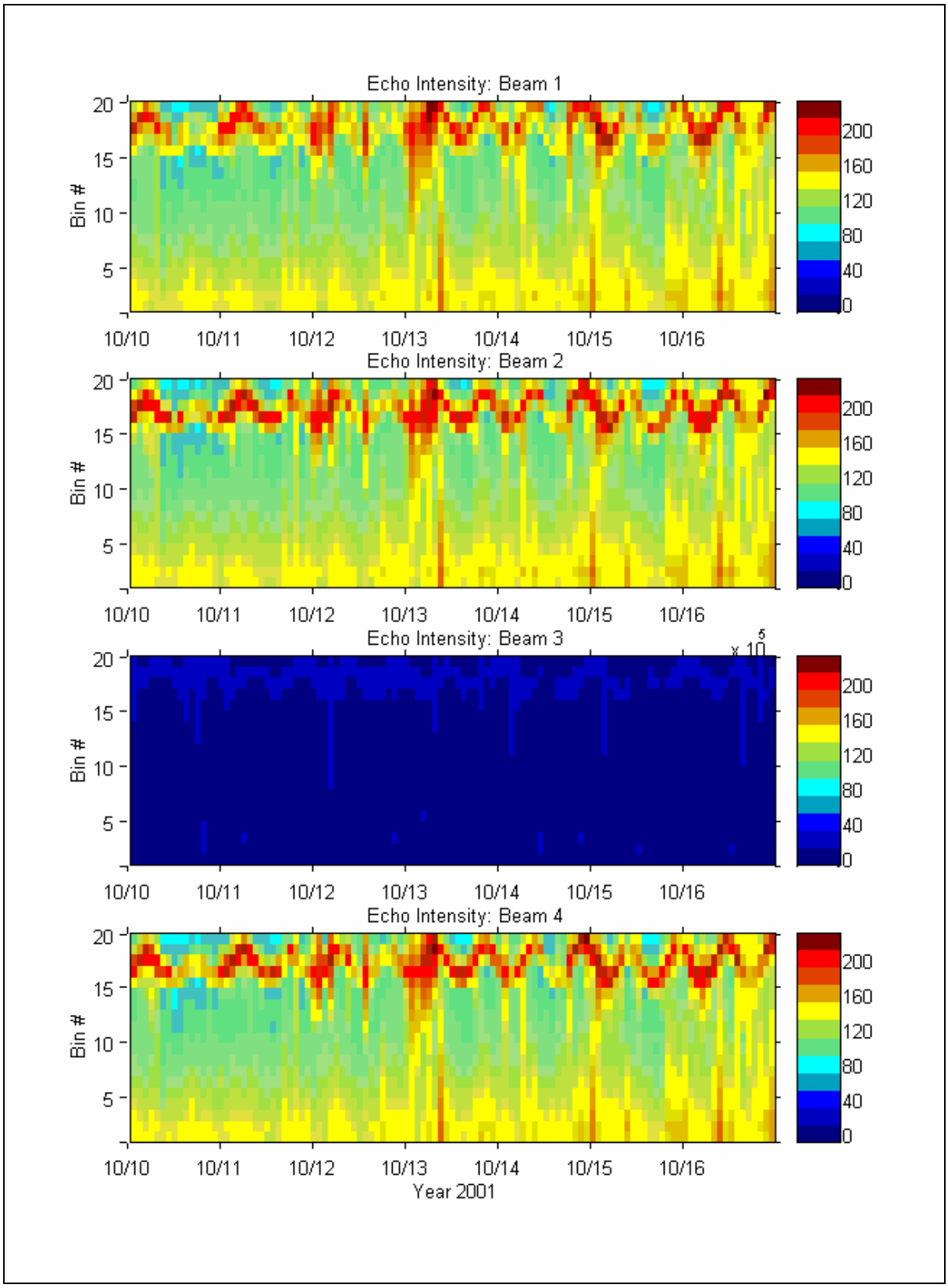

Figure C-1d. Time series of echo intensity profile data for 10 –16 October.

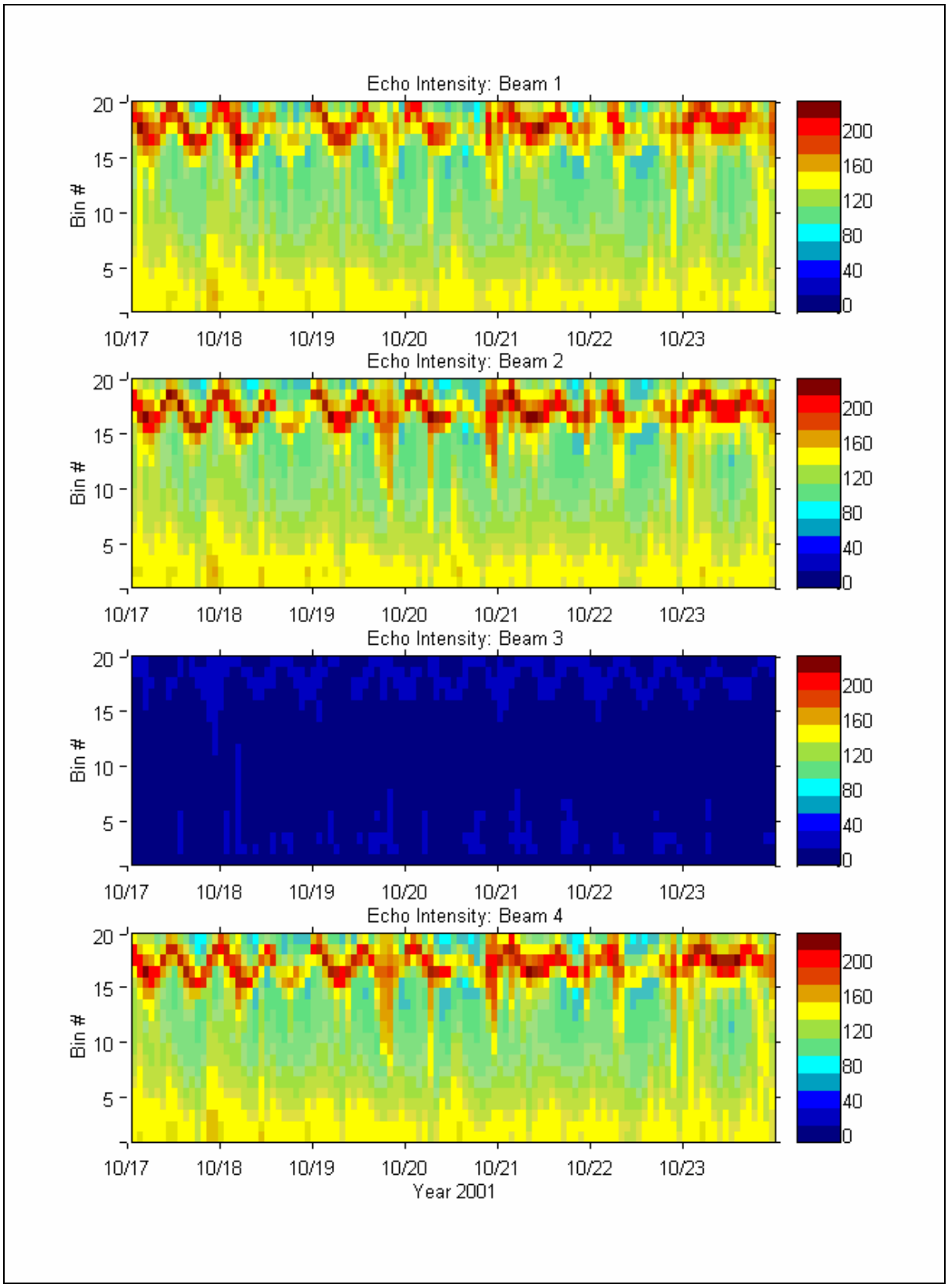

Figure C-1e. Time series of echo intensity profile data for 17 – 23 October.

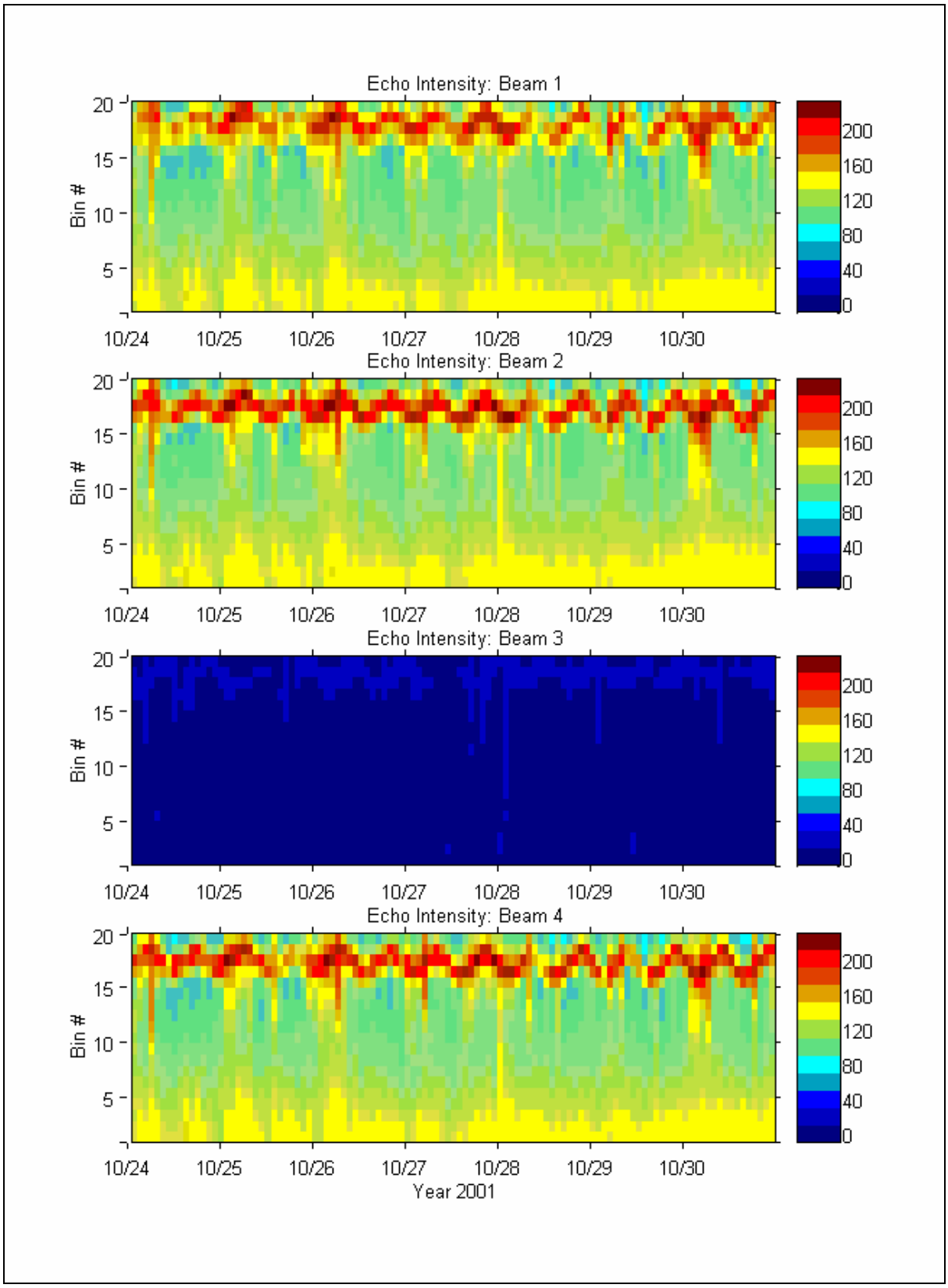

Figure C-1f. Time series of echo intensity profile data for 24 – 30 October.

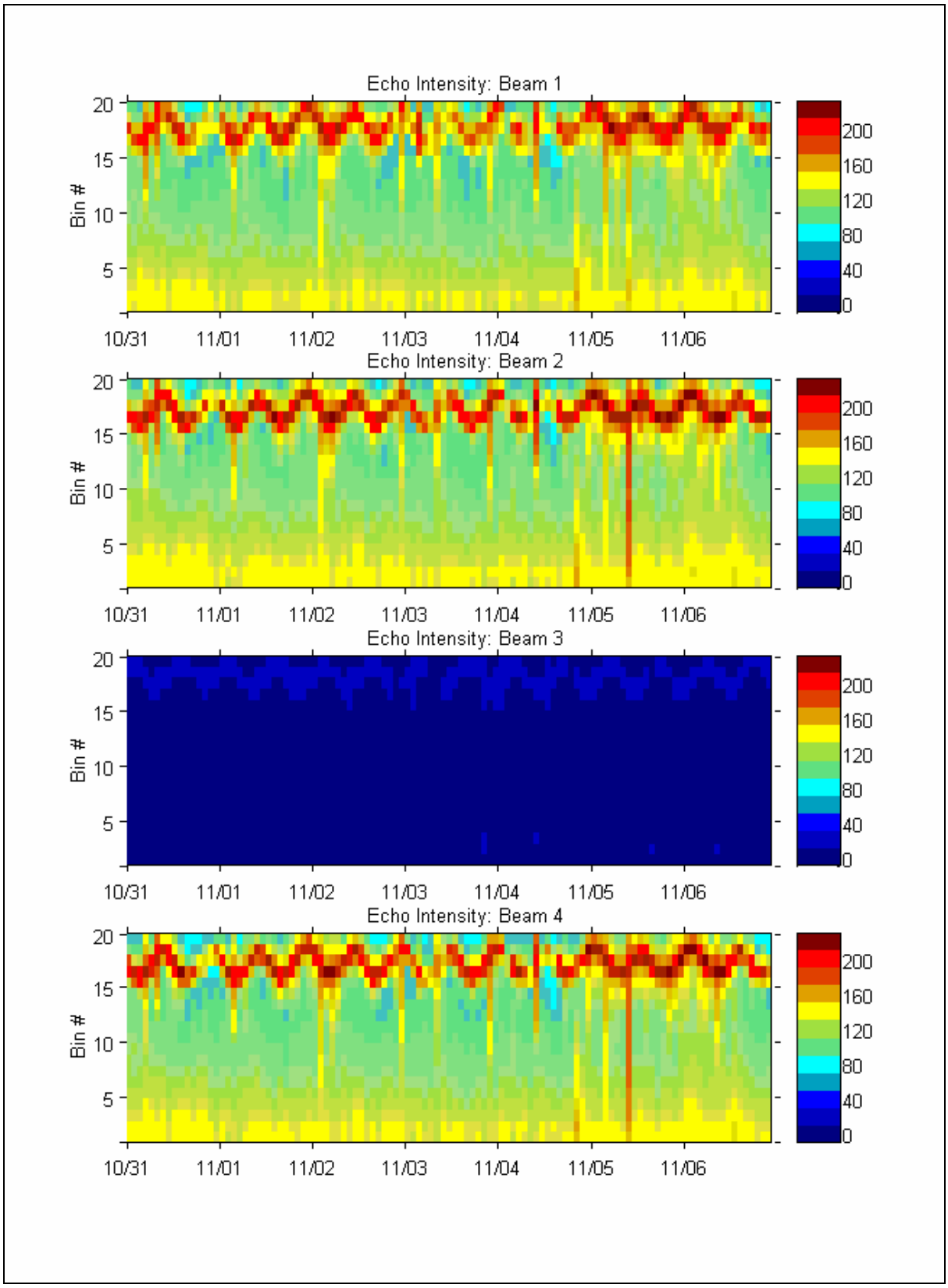

Figure C-1g. Time series of echo intensity profile data from 31 October to 6 November.

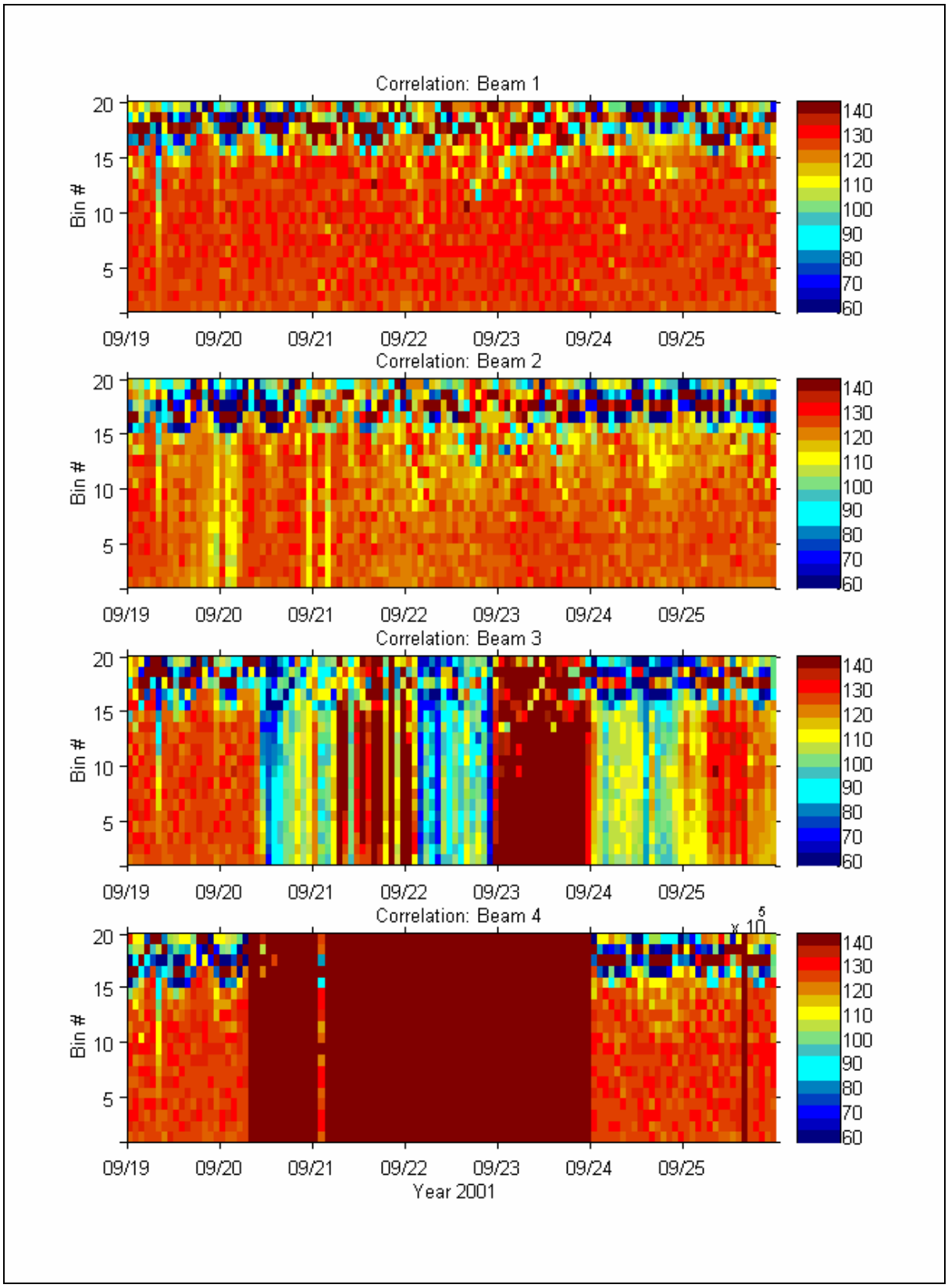

Figure C-2a. Time series of correlation profile data for 19 – 25 September.

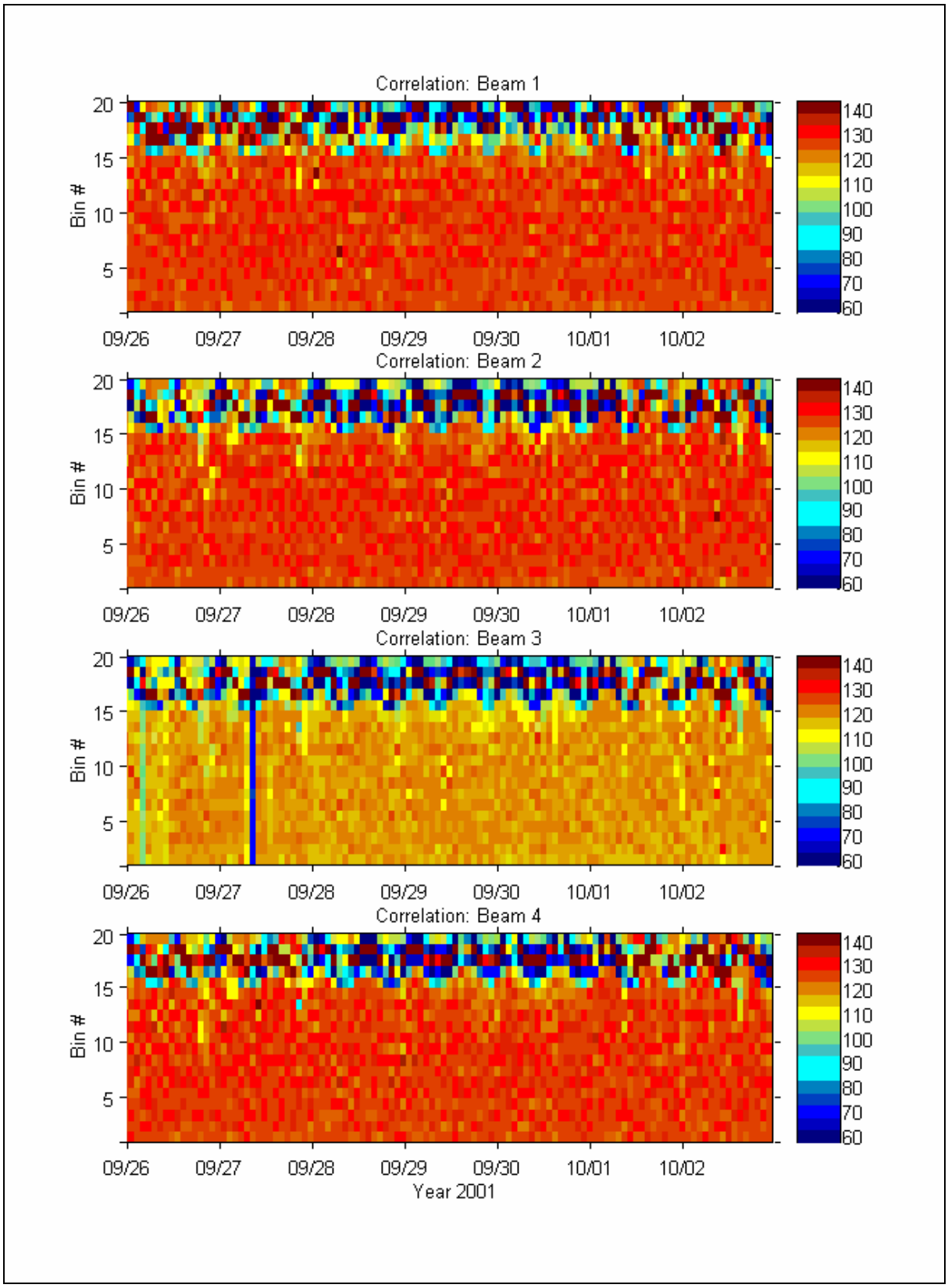

Figure C-2b. Time seies of correlation profile data from 26 September to 2 October.

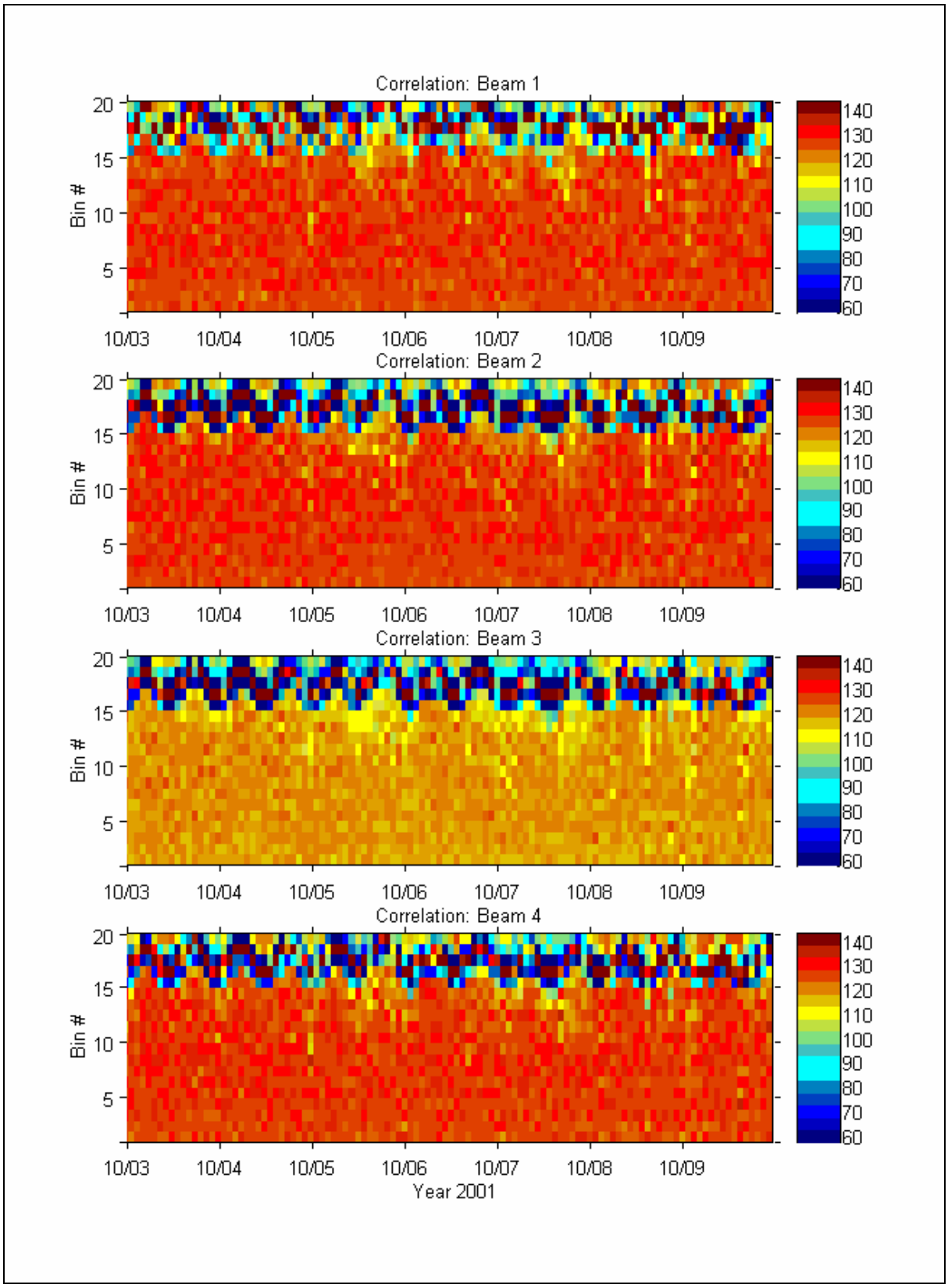

Figure C-2c. Time series of correlation profile data for 3 – 9 October.

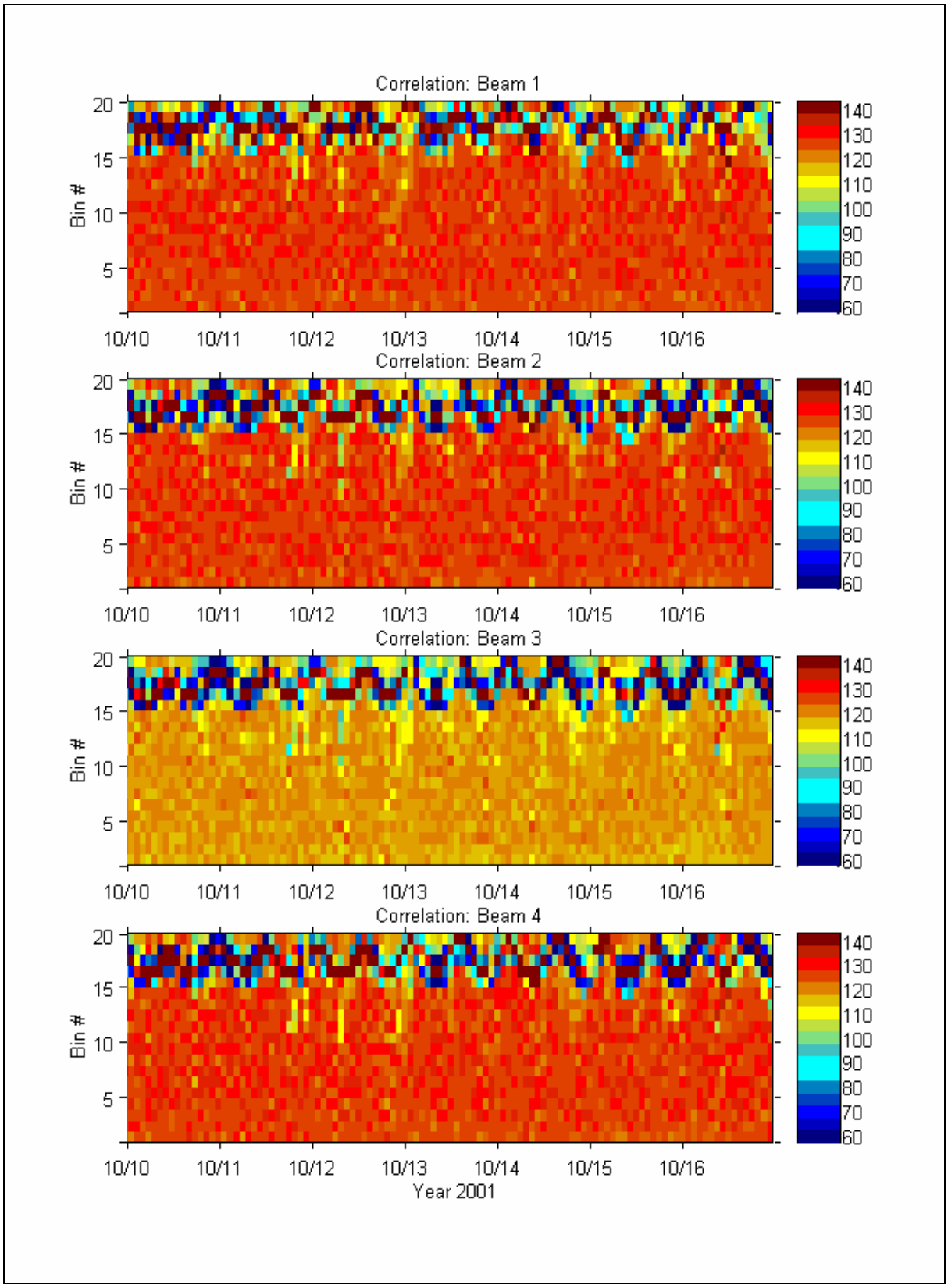

Figure C-d. Time series of correlation profile data for 10 – 16 October.

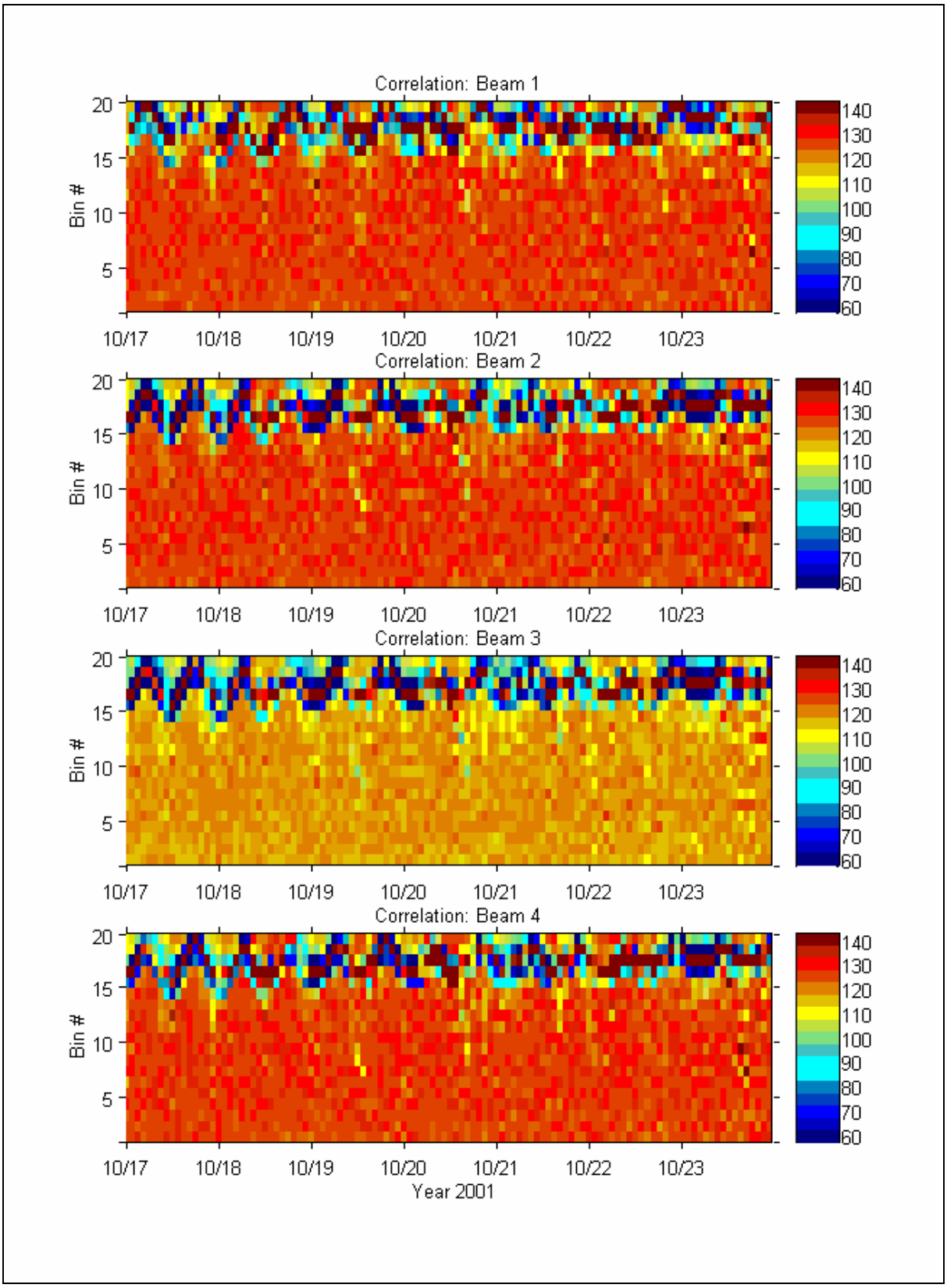

Figure C-2e. Time series of correlation profile data for 17 – 23 October.

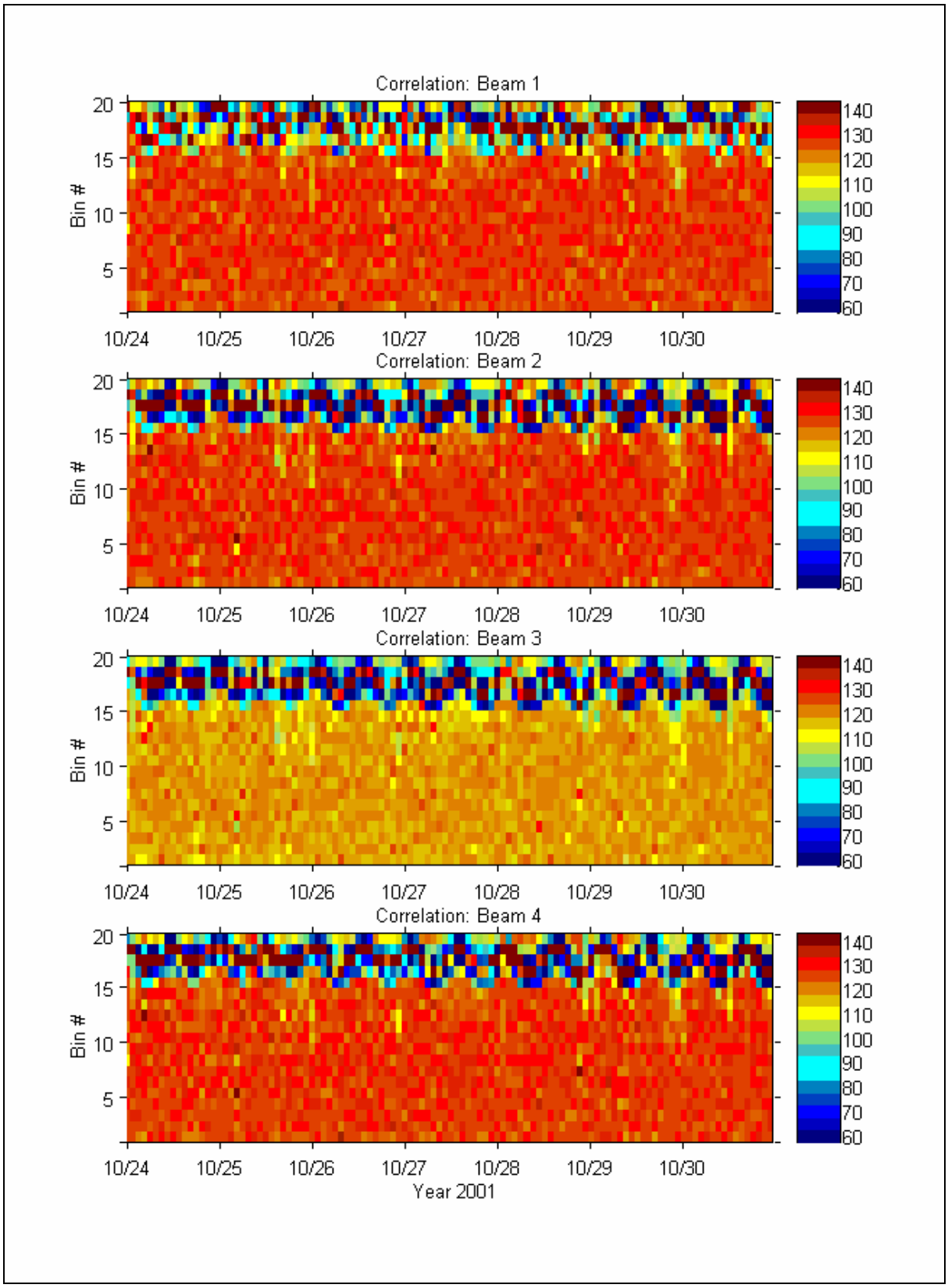

Figure C-2f. Time seies of correlation profile data for 24 – 30 October.

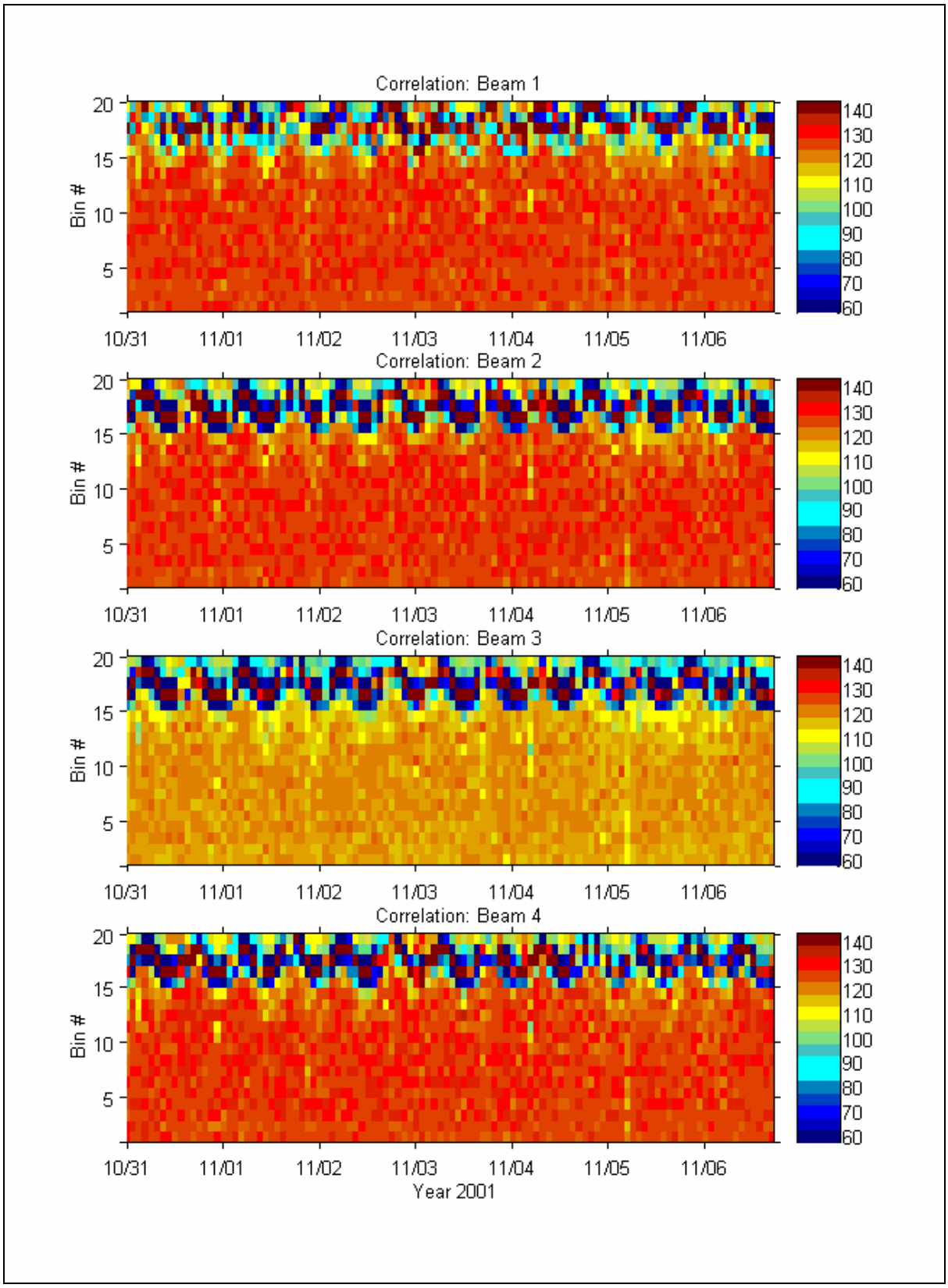

Figure C-2g. Time series of correlation profile data from 31 October to 6 November.

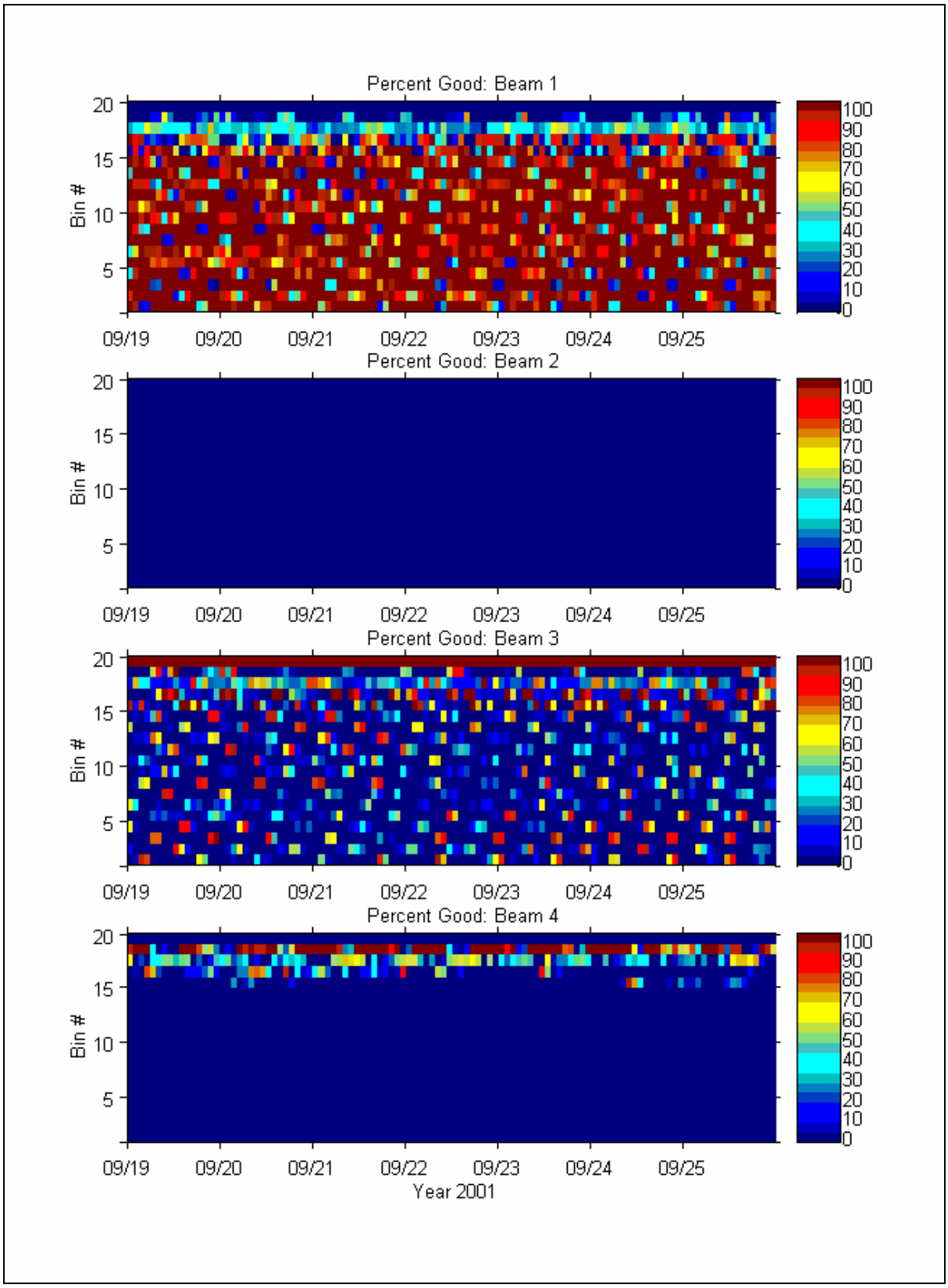

Figure C-3a. Time series of percent good profile data for 19 – 25 September.

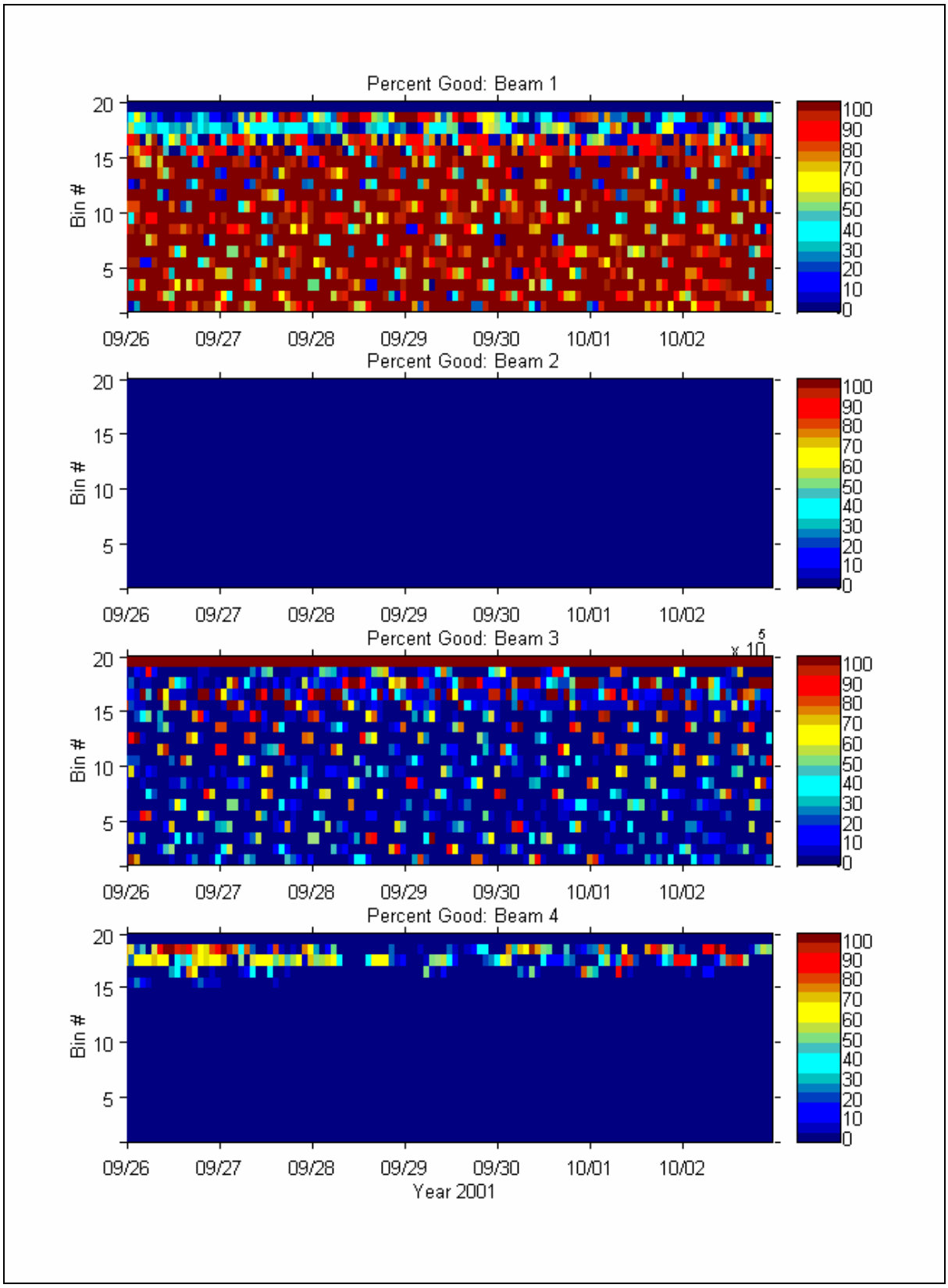

Figure C-3b. Time series of percent good profile data from 26 September to 2 October.

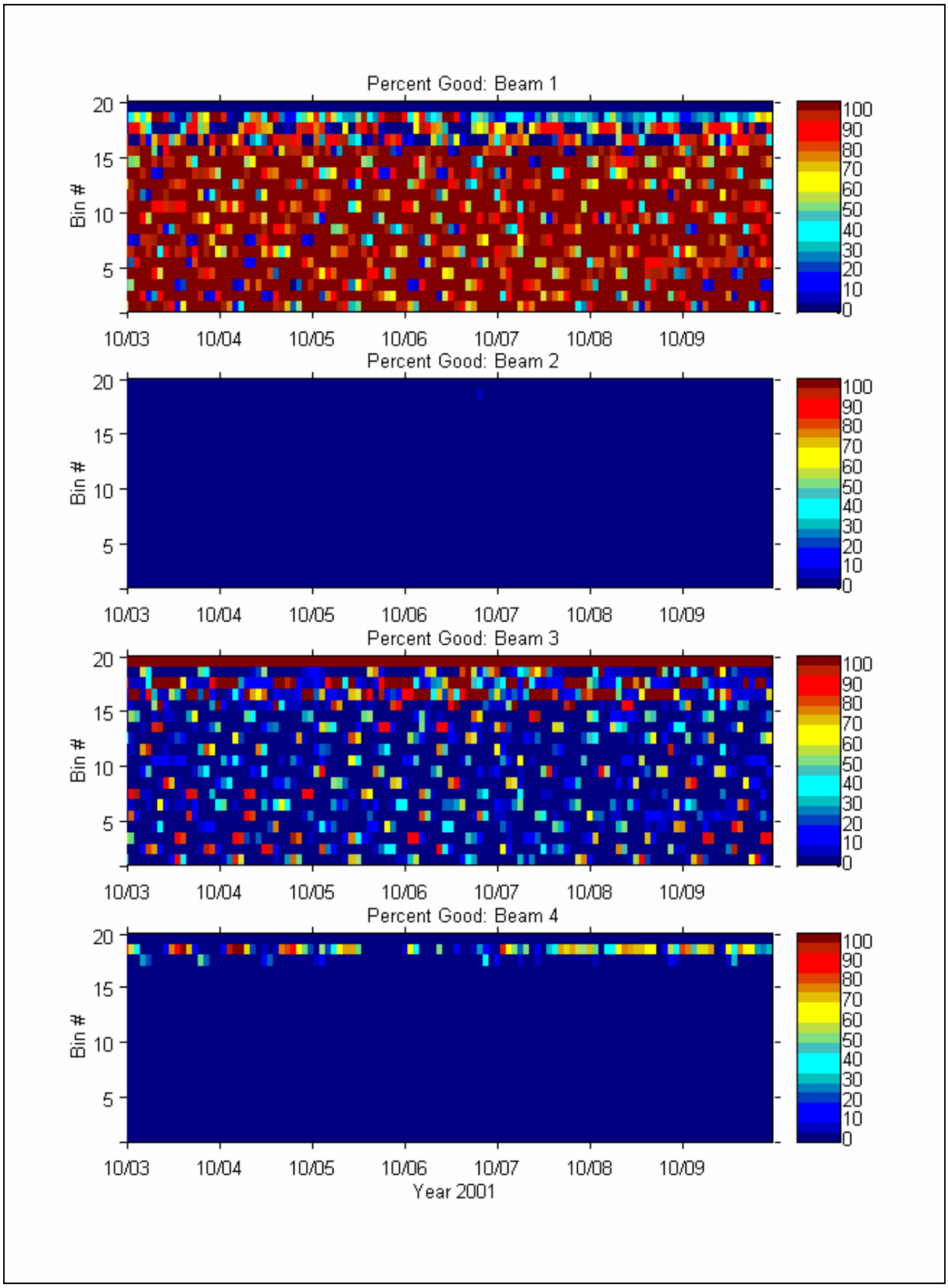

Figure B3-c. Time series of percent good profile data for 3 – 9 October.

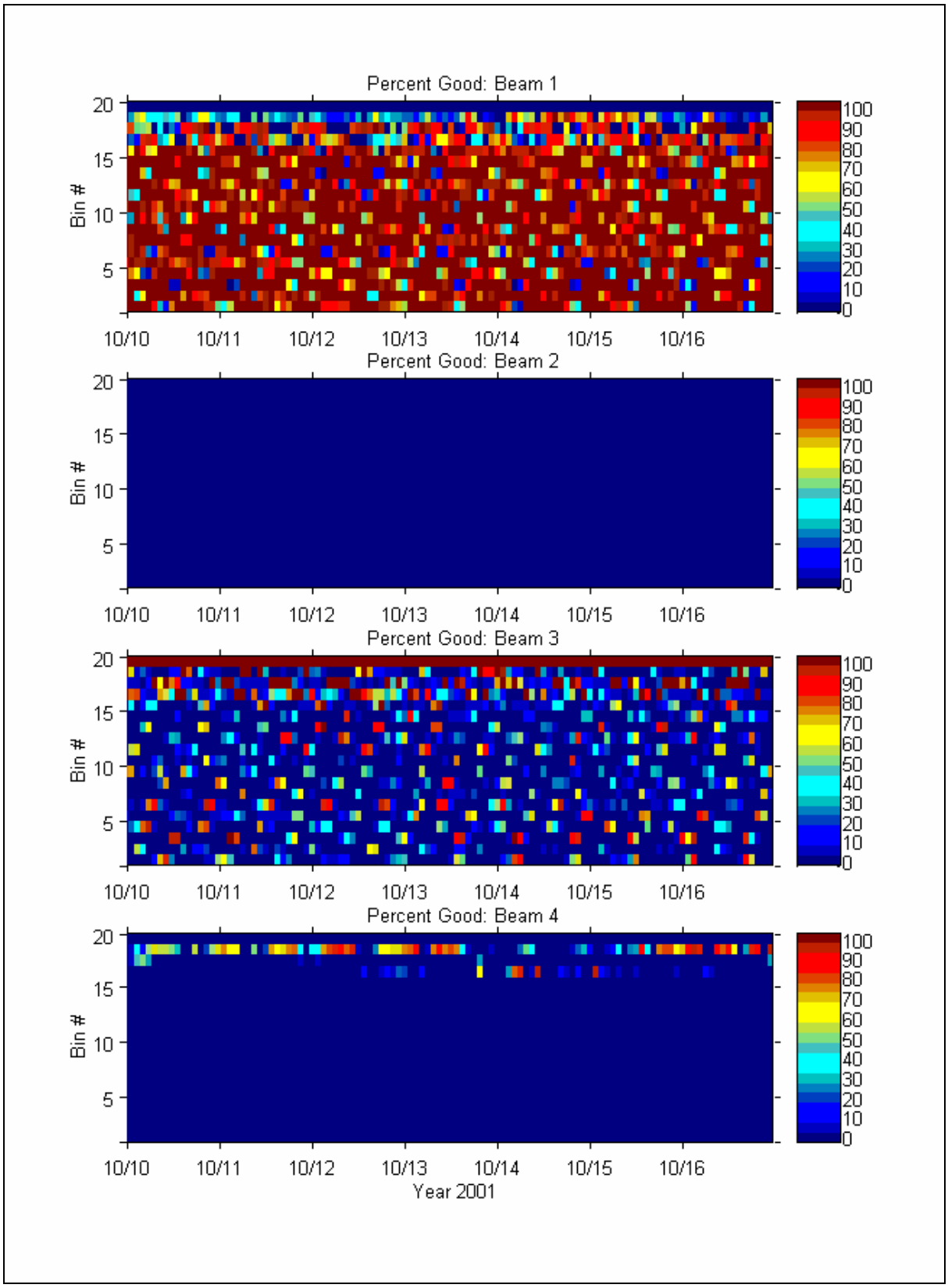

Figure C-3d. Time series of percent good profile data for 10 – 16 October.

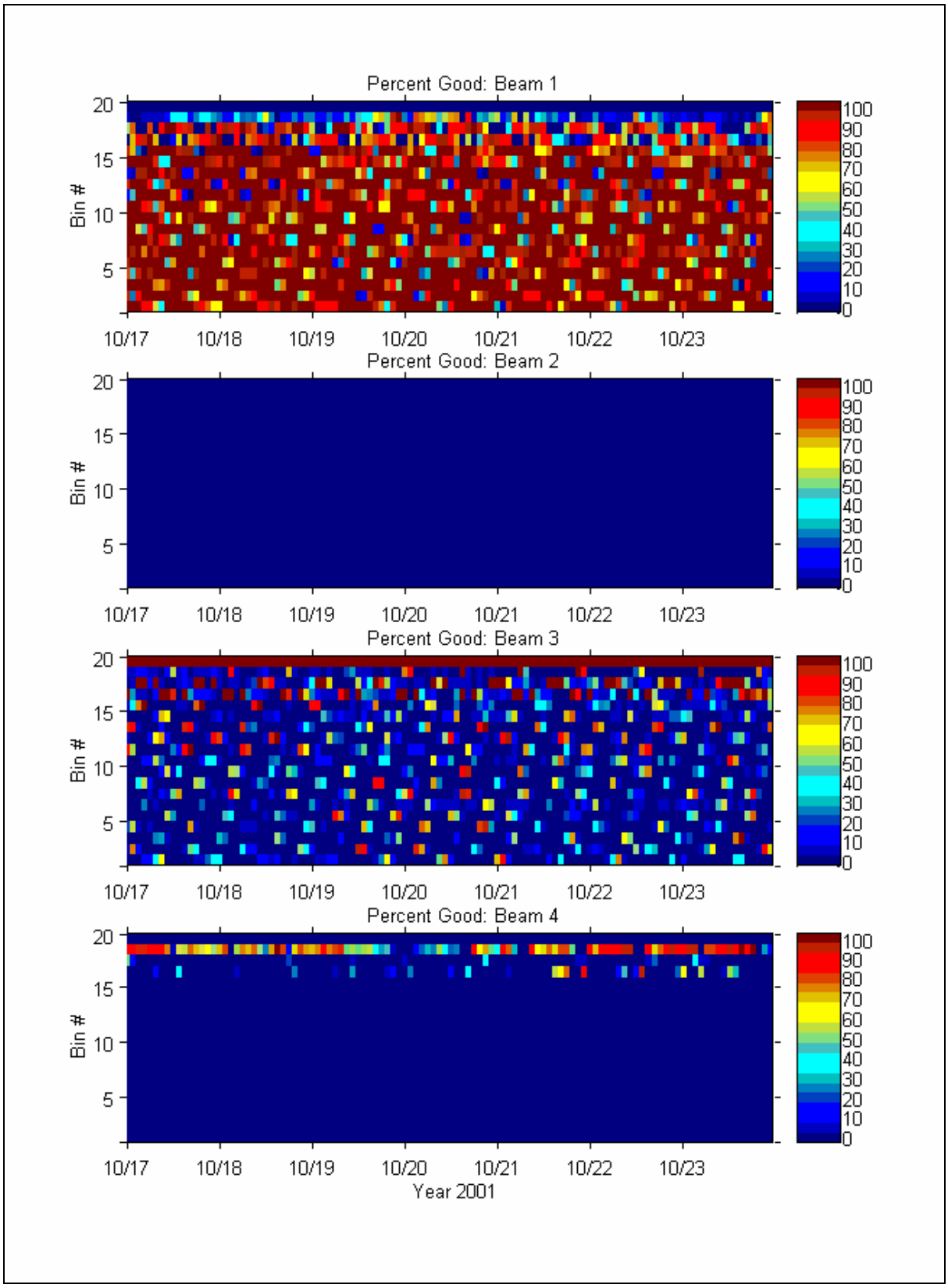

Figure C-3e. Time series of percent good profile data for 17 – 23 October.

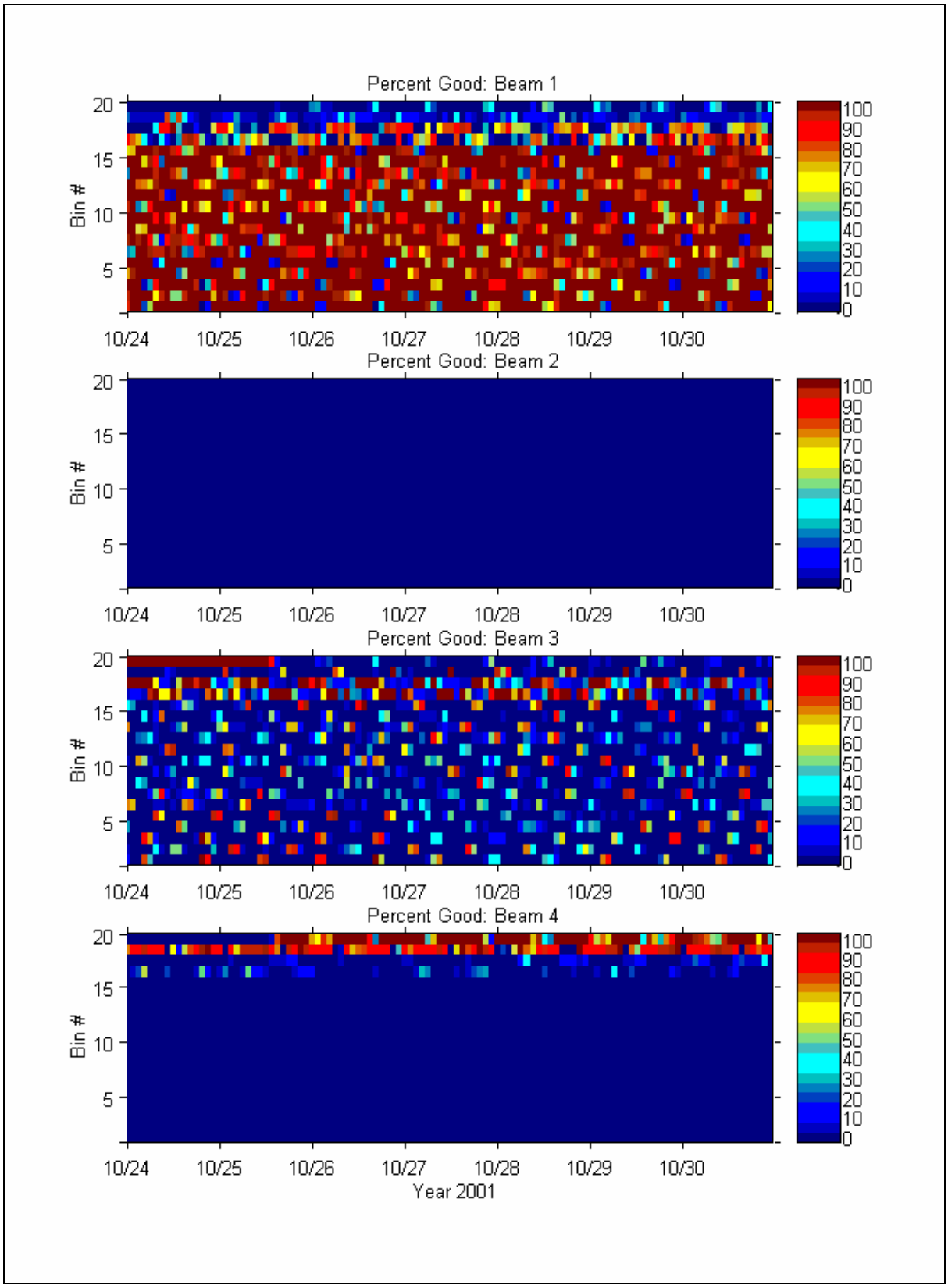

Figure C-3f. Time series of percent good profile data for 24 – 30 October.

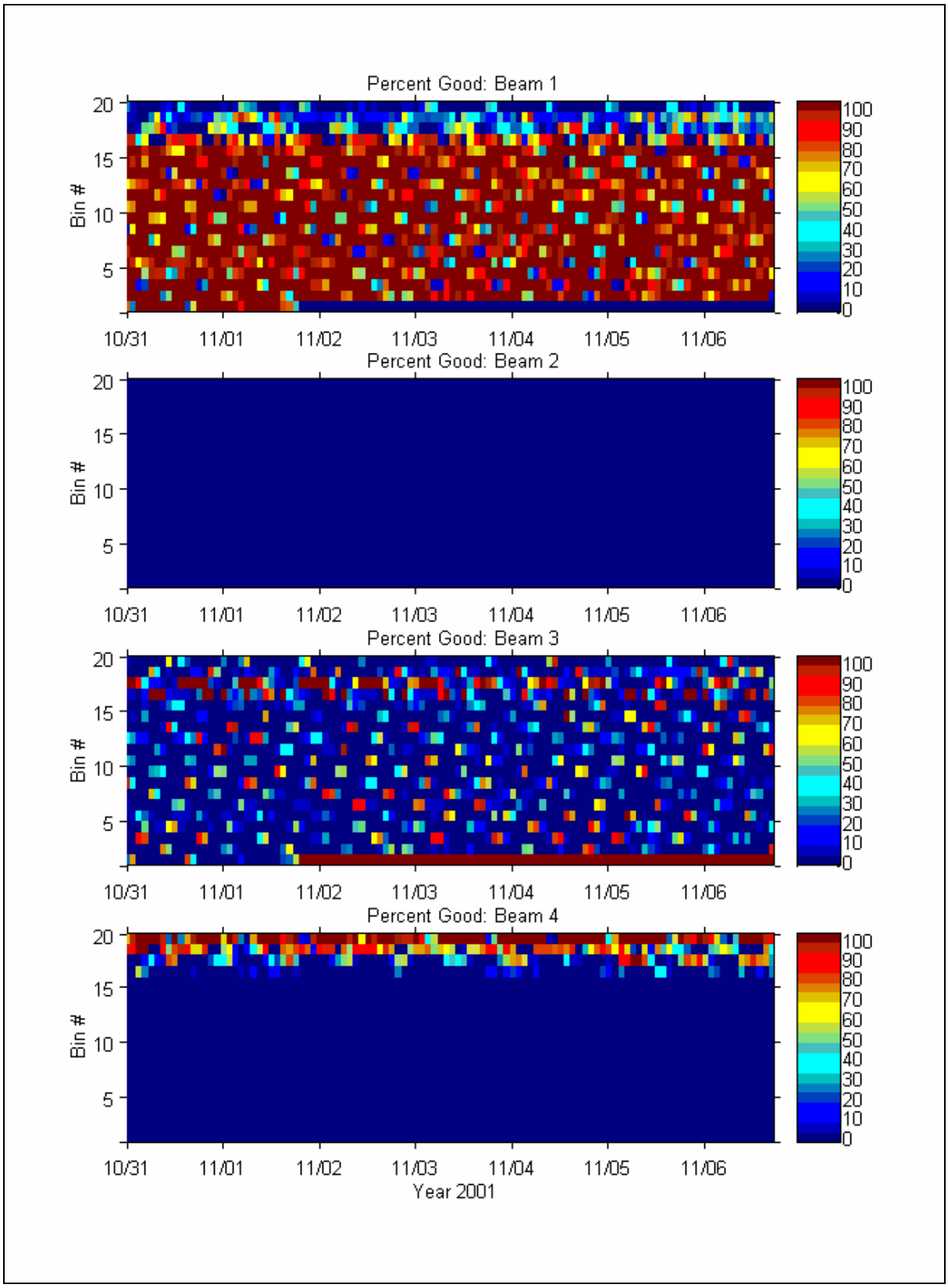

Figure C-3g. Time series of percent good profile data from 31 October to 6 November.